GEOMAR

The Importance of Natural and Anthropogenic Factors for the Coupling Between the Stratosphere and the Troposphere

Dissertation
zur Erlangung des Doktorgrades
der Mathematisch-Naturwissenschaftlichen Fakultät
der Christian-Albrechts-Universität zu Kiel

vorgelegt von

Felicitas K. Hansen

Kiel, 2015

Erste Gutachterin: Prof. Dr. Katja Matthes
Zweiter Gutachter: Prof. Dr. Richard Greatbatch

Tag der mündlichen Prüfung: 11.05.2015
Zum Druck genehmigt: 11.05.2015

gez. Dr. Wolfgang J. Duschl, Dekan

Abstract

This thesis describes several new aspects of the dynamical coupling between the stratosphere and the troposphere, and how this coupling is influenced by different natural and anthropogenic factors. A unique set of four long-term sensitivity experiments is designed to examine the importance of the Quasi-Biennial Oscillation (QBO) of equatorial stratospheric winds, modes of sea surface temperature (SST) variability like the El Niño Southern Oscillation (ENSO), anthropogenic greenhouse gases (GHGs) and ozone depleting substances (ODSs), for stratosphere-troposphere coupling. The model experiments are performed with NCAR's CESM model with the chemistry-climate model WACCM as its atmospheric component. The number and the length of the simulations performed here, given that the model includes both an interactive ocean and an interactive chemistry module and reaches up to the thermosphere, are exceptional.

Special emphasis is placed on major Stratospheric Sudden Warmings (SSWs) in the Northern hemisphere which are a prominent example of stratosphere-troposphere coupling and which can affect surface weather and climate. It is shown that the QBO strengthens the climatological stratospheric polar night jet (PNJ) and significantly reduces the major SSW frequency by reducing the propagation of planetary waves into the PNJ region. Variability in SSTs weakens the PNJ and significantly increases the major SSW frequency by enhancing planetary wave forcing. Extreme climate change conditions determine the prewarming phase of major SSWs. SST variability is needed to reproduce the observed tropospheric negative Northern Annular Mode pattern after major SSWs.

Further testing the sensitivity of WACCM experiments to the width of the QBO relaxation along the equator leads to a new contribution to the famous Holton-Tan mechanism in stratospheric dynamics and chemistry. The Holton-Tan mechanism, i.e., stronger zonal mean winds during QBO west phases (QBOW) in the PNJ region, is enhanced for a wider compared to a narrower QBO relaxation. The results suggest that at least two processes are involved in transmitting the equatorial QBO signal into the polar stratosphere: first, an effect of the zero wind line in the lower stratosphere which is shifted depending on the phase of the QBO, and second, the effect of the secondary QBO circulation in the middle to upper stratosphere. Both processes affect the direction of planetary wave propagation so that these waves disturb the stratospheric polar vortex more during QBO east phases (QBOE).

The first study which investigates a combined QBO-ENSO influence on the troposphere shows that large differences occur between the North Pacific and North Atlantic. The stratospheric equatorial QBO anomalies extend down to the troposphere over the North Pacific during boreal winter, but only during La Niña (not El Niño) events. The conditions for the genesis and intensification of synoptic-scale waves are improved during QBOW compared to QBOE conditions by linear QBO-ENSO interactions. In the North Atlantic, the non-linear interaction of QBOW with La Niña (QBOE with El Niño) results in a positive (negative) North Atlantic Oscillation pattern.

This thesis presents an improved understanding of the physical mechanisms that couple the stratosphere and the troposphere, which has the potential to improve tropospheric weather forecasting skill and moreover highlights the importance of the stratosphere for understanding and modeling tropospheric dynamics.

Zusammenfassung

Diese Arbeit beschreibt einige neue Aspekte der dynamischen Kopplung zwischen Stratosphäre und Troposphäre und wie diese Kopplung von verschiedenen natürlichen und anthropogenen Faktoren beeinflusst wird. Um die Bedeutung der quasi-zweijährigen Schwingung des Windes in der äquatorialen Stratosphäre (engl. Quasi-Biennial Oscillation, QBO), von Variabilitäten der Meeresoberflächentemperatur (engl. sea surface temperature, SST) wie z.B. die El Niño Southern Oscillation (ENSO), von anthropogenen Treibhausgasen und von ozonzerstörenden Substanzen für die Stratosphären-Troposphären-Kopplung zu untersuchen, wurde ein einzigartiges Set aus vier langen Sensitivitätsexperimenten entworfen. Die Modellexperimente wurden mit NCAR's CESM Modell durchgeführt, welches das Klima-Chemie-Modell WACCM als atmosphärische Komponente beinhaltet. Die Anzahl und die Länge der Simulationen mit solch einem komplexen Modellsystem, das sowohl einen interaktiven Ozean als auch ein interaktives Chemie-Modul enthält und das bis in die Thermosphäre hinaufreicht, sind außergewöhnlich.

Ein spezieller Fokus dieser Arbeit lag auf der Untersuchung von großen plötzlichen Stratosphärenerwärmungen in der Nordhemisphäre, da diese ein bekanntes Beispiel für Stratosphären-Troposphären-Kopplung darstellen und sogar das Wetter und Klima an der Erdoberfläche beeinflussen. Die Ergebnisse dieser Arbeit zeigen, dass die Präsenz der QBO den klimatologischen Polarnachtstrahlstrom in der Winter-Stratosphäre verstärkt und die Anzahl von großen Stratosphärenerwärmungen signifikant dadurch verringert, dass die Ausbreitung von planetarischen Wellen in die Polarnachtstrahlstrom-Region reduziert wird. Variable SSTs schwächen den Polarnachtstrahlstrom und erhöhen die Frequenz von großen Stratosphärenerwärmungen dadurch, dass die Wellenausbreitung in die Polarnachtstrahlstrom-Region verstärkt wird. Extreme Klimawandel-Bedingungen haben einen Einfluss auf die dynamische Entwicklung in den Wochen vor den großen Stratosphärenerwärmungen. Variable SSTs werden benötigt, um das beobachtete negative Signal der Nordatlantischen Oszillation in der Troposphäre im Anschluss an große Stratosphärenerwärmungen richtig zu reproduzieren.

Weitere Analysen bezüglich der Breite der QBO-Relaxierung am Äquator konnten zu einem besseren Verständnis des bekannten Holton-Tan-Mechanismus' beitragen. In dieser Arbeit wurde gezeigt, dass der Holton-Tan-Mechanismus, der stärkere Zonalwinde in der polaren Stratosphäre während QBO-West-Phasen bewirkt, verstärkt ist, wenn eine breitere QBO-Relaxierung gewählt wird. Zwei Prozesse scheinen hauptsächlich für die Übermittlung des äquatorialen QBO-Signals in die polare Stratosphäre verantwortlich zu sein: zum einen der Effekt der Nullwindlinie in der unteren Stratosphäre der niederen Breiten, die abhängig von der QBO-Phase verschoben wird, und zum anderen der Effekt der sekundären QBO-Zirkulation in der mittleren und oberen Stratosphäre der mittleren Breiten. Beide Effekte bewirken eine Änderung der Ausbreitungsrichtung von planetarischen Wellen, sodass diese während der QBO-Ost-Phase in Richtung des Polarnachtstrahlstromes gelenkt werden und den Polarwirbel stören und abschwächen.

In der ersten Studie, die den kombinierten QBO-ENSO-Einfluss auf die Troposphäre untersucht, konnte gezeigt werden, dass bei diesem Einfluss große Unterschiede zwischen dem Nord-Pazifik und dem Nord-Atlantik auftreten. Die QBO-Anomalien breiten sich aus der äquatorialen Stratosphäre bis in die Troposphäre über dem Nord-Pazifik aus, allerdings nur während La Niña- und nicht während El

Niño-Ereignissen. Durch lineare QBO-ENSO-Interaktionen herrschen hier während der QBO-West-Phasen bessere Bedingungen für die Genese und Intensivierung von synoptisch-skaligen Wellen als während der QBO-Ost-Phasen. Im Nord-Atlantik sorgen nicht-lineare Wechselwirkungen zwischen QBO-West-Phasen und La Niña-Bedingungen (QBO-Ost-Phasen und El Niño-Bedingungen) für die Entstehung eines positiven (negativen) Musters der Nordatlantischen Oszillation.

Diese Arbeit trägt zu einem besseren Verständnisses der physikalischen Prozesse von Stratosphären-Troposphären-Kopplung bei. Dies birgt Potenzial zur Verbesserung der Güte von troposphärischen Wettervorhersagen. Die Ergebnisse dieser Arbeit betonen auch die Relevanz der Stratosphäre für die Dynamik in der Troposphäre.

Contents

1 Introduction

The two lowermost layers in the Earth's atmosphere - the troposphere and the stratosphere - are not strictly separated but vertically coupled via various dynamical, chemical and radiative processes. Of these processes, the dynamical coupling deserves special consideration given that large stratospheric anomalies can propagate down into the troposphere and even have an effect on the surface. Thus, detailed understanding of dynamical stratosphere-troposphere coupling contains large potential to enhance skill for predictions of tropospheric weather and climate.
The coupling between the stratosphere and the troposphere can be influenced by those factors which determine atmospheric variability. The appearance of this modulation and the underlying physical mechanisms are far from being fully understood. However, it is crucial to separate and quantify the contributions from natural and anthropogenic factors for these mechanisms, e.g., in order to reliably estimate the anthropogenic contribution to the recent tropospheric warming and stratospheric cooling trend, and therefore improve projections of the future climate.
The goal of this thesis is to provide qualitative and quantitative estimates about the impact of different natural and anthropogenic factors on stratosphere-troposphere coupling. Underlying physical mechanisms for this coupling will be investigated.

1.1 Coupling between Stratosphere and Troposphere

Several theories exist on the mechanisms for the dynamical coupling between the stratosphere and the troposphere. Haynes et al. [1991] proposed the so-called "downward control" principle. It suggests that zonal forces which occur due to the dissipation of Rossby and gravity waves in the stratosphere induce a secondary circulation which extends down to the troposphere. Another idea involves the adjustment of the tropospheric flow to stratospheric potential vorticity anomalies [Hartley et al., 1998; Black, 2002; Black and McDaniel, 2004]. Other studies indicate a potential role of synoptic eddies for the downward coupling of stratospheric anomalies and the persistence of the signal in the troposphere [Kushner and Polvani, 2004; Song and Robinson, 2004; Simpson et al., 2009; Kunz and Greatbatch, 2013; Domeisen et al., 2013]. Kunz and Greatbatch [2013] report that quasi-geostrophic adjustment of the troposphere to stratospheric wave drag initiates a surface response to the stratospheric anomalies, and that this surface response is delayed up to several weeks with respect to the stratospheric signal due to eddy feedback processes.
For this thesis, stratosphere-troposphere coupling due to processes involving planetary waves is

considered. Planetary waves are generated in the troposphere by orography and land-sea contrasts. These waves propagate upward into the stratosphere where they either dissipate or are reflected downward to impact the troposphere again, e.g., through feedback processes with synoptic-scale waves.

Planetary waves can propagate only in a certain range of westerly wind regimes [Charney and Drazin, 1961]. When they dissipate in the stratosphere, they interact with the zonal-mean flow and accelerate or decelerate the prevailing background winds; the resulting anomalies can propagate downward. This process has been shown to be of potential importance for seasonal prediction and weather forecasts of tropospheric NH winter weather [Baldwin and Dunkerton, 2001; Thompson et al., 2002; Baldwin et al., 2003; Mitchell et al., 2013; Sigmond et al., 2013]. Several indices are used to assess this zonal-mean coupling. Many of them are based on the annular modes in both hemispheres (NAM and SAM, respectively), which are commonly defined as the leading empirical orthogonal functions (EOFs) of monthly-mean hemispheric geopotential height fields [Baldwin and Thompson, 2009]. Others use, e.g., the zonal mean wind at a certain latitude and height, or parameters at the polar cap. In a comparison of these indices, Baldwin and Thompson [2009] highlight the advantages of a methodology based on EOFs of daily zonally-averaged geopotential. According to their results, the daily evolution of stratosphere-troposphere coupling is seen most clearly with this method, it is robust, easy to apply to climate model output in zonal-mean form and computationally less expensive than other methods.

Especially weak and strong stratospheric events, defined via the various indices, have the potential to propagate downward and affect the troposphere. A prominent example of such an extreme event in the stratosphere is the weak polar vortex event, a so-called Stratospheric Sudden Warming (SSW; see below).

The process of planetary waves being reflected in the stratosphere to affect the troposphere again is called downward wave coupling. It represents another important source of stratosphere-troposphere coupling. Fundamental research on this topic has been mainly done by N. Harnik, J. Perlwitz and T. Shaw [e.g., Harnik and Lindzen, 2001; Perlwitz and Harnik, 2003, 2004; Harnik, 2009; Shaw et al., 2010]. They found that the occurrence of downward wave coupling is tied to a so-called "bounded wave geometry", meaning a well-defined high-latitude meridional waveguide in the lower stratosphere that is bounded above by a vertical reflecting surface.

Recent dynamical metrics of stratosphere-troposphere coupling are based on extreme stratospheric planetary-scale wave heat flux events [Shaw et al., 2014], tropospheric blockings [Davini et al., 2014], or Mark Baldwins idea of a stratospheric "plunger" (not published yet), meaning anomalies of potential vorticity affecting the tropopause height and thereby stratosphere-troposphere coupling.

1.1.1 Stratospheric Sudden Warmings (SSWs)

Planetary waves propagate upward from the troposphere into the stratosphere only in (not too strong) westerlies [Charney and Drazin, 1961]. Thus, they generally do not reach the stratosphere

during summer when easterly winds are prevailing. By the interaction of planetary waves with the zonal mean flow, the winter stratospheric polar vortex can be disrupted in its zonal symmetry [Matsuno, 1971]. It might then be displaced from the pole or split into two vortices, whereupon both processes lead to a fast (within a few days) and strong (up to several tens of °C) increase in temperatures in the polar stratosphere. If this temperature increase is accompanied by a reversal of the zonal mean zonal wind at 60°N on the 10hPa level from westerly to easterly, the World Meteorological Organization (WMO; see Labitzke and Naujokat [2000]) calls this event a major Stratospheric Sudden Warming (SSW). A major SSW is observed about every two years [Erlebach et al., 1996; Labitzke and Naujokat, 2000; Charlton and Polvani, 2007]. More details about major warmings and how they are influenced by different natural and anthropogenic factors can be found in Chapter 2.

At the end of each winter, the stratospheric winds switch from westerly to the easterly summer circulation; this event is called final warming. A major SSW occurring during this transition period without a circulation change back to the winter westerlies is called major final warming accordingly. When the polar temperature increases but the circulation at 10hPa does not reverse, the event is defined as a minor warming. Theoretically, major, minor and final warmings can occur in both hemispheres. However, since less waves are generated in the Southern hemisphere due to less land masses and hence dynamics which are very different from the NH, only one major warming occurred until now in the Southern Hemisphere (SH) since the beginning of detection in the 1940s [Krüger et al., 2005]. There exists no SH counterpart of the so-called Canadian warmings which happen in the NH in early winter.

Large stratospheric anomalies like those occurring during major SSWs have the potential to descend down into the troposphere and thus even affect surface weather and climate [Julian and Labitzke, 1965; Quiroz, 1977; Baldwin and Dunkerton, 2001; Thompson et al., 2002; Mitchell et al., 2013; Hitchcock and Simpson, 2014], and even the ocean [e.g., Reichler et al., 2012; O'Callaghan et al., 2014]. The resulting surface pattern strongly projects on the negative phase of the North Atlantic Oscillation (NAO) or the Arctic Oscillation (AO) [Baldwin and Dunkerton, 2001; Charlton and Polvani, 2007]. Examples of the surface influence of SSWs are an effect on North American, European [Mitchell et al., 2013] or northern Russia [Sigmond et al., 2013] surface temperatures, eastern Canada and North Atlantic precipitation [Sigmond et al., 2013], or 500hPa geopotential height over Europe [Domeisen et al., 2015].

1.2 Factors of natural climate variability

From the effect of stratospheric anomalies on tropospheric weather and climate it follows that the coupling mechanisms described above can be used to improve tropospheric weather forecasts and seasonal predictions for different latitudes and regions [Baldwin and Dunkerton, 2001; Thompson et al., 2002; Mitchell et al., 2013; Sigmond et al., 2013; Domeisen et al., 2015]. For that it is

mandatory to gain detailed understanding about the processes underlying this coupling, and of potential influencing factors. This thesis wants to contribute to this gain of understanding (and at the end to the enhancement of tropospheric prediction skill) by investigating the importance of different so-called "anthropogenic" and "natural" factors for stratosphere-troposphere coupling.
The factors which can be assumed to influence stratosphere-troposphere coupling are the factors which determine the variability of each of the two layers separately. Some of these factors, namely greenhouse gases (the most prominent example of them is carbon dioxide, CO_2) and ozone-depleting substances, have reached unsightly popularity in the last decades, as they have been shown to be responsible for the recent warming trend in global tropospheric temperatures and the accompanying cooling in the stratosphere (see assessment reports (AR) of the Intergovernmental Panel on Climate Change (IPCC), e.g. IPCC [2014]). The decline of the stratospheric ozone layer as well as changes in the ozone hole which forms over Antarctica each Southern hemisphere (SH) spring have been the focus of many chemistry studies. These studies agree that for the involved ozone depletion processes, catalytic chemistry including man-made chlorofluorocarbons are responsible [Solomon, 1999]. As GHGs and ODSs are produced and emitted due to human behavior, these factors are called "anthropogenic". Their counterpart are the so-called "natural" factors, causing natural or internal climate variability. Natural factors are, e.g., internal factors like the Quasi-Biennial Oscillation (QBO) of equatorial stratospheric winds, variations in sea surface temperatures (SSTs), volcanic eruptions, or external factors like variations in solar radiation. These natural factors and their importance for tropospheric and stratospheric variability shall be briefly introduced in the following. More detailed descriptions, especially of the QBO and SST variability patterns, can be found in the following chapters.

1.2.1 The Quasi-Biennial Oscillation

The QBO is the dominant natural variability mode in the equatorial stratosphere [Baldwin et al., 2001]. It is mainly driven by upward propagating tropical atmospheric waves like gravity, inertia-gravity, Kelvin and Rossby-gravity waves. These waves, which are smaller-scale compared to the previously introduced planetary waves, transfer momentum in the stratosphere and initiate the downward propagation of easterly and westerly wind regimes [Lindzen and Holton, 1968; Andrews and McIntyre, 1976; Baldwin et al., 2001] as can be seen in Figure 1.1. The wind regimes alternate with an average period of about 28 months. The amplitude of the wind regimes is asymmetric with a maximum of around $+20$ m/s in the westerly and -30 m/s in the easterly phase. By influencing the propagation of mid-latitude planetary waves and their interaction with the mean flow, the tropical QBO affects the mean state and variability in the extra-tropical and even polar stratosphere [Holton and Tan, 1980, 1982; Anstey and Shepherd, 2014]. In the latter, the stratospheric polar winter vortex is on average colder and less disturbed in QBO west phase winters, while it tends to be warmer and hence more disturbed in winters of dominating easterly QBO phase [Holton and Tan, 1980, 1982]. This is often referred to as the Holton-Tan effect and involves a shift of the zero wind

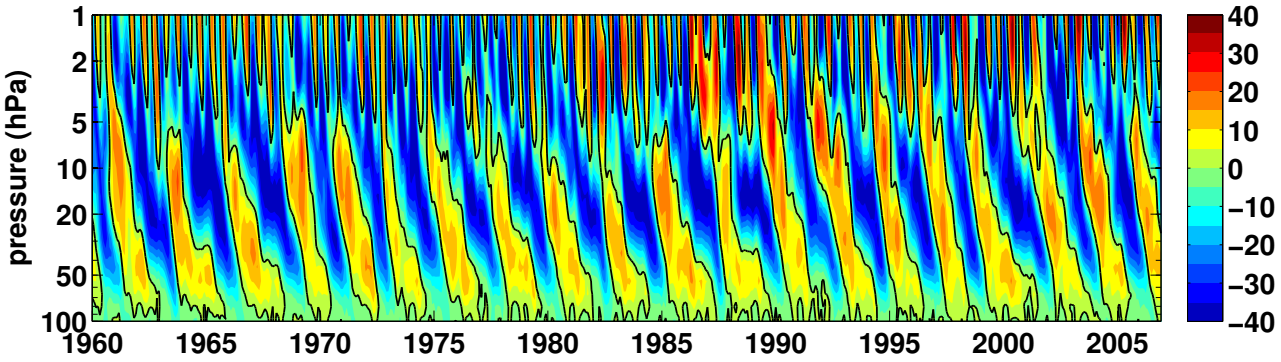

Figure 1.1: Zonal mean zonal wind (m/s) in the equatorial stratosphere, averaged between 2.8°S and 2.8°N. Contour interval 5 m/s; the black contour indicates the zero wind line. From the extended ERA40 data set (see Chapter 3).

line depending on the QBO phase, which hinders or allows planetary waves to propagate into the tropical stratosphere. However, more recent studies [Naoe and Shibata, 2010; Garfinkel et al., 2012] suggest that the underlying mechanism is more a combination of this effect with another effect in the mid-latitude stratosphere which includes the QBO secondary meridional circulation. In the mid-latitude stratosphere, a "barrier" for planetary waves is created depending on the QBO phase, leading to a convergence of these waves in the polar vortex region and hence a more disturbed vortex during QBOE. In Chapter 3 the importance of these two mechanisms for the QBO signal in the polar stratosphere will be addressed.

A detailed description of many more aspects of the QBO can also be found in Chapter 3.

Although the QBO is primarily a stratospheric phenomenon, there are at least two ways in which it can affect the troposphere: 1) directly in the tropics and subtropics by modifying, e.g., temperature and vertical wind shear along the tropopause and hence stratosphere-troposphere exchange [e.g., Gray et al., 1992], or 2) indirectly through its modulation of the stratospheric polar vortex which can be seen at the surface with a lag of 2–3 weeks [e.g., Baldwin and Dunkerton, 1999]. The tropospheric impact of the QBO then occurs, e.g., as an influence on European winter surface climate [Marshall and Scaife, 2009], as a modulation of the tropospheric subtropical jet [Garfinkel and Hartmann, 2011a,b] or as a modulation of tropical cyclone tracks [Ho et al., 2009] and their frequency [e.g., Shapiro, 1989].

1.2.2 Sea Surface Temperatures

Variations in SSTs also have a strong impact on the variability not only in the lower, but also in the middle to upper atmosphere [e.g., Sassi et al., 2004]. The dominant mode of SST variability between 60°S and N is the oceanic component of the El Niño-Southern Oscillation (ENSO) [Trenberth, 1997]. ENSO is a seesaw between warm and cold SST anomalies in the equatorial Pacific with consequences for the regional and global weather and climate. During a warm ENSO phase (El Niño), SSTs are

anomalously warm in the tropical Pacific ocean; during a cold ENSO phase (La Niña), SSTs are anomalously cold in this region. The coupled atmospheric component of ENSO, the Southern Oscillation, appears as according anomalies in sea level pressure (SLP), wind or temperature around the equatorial Pacific, i.e., high SLP over the western tropical Pacific during El Niño and low SLP in this region during La Niña.

Aside from ENSO, other important large-scale SST variability patterns are the Atlantic Multidecadal Oscillation [Schlesinger and Ramankutty, 1994], the North Pacific Oscillation/West Pacific pattern [e.g., Wallace and Gutzler, 1981; Linkin and Nigam, 2008], or the Pacific Decadal Oscillation [Mantua et al., 1997]. Figure 1.2 (from Blume [2012]) shows these variability patterns as the first four empirical orthogonal functions (EOFs) of observed monthly detrended SST anomalies.

Like the QBO, the effect of ENSO and other SST variability patterns is not restricted to their main occurrence regions. ENSO, although being a phenomenon of the tropical Pacific, has an effect on the global atmospheric circulation [e.g., Alexander et al., 2002]. There seems to be a tropospheric (via tropospheric teleconnections) and a stratospheric (mainly via SSWs) pathway of ENSO influencing the troposphere as recently summarized for reanalysis data by Butler et al. [2014]. Via tropospheric teleconnection patterns like, e.g., the Pacific-North American pattern (PNA; Wallace and Gutzler [1981]), ENSO modulates the climate over North America. Its influence on the stratospheric polar vortex has been, e.g., confirmed in observations by van Loon and Labitzke [1987] and in model studies by Sassi et al. [2004]; Manzini et al. [2006]; Ayarzagüena et al. [2013]. During ENSO warm phases, the Aleutian low is deepened, and the planetary wave number 1 interferes positively with the climatological wave structure [Ineson and Scaife, 2009]. The resulting stronger wave forcing in turn leads to a weaker stratospheric polar vortex [Manzini et al., 2006; Ayarzagüena et al., 2013] and more SSWs. Via this stratospheric pathway, ENSO affects the climate over the North Atlantic and Europe [Ineson and Scaife, 2009; Butler et al., 2014; Domeisen et al., 2015]. The resulting surface signal consists of a negative North Atlantic Oscillation (NAO) pattern, which leads, e.g., to cold late winters in Northern Europe during the ENSO warm phase [Ineson and Scaife, 2009].

Influencing the same regions, ENSO effects interact with the QBO. During El Niño (La Niña) phases, the amplitude of the QBO at the equator is weaker (stronger) and the period is shorter (longer) [Taguchi, 2010; Yuan et al., 2014]. In the stratospheric polar vortex region, El Niño interacts non-linearly with the easterly QBO phase [Garfinkel and Hartmann, 2007; Calvo et al., 2009].

1.2.3 Other natural factors

Volcanic eruptions can influence climate variability by the injection of aerosols into the atmosphere. Two processes are mainly involved in modulating global temperatures: first, the aerosol layer leads to an enhanced scattering of incoming solar radiation back to space, resulting in a cooling at the surface. Second, by absorbing solar and terrestrial radiation, stratospheric temperatures increase [Robock, 2000]. Although stratospheric ozone depletion is enhanced after an eruption through heterogeneous chemical reactions which involve the volcanic aerosols [Solomon, 1999] leading to less ultraviolet

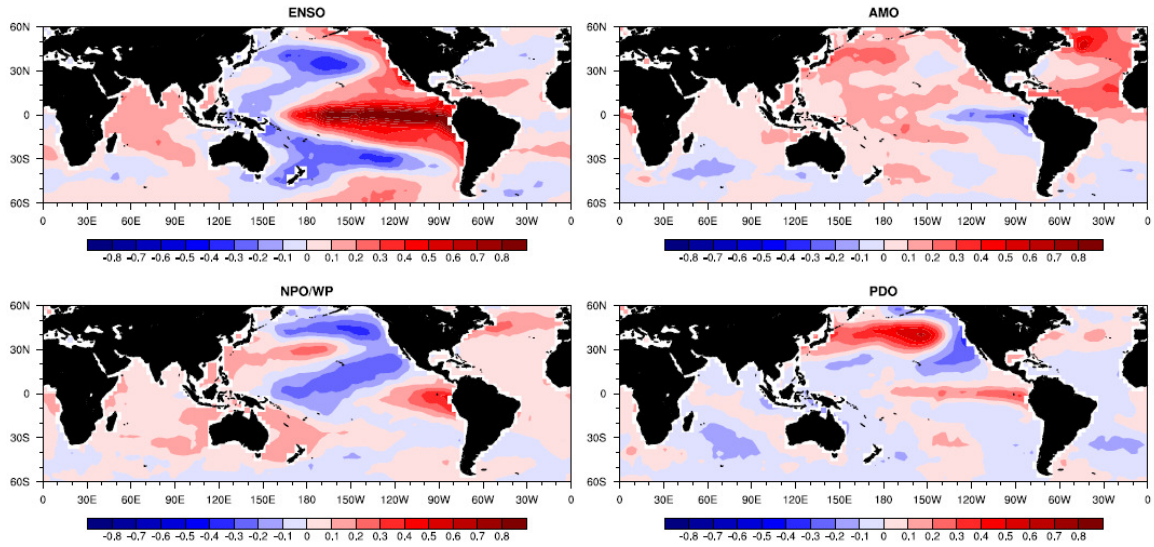

Figure 1.2: The first four empirical orthogonal functions (EOFs) of monthly observed detrended SST anomalies in Kelvin. Figure from Blume [2012].

absorption and hence reduced radiative heating in the stratosphere, the net stratospheric effect is still heating. Because this stratospheric warming is stronger at low than at high latitudes, the equator-to-pole temperature gradient is enhanced which results in a stronger stratospheric polar vortex. A global influence of volcanic eruptions is more likely when the eruptions take place close to the equator: by tropical convection, the injected aerosols are transported higher up into the atmosphere and are distributed globally with the Brewer-Dobson circulation, the meridional overturning circulation in the stratosphere [Brewer, 1949; Dobson, 1952]. Prominent examples of volcanic eruptions which were followed by a significant decrease in global surface temperature and an increase in stratospheric temperatures are the eruptions of Mt. Agung (1963), El Chichón (1982), and Mt. Pinatubo (1991). The stratospheric warming following such strong volcanic eruptions can last 1–2 years, the surface cooling even 1–3 years [Robock, 2000].

Another non-negligible part of the variability in the climate system is generated by variations in solar irradiance (see review paper by Gray et al. [2010]). Strong variations in various atmospheric parameters like, e.g., ozone and temperatures occur with a period of 11 years [e.g., Haigh, 1994, 1996; Matthes et al., 2006; Frame and Gray, 2010] which is referred to as the 11-year solar cycle. These variations are induced by a varying number of sunspots and faculae on the Sun's surface. Although the total solar irradiance changes only by about 0.07% between sunspot maximum and minimum [Gray et al., 2010], differences in the ultra-violet (UV) band of the spectrum can reach up to 8% [Lean et al., 1997]. This is of special importance for the ozone layer in the middle atmosphere where UV radiation is absorbed which in turn directly affects the radiation budget and hence atmospheric temperatures. Solar cycle induced changes in the meridional temperature gradient lead to changes in wind fields due to thermal wind balance. It occurs that the stratospheric polar vortex is stronger during solar maximum years than during solar minimum years. The solar

influence on the atmosphere interacts with effects of the QBO in such way that the Brewer-Dobson circulation is weakened during solar maximum conditions and the easterly phase of the QBO, and strengthened during solar maximum and the westerly QBO phase [Matthes et al., 2010].

1.2.4 Impact on NH zonal mean temperature

Both natural and anthropogenic factors have an influence on the whole atmosphere, albeit in different strength, depending, amongst others, on the altitude, the latitudinal region and the season. As the factors vary on different time scales and also interact with each other in a complex, non-linear way, it is difficult to separate their individual contributions and quantify their respective roles for the total variability. Some parts of the total variability might also be due to chaotic behavior [e.g., Holton and Mass, 1976; Yoden, 1987a,b; Christiansen, 2000; Badin and Domeisen, 2013].
Figure 1.3, left, shows zonally averaged NH tropospheric and stratospheric temperatures, and Figure 1.4 provides an estimate of the relative importance of the different factors for these temperatures. For Figure 1.4, the Linear Discriminant Analysis (LDA) is chosen and applied in a similar way as in Blume [2012]. The time series of zonal mean temperatures at each grid point in the zonal mean plane is modeled using a linear and stationary regression model where the time series of the different factors serve as forcing factors. The output of the LDA is a coefficient for each of the forcing factors, and from these coefficients the normalized impacts of the respective factors (which are shown in Figure 1.4) for zonal mean temperatures can be computed (see Appendix A.1 for details). Data are taken from a simulation of the recent past (1955–1999) with the Community Earth System Model (CESM) (20th century part of the "GHG" simulation described in chapter 2).
Figure 1.4 shows that in the tropical troposphere, zonal mean temperature variability is dominated by variability in SSTs (maximum impact larger than 60%; Figure 1.4 a), originating mainly from ENSO (not shown)[1]. Higher up in the tropical stratosphere, the QBO becomes apparent as the dominant mode not only in zonal mean zonal wind but also in zonal mean temperatures (maximum impact larger than 60%; Figure 1.4 b). Its dominant influence reaches into the stratospheric subtropics, where a secondary QBO signal is induced in order to maintain thermal wind balance [Plumb and Bell, 1982]. In the upper tropical stratosphere, temperature variability is dominated by the stratospheric semi-annual oscillation (SAO; Figure 1.4 e) [Reed, 1966; Belmont et al., 1974; Gray and Pyle, 1986].
The largest impact - more than 70% - on extra-tropical NH zonal mean temperatures in both the troposphere and the stratosphere comes from variations due to the seasonal cycle (Figure 1.4 f). The other factors are of secondary importance in the extra-tropics and play a role only locally, like, e.g., the SSTs in the mid-latitude lower stratosphere and high-latitude lower and upper stratosphere. The impact of volcanic eruptions is strongest along the subtropical tropopause and in the upper

[1] As described in Appendix A.1, the LDA has been performed separately for the first four EOFs of daily detrended SST anomalies. The tropical tropospheric signal in Figure 1.4 (a) is dominated by the signal coming from the first EOF, which corresponds to ENSO.

stratosphere (Figure 1.4 d). However, with a maximum impact of around 25%, its relative importance for NH zonal mean temperatures is small compared to the other factors. The same is true for the solar cycle (Figure 1.4 c). The influence of these factors on climate can be better seen using other methods, like in anomaly composites as done, e.g., in Kodera and Kuroda [2002]; Matthes et al. [2006]; Ineson et al. [2011]. The LDA applied here is not able to bare comparatively small signals which can be amplified by feedback processes; however, the method is sufficient to provide a estimate of the mean relative importance of the factors.

Compared to the other factors, the linear trend (Figure 1.4 g) is of special importance for the NH zonal mean temperature in the tropical troposphere (impact of $\sim$30%), the subtropical upper stratosphere ($\sim$40%) and along the mid-latitude tropopause and stratosphere (10–20%) during the period 1955–1999.

The general picture presented here is consistent with the results from Mitchell et al. [2014] where multilinear regression techniques are applied to nine reanalysis data sets, and with other model studies [e.g., Robock, 2000; Butchart et al., 2003; Giorgetta et al., 2006; Manzini et al., 2006].

From the method applied for Figure 1.4, we can get a rough idea about the impact of the respective factors on NH *global zonal mean* temperature; however, the real impact is not zonally symmetric around the globe. Chapter 4 of this thesis partly discusses this issue using the example of the QBO and its influence on different tropospheric sectors.

The impact of the different factors might change over time, e.g., due to changing atmospheric background states like the increase in GHGs since the industrial revolution which results in a tropospheric warming and stratospheric cooling trend (see Figure 1.3, right). Figure 1.5 shows how this impact change could look like for the period 2050–2099, using again the CESM "GHG" simulation, but now forced with the so-called Representative Concentration Pathways (RCP) Scenario 8.5. The RCP8.5 scenario is a strong GHG scenario which assumes an increase in radiative forcing of 8.5 W/m^2 relative to preindustrial values. Following this scenario, the impact of the linear trend increases especially in the tropical and subtropical troposphere and stratosphere by 10%, and this increase mainly counterbalances the decreasing impact of SSTs in this region. The SSTs become increasingly important ($+$10%) in the polar lower stratosphere, and the impact of the QBO increases by $\sim$10% in the mid-latitude lower stratosphere.

Altogether, it can be seen from this analysis that the natural and anthropogenic factors introduced before all have an impact on the stratosphere and the troposphere. However, as these two layers are not dynamically separated but vertically "coupled", the different factors also affect the stratosphere-troposphere coupling. Besides the seasonal cycle, the QBO and SSTs have the largest impact on NH zonal mean temperatures. This is why these two natural factors are chosen for this thesis for the following more detailed analysis on their importance for stratosphere-troposphere coupling, while the solar cycle, volcanic eruptions and the SAO are not further investigated here.

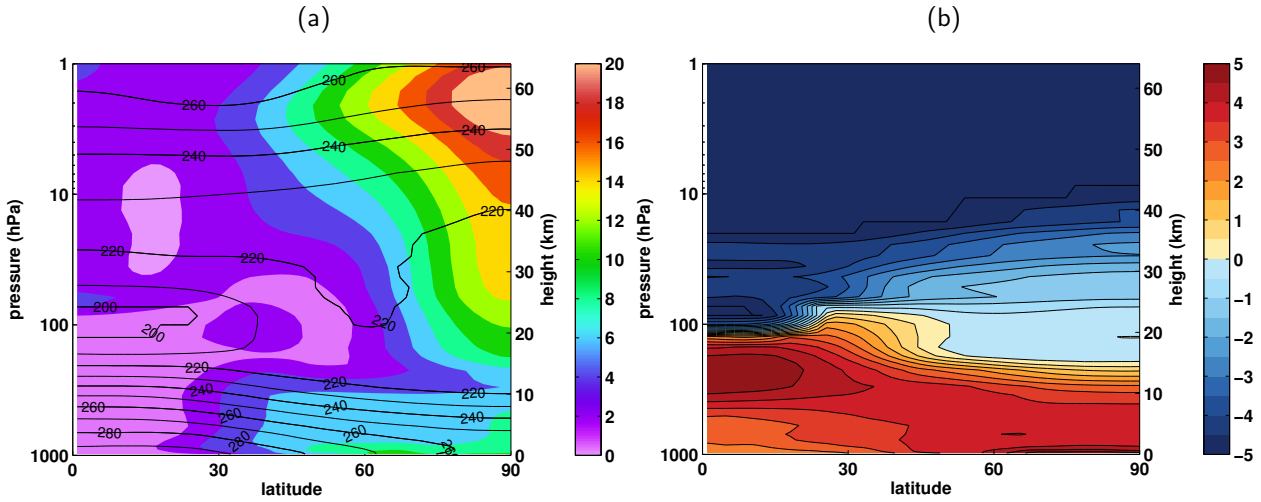

Figure 1.3: Annual NH zonal mean temperatures. Mean (contours, contour interval 10K) and standard deviation (colours, contour interval 2 K) for the period 1955–1999 (a), and the difference between the 2050–2099 average and the 1955-1999 average (b; contour interval 0.5 K). Data from CESM "GHG" simulation (see Chapter 2).

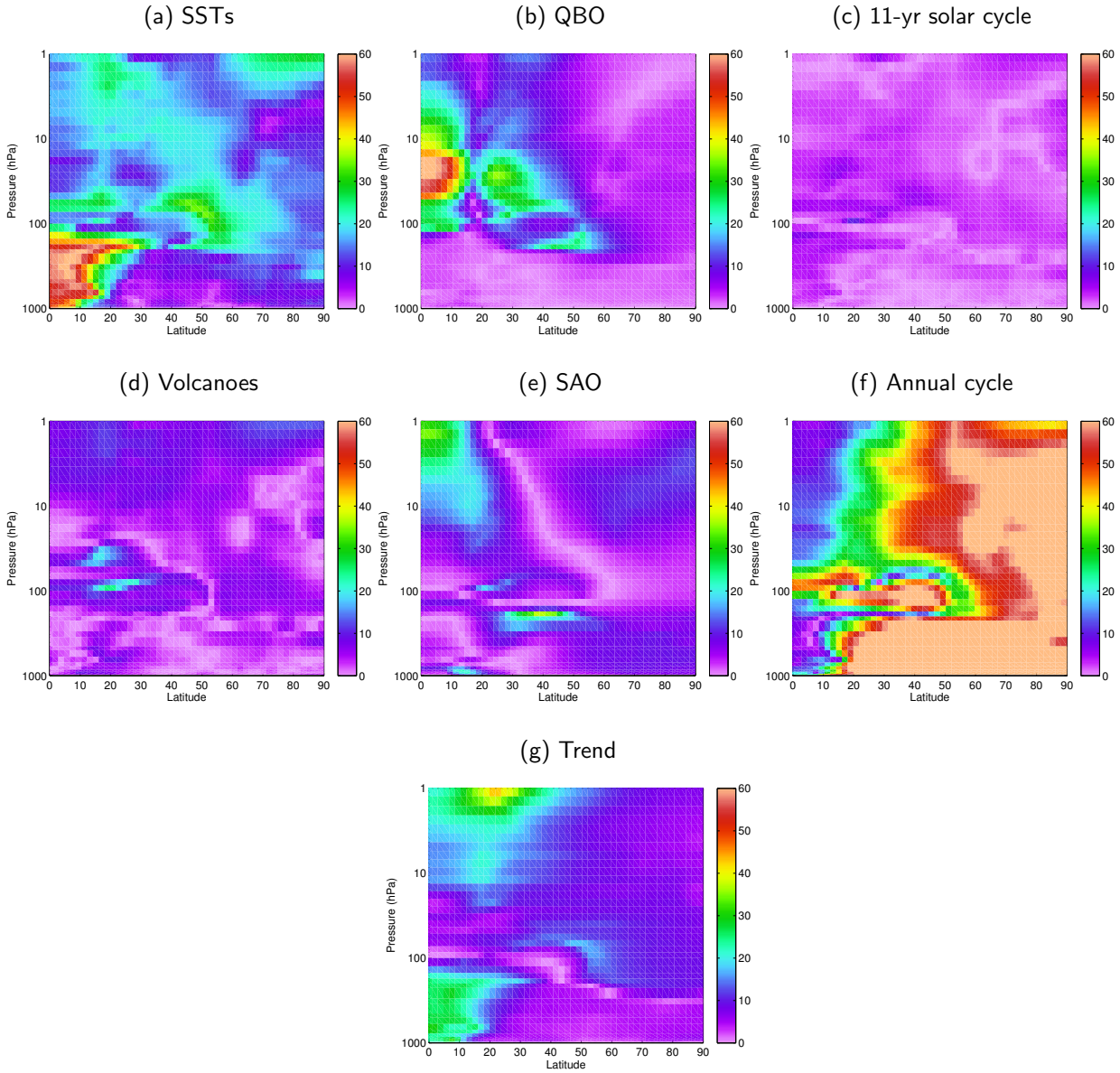

Figure 1.4: Impact (in %) of different natural (1st and 2nd row) and anthropogenic (3rd row) factors on annual NH zonal mean temperatures during 1955–1999. For details about the computation of the impact and about the single factors see Appendix A.1. Data from CESM "GHG" simulation (see Chapter 2).

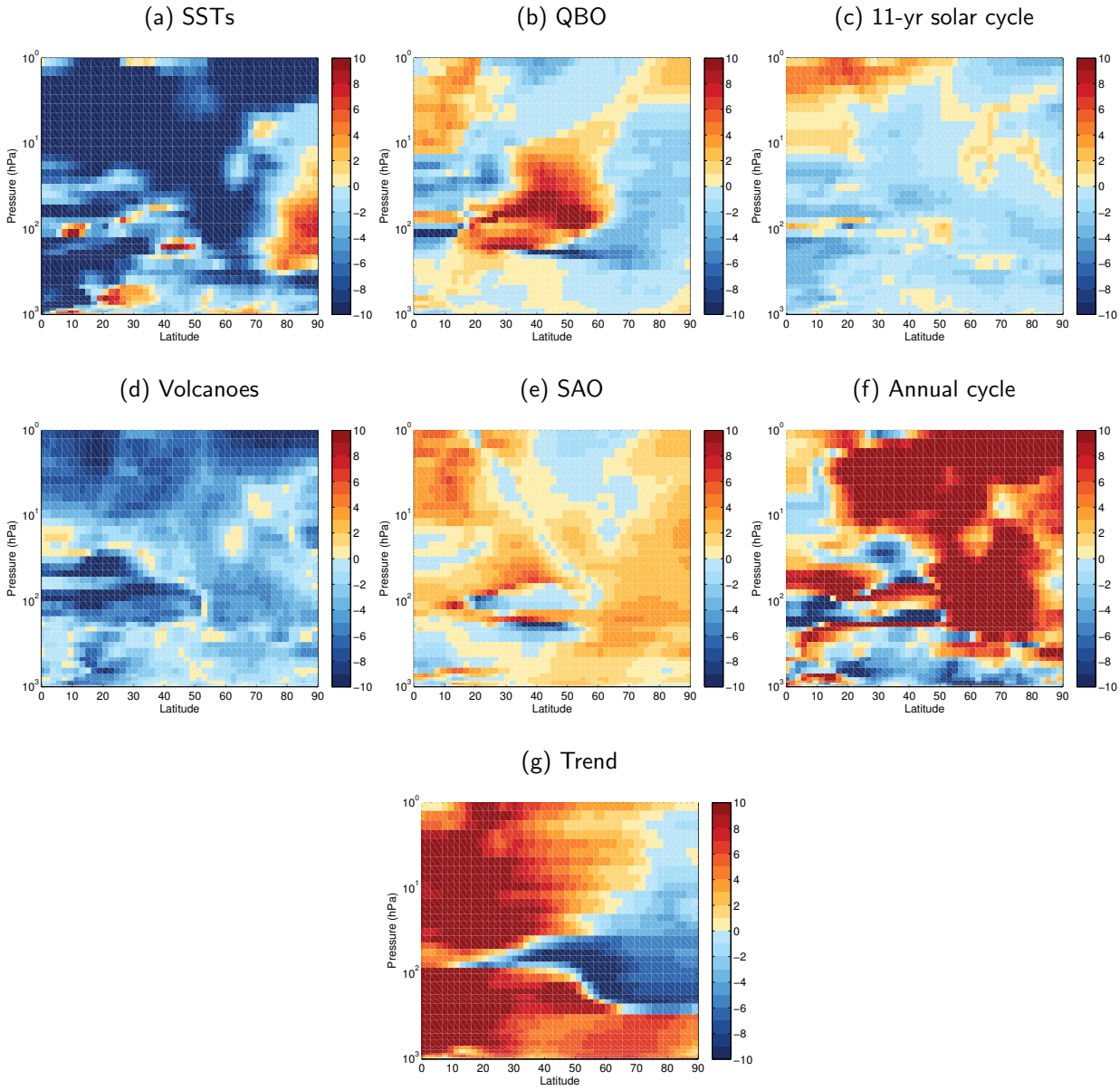

Figure 1.5: Change of impact (in %) of different natural (1st and 2nd row) and anthropogenic (3rd row) factors on annual NH zonal mean temperatures during 2050–2099 relative to 1955-1999. Data from CESM "GHG" simulation (see Chapter 2).

1.3 The need for climate models

When influencing the coupling between the stratosphere and the troposphere, the different natural and anthropogenic factors partly interact in a complex, non-linear way. This makes it complicated, if not impossible, to separate their contributions to, e.g., polar stratospheric temperatures if only one observational time series of these temperatures is available. Observations which have a spatial and temporal resolution that is high enough for this purpose (e.g., temporal resolution has to be higher than monthly means) are rare in general, but especially for the stratosphere these observational records are short and do not cover more than some decades as they are mainly obtained from satellite observations which were established in 1979. These shortcomings can be overcome in climate model simulations. The advantages of climate models are, e.g., the ability to perform long simulations from which statistically reliable results can be obtained or the ability to perform an ensemble of simulations with slightly altered initial conditions.

During the last decade, more and more international modeling groups became aware of the need to resolve the stratosphere and higher atmospheric layers in climate models to obtain realistic results for their tropospheric research questions. Outcomes of international projects like the Coupled Model Intercomparison Project 5 (CMIP5) [Taylor et al., 2009, 2012] begin to convince the research community of the significance of stratospheric processes for the troposphere. Charlton-Perez et al. [2013], e.g., showed that CMIP5 models with a comparably low upper boundary systematically underestimate stratospheric variability on daily to interannual time scales. Manzini et al. [2006] also provide evidence of the need to resolve the stratosphere in models in the context of narrowing uncertainties for future projections of sea level pressure changes. An underestimation was also found for stratospheric planetary wave activity in the so-called low-top models (model lid below 1hPa) in a recent study by Lee and Black [2015]. Several studies conclude that knowledge of stratospheric conditions could improve seasonal (tropospheric) forecasts substantially [e.g., Thompson et al., 2002; Sigmond et al., 2013; Butler et al., 2014].

The use of a climate model instead of observational time series allows to perform sensitivity experiments, where single processes or factors can be easily switched on or off. The comparison of different experiments with or without the phenomenon enables to estimate the importance of this specific phenomenon. This is not possible from observations, which are the sum of the interactions of all phenomena and processes. Therefore for this thesis a unique set of model experiments has been designed and analyzed.

1.3.1 A special problem: the QBO in climate models

One example for a phenomenon which is difficult to include in climate models is the QBO. Its representation in climate models is still a well-known shortcoming and one of the major challenges in simulating middle atmosphere processes [e.g., SPARC CCMVal, 2010]. During the last 15 years, a growing number of climate models has succeeded in simulating the QBO internally [Scaife et al.,

2000; Giorgetta et al., 2002; Shibata and Deushi, 2005; Kulyamin et al., 2009; Kawatani et al., 2010; Anstey et al., 2010; Xue et al., 2012; Kawatani and Hamilton, 2013; Richter et al., 2014; Rind et al., 2014]. However, the majority of climate models is still not able to generate a spontaneous QBO. Reasons for that are insufficient spatial or vertical resolution or problems in realistically simulating small-scale processes like tropical convection [Scaife et al., 2000; Giorgetta et al., 2002; Shibata and Deushi, 2005; Richter et al., 2014]. To overcome this deficiency, models without an internally-generated QBO employ a so-called "nudging" technique. A certain parameter in the model (in this case the equatorial zonal mean zonal wind) is forced towards an observed time series of this parameter. This can represent a strong intervention into the model dynamics because no feedback processes can occur then between the tropics (where the nudging is applied) and the extratropics. This has to be kept in mind when analyzing model simulations of such kind of climate model. This thesis addresses - besides the main question of the importance of different factors for stratosphere-troposphere coupling - the question of how the width of the QBO nudging influences stratospheric dynamics and chemistry (Chapter 3).

1.4 Scientific questions of this thesis

This thesis investigates the influence of different natural and anthropogenic factors such as the QBO, SSTs, GHGs and ODSs on the dynamical coupling between the stratosphere and the troposphere. The following questions are addressed in the coming chapters, which are all reprints of publications accepted in or submitted to scientific journals.

- **How do the different natural and anthropogenic factors influence extreme events in the NH stratosphere - major Stratospheric Sudden Warmings (SSWs) - which are a prominent example of stratosphere-troposphere coupling?** (Chapter 2)
- **How does the width of the QBO in a climate model influence the connection between the equatorial and the polar stratosphere, which is often referred to as the Holton-Tan mechanism?** (Chapter 3)
- **How does the stratospheric QBO influence tropospheric weather and climate?** (Chapter 4)

To answer these questions, different simulations have been performed and the model output has been analyzed from the Community Earth System Model (CESM), developed at the National Center for Atmospheric Research (NCAR), and from the Whole Atmosphere Community Climate Model (WACCM). CESM is a state-of-the-art coupled model system which includes an ocean, land, sea ice and atmosphere (in the model configuration used here: WACCM) component. WACCM is a fully interactive chemistry-climate model extending from the Earth's surface to ∼145 km. It is used both as the atmospheric component of CESM as well as a stand-alone atmosphere-only model

in this thesis. The set of model simulations performed and analyzed here is unique, considering that it consists of various long-term (up to 145 years) experiments performed with a complex model system which reaches up to the thermosphere and includes both an interactive ocean and interactive chemistry. Both CESM-WACCM and WACCM stand-alone have been evaluated before and have been found to exhibit a realistic middle atmosphere mean state and variability (Marsh et al. [2013] and Richter et al. [2008], respectively). Especially WACCM has been used independently in many studies of middle to upper atmosphere dynamics and chemistry [e.g., Garcia et al., 2007; Matthes et al., 2010; Garcia et al., 2011; Smith et al., 2011; Limpasuvan et al., 2012; Matthes et al., 2013]. Details of the model and the setup of the simulations can be found in the respective chapters of this thesis.

2 The influence of natural and anthropogenic factors on Major Stratospheric Sudden Warmings

Different natural and anthropogenic factors can have an influence on the NH polar stratosphere, as has been introduced in the previous chapter. Besides this general influence, these factors might also affect the "extreme events" in this region, which are major Stratospheric Sudden Warmings (SSWs). Major SSWs represent an important example for the coupling between the stratosphere and the troposphere. In this chapter, which is a reprint of an article of the same title published in *Journal of Geophysical Research - Atmospheres*, the impact of the QBO, SST variability and GHGs on different characteristics of major SSWs is investigated.

Citation: **Hansen, F., K. Matthes, C. Petrick, and W. Wang, 2014: The influence of natural and anthropogenic factors on major Stratospheric Sudden Warmings. J. Geophys. Res.-Atmos., 119, 8117–8136, doi:** $10.1002/2013JD021397$**.**

The authors' contributions to this publication are as follows:

- *F. Hansen performed one of the four model simulations, did all the analyses, produced all figures and wrote the manuscript.*
- *K. Matthes initiated the model experiments, contributed with ideas and discussions on the analysis and with comments on the manuscript.*
- *C. Petrick performed two of the four model simulations.*
- *W. Wang performed one of the four model simulations and contributed to the script to calculate daily values for the Eliassen-Palm flux and its divergence.*

AGU PUBLICATIONS

JGR

Journal of Geophysical Research: Atmospheres

RESEARCH ARTICLE

10.1002/2013JD021397

Key Points:
- The QBO reduces the frequency of major SSWs; SST variability increases it
- Anthropogenic GHGs and ODSs determine the prewarming phase of major SSWs
- Two-way ocean/atmosphere coupling is needed for the negative AO response after SSWs

Correspondence to:
F. Hansen,
fhansen@geomar.de

Citation:
Hansen, F., K. Matthes, C. Petrick, and W. Wang (2014), The influence of natural and anthropogenic factors on major stratospheric sudden warmings, *J. Geophys. Res. Atmos.*, *119*, 8117–8136, doi:10.1002/2013JD021397.

Received 19 DEC 2013
Accepted 18 JUN 2014
Accepted article online 24 JUN 2014
Published online 15 JUL 2014

The influence of natural and anthropogenic factors on major stratospheric sudden warmings

F. Hansen[1], K. Matthes[1], C. Petrick[2,3], and W. Wang[1,4]

[1]GEOMAR Helmholtz Centre for Ocean Research Kiel, Kiel, Germany, [2]Formerly at GEOMAR Helmholtz Centre for Ocean Research Kiel, Kiel, Germany, [3]Formerly at GFZ German Research Center for Geosciences, Potsdam, Germany, [4]Institute of Meteorology, Freie Universität Berlin, Berlin, Germany

Abstract Major stratospheric sudden warmings are prominent disturbances of the Northern Hemisphere polar winter stratosphere. Understanding the factors controlling major warmings is required, since the associated circulation changes can propagate down into the troposphere and affect the surface climate, suggesting enhanced prediction skill when these processes are accurately represented in models. In this study we investigate how different natural and anthropogenic factors, namely, the quasi-biennial oscillation (QBO), sea surface temperatures (SSTs), anthropogenic greenhouse gases, and ozone-depleting substances, influence the frequency, variability, and life cycle of major warmings. This is done using sensitivity experiments performed with the National Center for Atmospheric Research's Community Earth System Model (CESM). CESM is able to simulate the life cycle of major warmings realistically. The QBO strengthens the climatological stratospheric polar night jet (PNJ) and significantly reduces the frequency of major warmings through reduction of planetary wave propagation into the PNJ region. Variability in SSTs weakens the PNJ and significantly increases the major warming frequency due to enhanced wave forcing. Even extreme climate change conditions (RCP8.5 scenario) do not influence the total frequency but determine the prewarming phase of major warmings. The amplitude and duration of major warmings seem to be mainly determined by internal stratospheric variability. We also suggest that SST variability, two-way ocean/atmosphere coupling, and hence the memory of the ocean are needed to reproduce the observed tropospheric negative Northern Annular Mode pattern after major warmings.

1. Introduction

Stratospheric sudden warmings (SSWs) are prominent disturbances of the Northern Hemisphere (NH) winter stratospheric polar vortex and are also a clear manifestation of the dynamical coupling in the stratosphere-troposphere system. They were first discovered by *Scherhag* [1952] and are induced by the interaction of upward propagating planetary waves of tropospheric origin with the zonal mean flow [*Matsuno*, 1971]. By this interaction, the vortex is disrupted in its zonal symmetry and displaced from the pole or split into two vortices, leading to increased temperatures in the polar stratosphere. If additionally the wind at 60°N, 10 hPa reverses from westerly to easterly, the warming is called a major warming, according to the definition of the World Meteorological Organization (WMO; *Labitzke and Naujokat* [2000]). The signature of major sudden warmings can descend to the troposphere and thus even affect surface weather and climate [*Quiroz*, 1977; *Baldwin and Dunkerton*, 2001; *Thompson et al.*, 2002; *Mitchell et al.*, 2013]; therefore, the accurate simulation of SSWs and their downward propagating dynamical disturbances yield potential for improving the tropospheric weather prediction skill in climate models [*Baldwin and Dunkerton*, 2001; *Thompson et al.*, 2002; *Mitchell et al.*, 2013].

A major warming is observed about every 2 years [*Erlebach et al.*, 1996; *Labitzke and Naujokat*, 2000; *Charlton and Polvani*, 2007], though *Labitzke* [1977], *Labitzke and Naujokat* [2000], and *Schimanke et al.* [2011] pointed out (in observations and a model study, respectively) that SSW occurrence has large interannual to interdecadal variability. SSWs dominate the interannual variability of the NH polar winter stratosphere [*Labitzke and Naujokat*, 2000]. There are various natural and anthropogenic factors that influence both the mean state and the variability of the polar vortex, suggesting a possible impact of these forcings on SSWs. Natural factors include, e.g., the quasi-biennial oscillation (QBO) of equatorial stratospheric winds, variations in sea surface temperatures (SSTs) such as the El Niño Southern Oscillation (ENSO), the 11 year solar cycle, and volcanic eruptions. Anthropogenic factors involve changes in greenhouse gases

(GHGs) and ozone-depleting substances (ODSs). By affecting either the background winds, the generation and propagation of waves, or the wave-mean flow interaction, these factors impact the polar vortex and hence the frequency and characteristics of SSWs. These dynamical mechanisms are not yet well understood and will be investigated in this study for some of the above mentioned factors.

The influence of the QBO on the polar stratosphere was first examined by *Holton and Tan* [1980, 1982]. On average, the polar stratospheric vortex is colder and less disturbed in QBO west-phase winters, leading to a lower frequency of SSWs, while winters during QBO east phase tend to be warmer and more disturbed, and more SSWs are observed. The mechanism behind this is not fully understood yet; it is likely that both the position of the zero wind line (known as the Holton-Tan mechanism; *Holton and Tan* [1980, 1982]; *Watson and Gray* [2014]) and also the QBO-induced secondary meridional circulation [*Naoe and Shibata*, 2010; *Garfinkel et al.*, 2012] influence the propagation of planetary waves which are then responsible for the stronger or weaker disturbance of the polar vortex.

The influence of SST variations on the polar vortex largely happens within ENSO events. *Van Loon and Labitzke* [1987] found in observations that warm ENSO events (El Niños) seem to be associated with an anomalously weak and warm polar vortex and hence more SSWs. *Manzini et al.* [2006] confirmed in a model study the statistical significance of this relationship and also highlighted its nonlinear character, i.e., that cold ENSO events (La Niñas), on the other hand, do not have an equivalent influence significantly distinguishable from internal variability. This was also confirmed in model studies by, e.g., *Sassi et al.* [2004] and *Taguchi and Hartmann* [2006] and observational studies by *Camp and Tung* [2007] and *Mitchell et al.* [2011]. By analyzing general circulation model simulations, *Manzini et al.* [2006] and *Ayarzagüena et al.* [2013] suggested that the large-scale, extratropical ENSO teleconnection pattern in NH winter includes a deepening of the Aleutian low during El Niño events which enhances the forcing and vertical propagation of quasi-stationary planetary waves, resulting in a weaker stratospheric polar vortex. However, *Butler and Polvani* [2011] and *Garfinkel et al.* [2012] found that the SSW frequency is enhanced during both El Niño and La Niña years in reanalysis data and climate model simulations, despite the opposite-signed influence of the ENSO phases on the polar vortex. In general, two-way coupling between the atmosphere and the ocean in climate models has been shown to increase the low-frequency variability in both media [*Barsugli and Battisti*, 1998]. Recently, *Omrani et al.* [2014] suggested in a model study that decadal variability in North Atlantic SSTs might influence stratospheric background winds and SSWs.

Other natural factors that modify the polar vortex and hence may affect the frequency of SSWs directly or by interaction with other factors are the 11 year solar cycle [e.g., *Gray et al.*, 2010] and volcanic eruptions [e.g., *Robock*, 2000].

The influence of anthropogenic GHGs and ODSs on the polar vortex and SSWs is mainly addressed in model studies using 21st century GHG emission scenarios and comparing them to observations or model simulations of the 20th century. The results are, however, not concordant: while the majority of recent studies shows an increase in SSW frequency under increased GHG forcings [e.g., *Huebener et al.*, 2007; *Charlton-Perez et al.*, 2008; *Bell et al.*, 2009; *Schimanke et al.*, 2013; *Ayarzagüena et al.*, 2013], one general circulation model study shows a decrease [*Rind et al.*, 1998] and others no significant trend [*Butchart et al.*, 2000; *SPARC CCMVal*, 2010; *Mitchell et al.*, 2012]. Possible causes for changes in SSW frequency under increased GHG conditions are found to be changes in the stratospheric meridional overturning circulation, which itself occurs due to a combination of changes in wave flux from the troposphere into the stratosphere [*Ayarzagüena et al.*, 2013; *Schimanke et al.*, 2013], and changes in middle atmospheric zonal winds [*McLandress and Shepherd*, 2009; *Schimanke et al.*, 2013].

There are still a number of open questions about the influence of natural and anthropogenic factors on the polar vortex and the frequency of SSWs. Nonlinear interactions between the single forcing factors complicate the gain of insight, e.g., because QBO east years tend to coincide with El Niño years. Since observational records of the stratosphere are short and it is complicated if not impossible to separate the influence of the respective factors, we designed sensitivity simulations with a high-top stratosphere-resolving chemistry-climate model (CCM) to systematically switch on and off the single factors and analyze their respective roles. We use National Center for Atmospheric Research (NCAR)'s Community Earth System Model (CESM) version 1.0.2, a state-of-the-art coupled model system with the Whole Atmosphere Community Climate Model (WACCM) version 4 as its atmospheric component.

Our paper extends the study of *Richter et al.* [2011], who analyzed the influence of the QBO and ENSO on SSW frequency in a set of 30 year model simulations. They found no significant change in the number of SSWs when they removed the QBO or variable SSTs from their simulations but a significant drop in the frequency when both factors were removed at once. We now investigate longer simulations (two 56 year and two 145 year simulations) and additionally consider the influence of anthropogenic forcings. In this study, we investigate not only the frequency of major warmings but also their life cycle, starting from its preconditioning in the troposphere to the warming event itself and the downward coupling to the troposphere afterward.

Several studies investigated the preconditioning of major SSWs and found a geographically dependent connection between different types of SSWs and tropospheric blockings [e.g., *Quiroz*, 1986; *Taguchi*, 2008; *Martius et al.*, 2009; *Woollings et al.*, 2010; *Castanheira and Barriopedro*, 2010; *Nishii et al.*, 2011; *Bancala et al.*, 2012]. Blockings are quasi-stationary and persistent anticyclonic systems with a strong meridional component that interrupts the zonal flow. *Nishii et al.* [2011] found that tropospheric blockings over the Euro-Atlantic sector tend to enhance upward planetary wave propagation and can lead to major warmings, while blockings over the western Pacific region tend to suppress planetary wave propagation and hence the development of SSWs. *Martius et al.* [2009] and *Castanheira and Barriopedro* [2010] distinguish between the influence of blockings on different types of SSW events: the vortex displacement events—where the vortex is shifted off the pole—which are often preceded by blockings in the Euro-Atlantic basin, and the vortex-splitting events—where the vortex breaks up into two subvortices of comparable size—which are more favorable after blockings in the Pacific. *Bancala et al.* [2012], on the other hand, distinguish between "wave number-1" and "wave number-2" events based on the dominant wave pattern responsible for initiating the warming. They found that blockings in the Euro-Atlantic mostly lead to the development of wave number-1 events, and blockings in the Pacific mostly precede wave number-2 SSWs.

The warming event itself can be characterized by several benchmarks like its type (wave number-1 or wave number-2 [*Yoden et al.*, 1999], "split" or "displacement"), its strength, and its duration [*de la Torre et al.*, 2012]. In this study, we investigate if and how natural and anthropogenic factors influence these characteristics of major warmings.

We also analyze possible differences in the surface response following a major warming. When the geopotential height anomaly propagates down to the troposphere after major warmings [*Quiroz*, 1977; *Kodera and Chiba*, 1995; *Baldwin and Dunkerton*, 2001; *Thompson et al.*, 2002; *Mitchell et al.*, 2013], the resulting surface pattern strongly projects onto the negative phase of the North Atlantic Oscillation (NAO) or the Arctic Oscillation (AO) [*Baldwin and Dunkerton*, 2001; *Charlton and Polvani*, 2007]. *Mitchell et al.* [2013] showed by analyzing reanalysis data that vortex split events lead to positive (negative) temperature anomalies over North America (Europe) while the surface response to vortex displacement events is much weaker. *Charlton and Polvani* [2007] found an additional surface anomaly to occur over the Pacific after SSW events which is reminiscent of the Pacific-North American pattern (PNA) [*Wallace and Gutzler*, 1981].

This paper is structured as follows: section 2 describes the CESM model and the CESM sensitivity experiments. Section 3 explains the major warming identification algorithm and the blocking index used in our analysis. In section 4, the SSW frequency as well as the climatological background state of the NH polar winter stratosphere are analyzed for the different sensitivity experiments. Section 5 then examines differences in the evolution of SSW events (preconditioning, mature and declining phase) for all simulations. Finally, the results are summarized and discussed in section 6.

2. Model Description, Experiments, and Reanalysis Data

The forcing experiments analyzed in this study were performed with the Community Earth System Model (CESM), developed at the National Center for Atmospheric Research (NCAR). CESM is a state-of-the-art coupled model system which is based upon the Community Climate System Model (CCSM4) [*Gent et al.*, 2011]. It includes an interactive ocean Parallel Ocean Program (POP), land Community Land Model (CLM), sea ice Community Ice CodE (CICE), and atmosphere (optionally WACCM or Community Atmosphere Model (CAM)) component [*Marsh et al.*, 2013]. For the simulations analyzed here, CESM was used in its version 1.0.2 with the Whole Atmosphere Community Climate Model (WACCM) version 4 as the atmospheric component, designated CESM1(WACCM) in *Marsh et al.* [2013]. WACCM is a fully interactive chemistry-climate model which has been used independently in many studies of middle to upper atmosphere dynamics and

Table 1. Summary of CESM Experiments

Name	Period	GHGs and ODSs	SSTs/Sea Ice	QBO
GHG	1955–2099 (145 years)	observations and RCP8.5 scenario	interactively	nudged
NATURAL	1955–2099 (145 years)	fixed at 1960s level	interactively	nudged
Fixed SSTs	1955–2010 (56 years)	fixed at 1960s level	climatological annual cycle from NATURAL	nudged
NOQBO	1955–2010 (56 years)	fixed at 1960s level	interactively	no

chemistry [e.g., *Taguchi and Hartmann*, 2006; *Matthes et al.*, 2010; *Garcia et al.*, 2011; *Smith et al.*, 2011; *Limpasuvan et al.*, 2012; *Matthes et al.*, 2013]. It extends from the Earth's surface to ~140 km altitude [*Garcia et al.*, 2007; *Richter et al.*, 2010] and is used here on a horizontal grid of $1.9 \times 2.5°$ (latitude × longitude) and on 66 vertical levels. Chemistry is calculated interactively in the chemistry module based on version 3 of the Model for OZone And Related chemical Tracers (MOZART) [*Kinnison et al.*, 2007]. The interactive ocean and sea ice components are run on a $1° \times 1°$ triangular horizontal grid and are described in *Holland et al.* [2012] and *Danabasoglu et al.* [2012]. Note that the amplitude of ENSO is overestimated compared to observations [*Marsh et al.*, 2013].

To study the influence of natural and anthropogenic factors on SSWs, four different simulations were performed where these factors were systematically switched on and off to allow the separation of the individual contributions. A summary of the experiments is given in Table 1. Due to the complexity of the model system and the fact that chemistry is calculated interactively in WACCM, the computational effort of CESM is extremely high so that only one run per experiment could be performed.

All factors considered in this study, namely, anthropogenic forcings, the QBO, and SSTs (including sea ice concentrations), were used for the 145 year CESM "GHG" experiment. GHGs and ODSs follow observations from 1955 to 2005, and the Coupled Model Intercomparison Project 5 (CMIP5) Representative Concentration Pathways (RCP) Scenario 8.5 thereafter until 2099 [*Meinshausen et al.*, 2011; *Taylor et al.*, 2012]. The QBO is nudged between 22°S and N as described in *Matthes et al.* [2010] and *Hansen et al.* [2013] and extended into the future by projecting Fourier coefficients of the oscillation. The solar cycle is prescribed as spectrally resolved daily variations following *Lean et al.* [2005]; for the 21st century, the last four solar cycles before 2005 are repeated. Of all the experiments which were performed, the GHG simulation is the one whose forcings are closest to observations in the twentieth century. This simulation is similar to the CESM1 (WACCM) RCP8.5 simulation submitted to CMIP5 by the NCAR CESM group [*Hurrell et al.*, 2013].

In the "NATURAL" experiment only natural and no anthropogenic forcings are considered. This is done by keeping GHGs and ODSs fixed at the 1960s level over the whole simulation period (1955–2099; for CO_2, e.g., this means an annual mean value of 316 ppmv). All other settings are equivalent to the GHG experiment.

The "Fixed SSTs" simulation uses the same forcings as the NATURAL experiment except that the underlying SSTs and sea ice for the 56 simulated years (1955–2010) were computed as the climatological monthly varying fields from the NATURAL experiment. As this simulation does not contain interannual variations in SSTs, the interannual memory of the ocean is switched off and it does not include oceanic phenomena such as ENSO or extratropical interdecadal and intradecadal Atlantic and Pacific variability. Of the factors investigated in this study, the only interannually varying forcing here is the QBO. Consequently, this experiment can be used to investigate the pure QBO effect without any influence of oceanic variability signals.

The 56 year "NOQBO" experiment (spanning the period 1955–2010 as in Fixed SSTs) uses again the same settings as the NATURAL simulation but without the QBO nudging. This leads to relatively constant weak easterlies of about −10 m/s in the equatorial stratosphere instead of the quasi-biennial oscillation between westerly and easterly winds in this region. Thus, the SSTs and sea ice are the only interannually varying forcing in this experiment which makes it well suited for analyzing pure SST and sea ice induced signals, especially those associated with ENSO.

This set of sensitivity experiments will be used in the following to systematically study the influence of natural and anthropogenic factors on SSWs. We compare the results of the sensitivity simulations to the European Centre for Medium-Range Weather Forecasts Re-Analyis (ERA) products ERA40 [*Uppala et al.*, 2004] and ERA-Interim [*Simmons et al.*, 2006], which have been combined into one data set as described in *Blume et al.* [2012], referred to as "ERA" hereafter. This combined data set resolves the stratosphere up to 1 hPa and spans the period from 1958 to 2012.

3. Methods

3.1. Identification of Stratospheric Sudden Warmings

According to the WMO definition, a major SSW occurs if the zonal mean temperature difference between 60°N and 90°N increases significantly in a couple of days and the zonal mean zonal wind at 60°, 10 hPa reverses from westerly to easterly [*Andrews et al.*, 1987; *Labitzke and Naujokat*, 2000]. Many studies which deal with different questions on SSWs consider the wind criterion only and neglect the temperature difference between 60°N and 90°N [e.g., *Charlton and Polvani*, 2007; *Garfinkel et al.*, 2012; *Schimanke et al.*, 2013]. Another approach is to use the first empirical orthogonal function (EOF) and its respective principal component (PC), e.g., of geopotential height anomalies (which then defines the Northern Annular Mode (NAM) [*Baldwin and Dunkerton*, 2001]) or of zonal mean zonal wind anomalies at 50 hPa (as done by *Limpasuvan et al.* [2004]) to define disturbed NH winter states.

Black and McDaniel [2004] analyzed potential vorticity in the context of stratospheric NAM events, and recently *Mitchell et al.* [2013] used the distribution of potential vorticity for the definition of weak vortex events.

We follow the original WMO definition of SSWs: a major warming is identified if between November and April (1) the zonal mean zonal wind at 60°N, 10 hPa is easterly and (2) the temperature difference between 60 and 90°N at 10 hPa is positive for at least 5 days within the period from 10 days before to 4 days after the day of the wind reversal, which is referred to hereafter as the central date of the warming (following WMO; *Labitzke and Naujokat* [2000]). No second warming can be defined within a period of 20 days after a major warming event, and all fluctuations around zero wind speed during this period are then counted as one event.

In this study, we will neglect minor warmings, which are disturbed states of the NH winter stratosphere with an anomalous increase in temperature but without a reversal of the circulation [*Labitzke and Naujokat*, 2000], and final warmings, which indicate the return to the summer circulation. We will focus only on major warmings, as they are the strongest manifestation of the dynamical coupling between the stratosphere and the troposphere.

Applying our identification algorithm to ERA leads to a total number of 26 major warmings in the period 1958–2002, i.e., three fewer than in *Charlton and Polvani* [2007] which is due to the additionally applied temperature criterion, and 31 major warmings in the period 1958–2012.

We used the method described in *Charlton et al.* [2007] to compute the statistical significance of the difference in major warming frequency between two different data sets with a two-sided *t* test. *Charlton et al.* [2007] argue that one can assume every winter to be an independent observation of the major warming frequency per winter. Then, an expected value and a standard error of the frequency can be computed, and two data sets can be compared with a two-sided *t* test.

3.2. Blockings

Several studies found a relation between the occurrence of SSWs and tropospheric blockings in the Euro-Atlantic and Pacific region [e.g., *Quiroz*, 1986; *Taguchi*, 2008; *Martius et al.*, 2009; *Woollings et al.*, 2010; *Castanheira and Barriopedro*, 2010; *Bancala et al.*, 2012]. We will test in this study whether this relationship holds in our model and how it depends on the different factors. We compute a daily blocking index following *Tibaldi and Molteni* [1990] which depends on the geopotential height fields at 500 hPa and compares midlatitudes (60°N) with higher (80°N) and lower (40°N) latitudes. According to this definition, a longitude is defined as being blocked if the geopotential height gradient between midlatitudes and lower latitudes is positive and the gradient between high latitudes and midlatitudes falls below −10 m per degree. This has to be fulfilled over at least three adjacent longitudes (i.e., 5° for our longitudinal resolution of 2.5°) and for at least 5 days.

4. Stratospheric Sudden Warming Frequency

In this section the seasonal distribution of major warmings over NH winter months is presented for the different experiments. Afterward, we address differences in the major warming distributions by examining differences in the climatological background winds, waves, and wave-mean flow interaction.

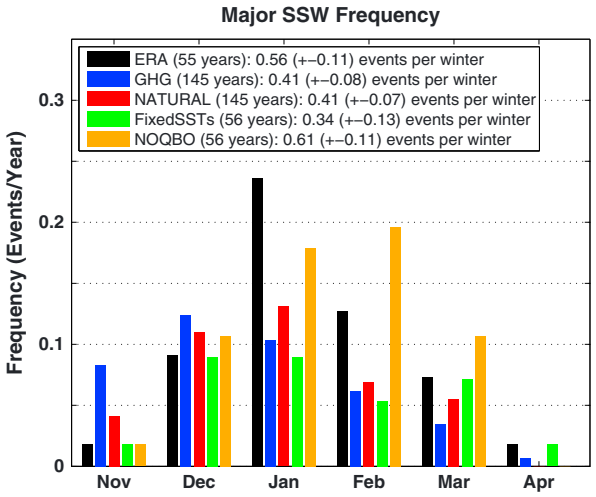

Figure 1. Frequency of major warmings in NH winter months in ERA and CESM sensitivity simulations. Numbers in brackets indicate the standard error of the SSW total winter frequency.

4.1. SSW Seasonal Distribution

Figure 1 shows the seasonal distribution (November through April) of major warmings for ERA and our four CESM sensitivity experiments in relative frequency of warming events per month and year. The observed SSW distribution (ERA, black bars) is well known: the frequency of major warmings increases steadily from November until its maximum of 0.23 events per year in January and decreases steadily afterward until the end of the winter. The average frequency of major warmings for the period 1958–2012 obtained for ERA with our selection algorithm is 0.56 events per year.

For the GHG experiment, we analyzed the 20th and 21st centuries separately (not shown) to detect potential differences in major warming frequency that might occur due to the strong GHG forcing (the RCP8.5 scenario). We neither found an increase in the number of major warmings until the end of the 21st century as was reported, e.g., in *Huebener et al.* [2007], *Charlton-Perez et al.* [2008], *Bell et al.* [2009], *Schimanke et al.* [2013], and *Ayarzagüena et al.* [2013], nor a decrease as found by *Rind et al.* [1998], so our results are in line with *Butchart et al.* [2000]; *SPARC CCMVal* [2010] and *Mitchell et al.* [2012]. Therefore, we will not distinguish between the two centuries in the following analysis but analyze the entire period from 1955 to 2099.

No large differences in SSW frequency are seen between ERA and the CESM sensitivity experiments in early winter (November and December), with the exception of the GHG experiment (blue bars) showing a higher major warming frequency in November. During January and February, all simulations show a lower major warming frequency than ERA, except the NOQBO experiment (orange bars), which shows a higher SSW frequency than ERA in February and a notably higher frequency than the other three runs in both months. This endures until March, although the differences become smaller.

Over the whole winter season, we find the highest SSW frequency in the NOQBO experiment, where 0.61 events per winter occur during the simulation period (1955–2010). The fewest SSWs occur in the Fixed SSTs run (green bars; 0.34 events per year between 1955 and 2010) where the seasonal distribution is very flat. The applied *t* test reveals that the differences between the major warming frequencies in NOQBO and Fixed SSTs are statistically significant at the 95% confidence interval and between the major warming frequencies in NOQBO and both GHG and NATURAL at the 90% confidence interval. That means that in our simulations variable SSTs and the QBO influence the number of SSWs significantly, while anthropogenic GHGs and ODSs do not have a measurable effect. A summary of the number and frequency of major warmings in ERA and the CESM sensitivity experiments can be found in the second and third columns in Table 2.

Table 2. Summary of SSW Characteristics in ERA and CESM Forcing Experiments[a]

Name	SSWs	SSW Frequency	Blocking ATL/PAC/Both	Prewarming W1/W2/W3	Duration (Days) Mean (Max/Min)	Amplitude (°C) Mean (Max/Min)	Displace/Split
ERA	31 (55 years)	0.56	11 / 3 / 11	24 / 7 / 0	8.0 (30 / 1)	13.6 (28.4 / −2.1)	18 / 13
GHG	60 (145 years)	0.41	17 / 4 / 3	57 / 3 / 0	6.1 (27 / 1)	13.8 (28.2 / 3.3)	55 / 5
NATURAL	60 (145 years)	0.41	13 / 6 / 5	57 / 1 / 2	6.8 (26 / 1)	13.8 (24.5 / −2.4)	56 / 4
Fixed SSTs	19 (56 years)	0.34	5 / 3 / 3	17 / 2 / 0	6.5 (25 / 1)	14.6 (23.1 / 7.8)	15 / 4
NOQBO	35 (56 years)	0.61	6 / 4 / 4	35 / 0 / 0	6.9 (22 / 1)	14.2 (22.7 / 1.8)	30 / 5

[a]In the fourth column, the three numbers indicate how many of the total number of SSWs (see first column) are preceded by a blocking in either the Atlantic or the Pacific or in both of the regions. The fifth column divides the total number of SSWs in wave numbers 1, 2, and 3 SSWs, and the eighth column in displace and split SSWs. See text for further details.

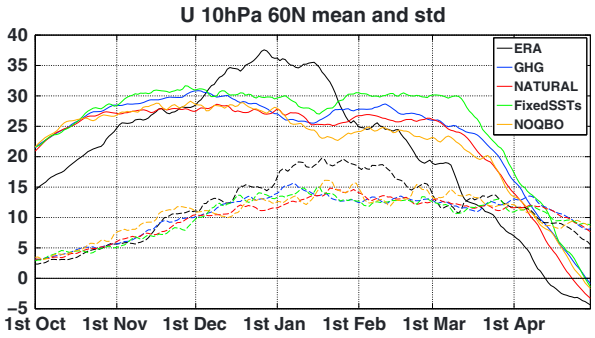

Figure 2. Development of the long-term mean (solid lines) and interannual standard deviation (dashed lines) of daily zonal mean zonal wind at 60°N, 10 hPa for ERA and CESM sensitivity simulations.

Our result that removing one factor, the QBO or variable SSTs, significantly changes (increases or decreases, respectively) the SSW frequency is different from the results of *Richter et al.* [2011] who only found a significant decrease (and a significant impact on the climatological background state) when both QBO and SST variability were removed. However, our simulations are almost twice as long and therefore provide better statistics for the detection of variability beyond the internal variability of the polar vortex.

In our simulation, we find clusters of major SSWs throughout the different simulations which are similar to observations (not shown). In GHG, NATURAL, and Fixed SSTs, there are two to three periods of about 10 years without any major SSWs, and in all simulations there is at least one decade with eight or nine major SSWs. However, the time series are too short for a detailed analysis of low-frequency fluctuations of major SSW occurrence.

4.2. Climatological NH Winter Conditions

SSWs are prominent examples of wave-mean flow interaction. Therefore, the differences in the major warming frequency between the different sensitivity experiments may arise from either (a) differences in the climatological stratospheric polar night jet (PNJ) (which is influenced by the natural and anthropogenic factors), (b) differences in planetary wave generation and/or propagation, (c) differences in the interaction between these waves with the mean flow, or from a combination of all. This will be investigated in the following section.

4.2.1. PNJ Strength and Variability

Shown in Figure 2 is the development of the daily zonal mean zonal wind at 60°N, 10 hPa, showing the average (solid lines) and the interannual standard deviation (dashed lines) over all winters for ERA and the CESM sensitivity experiments. The PNJ strength and evolution differ remarkably between ERA and the CESM simulations: while in ERA the wind increases until the end of December to a maximum of about 37 m/s, it stays almost constantly around 30 m/s from November on in CESM.

The zonal mean zonal wind develops similarly in the CESM experiments until the middle of January. Then two "extreme" cases develop: the highest PNJ wind speeds are found in the Fixed SSTs experiment and the lowest wind speeds in the NOQBO experiment, with differences of up to about 6–8 m/s in February and March. These two experiments also have statistically significant differences between the major warming frequency (see previous section), which are most prominent in January through March and therefore consistent with the findings here. The GHG and NATURAL experiments show PNJ strengths that lie between the two extreme cases.

Our knowledge about the dynamics between the equatorial QBO and the polar stratosphere implies a comparably weaker, and hence more easily disturbed, vortex in the NOQBO simulation, because the equatorial stratospheric winds in this experiment resemble a permanent easterly phase of the QBO. The effect of removing the QBO westerly phase is strongest from the end of December until the middle of March, which is consistent with the influence on major warming frequency which is also strongest in these months.

In the Fixed SSTs run, in contrast, the vortex is stronger and therefore less easily disturbed, probably because this simulation lacks El Niño events, which have been shown to significantly weaken the stratospheric polar vortex due to enhanced tropospheric wave forcing [*Van Loon and Labitzke*, 1987].

In our GHG simulation, a weakening of the stratospheric PNJ occurs poleward and upward of 60°N, 10 hPa, until the end of the 21st century due to increasing anthropogenic GHGs, together with a strengthening

(and shift) of the tropospheric subtropical jet (not shown), which is a robust outcome of tropospheric warming and stratospheric cooling under increased GHGs [see, e.g., *Shepherd and Mclandress*, 2011]. The region around 60°N, 10 hPa, which is shown in Figure 2 and where the wind criterion for the major warming definition is applied, lies exactly in the transition between these two opposed signals, so that no trend is seen here. Therefore, it is consistent to see no change in SSW frequency due to increasing anthropogenic GHGs in our study.

From the middle of April on, the PNJ strength again evolves very similarly in the CESM experiments, though a remarkably large difference of about half a month exists in the vortex breakup day, i.e., the return to summer circulation, between ERA (13 April) and CESM (23 to 28 April).

The interannual variability, shown as interannual standard deviation in dashed lines in Figure 2, is higher in ERA than in the CESM simulations throughout January and February. This is consistent with the finding of a higher major warming frequency in ERA, especially in January, but the differences in standard deviation between ERA and CESM become smaller in PNJ regions closer to the pole. However, no remarkable differences are seen between the simulations.

4.2.2. Wave Generation

Besides an impact on the PNJ strength and variability, the different factors might have an impact on the generation of waves in the troposphere, which could then lead to differences in the propagation of these waves into the stratosphere and the PNJ region and hence have an effect on SSWs. To analyze a possible influence on wave generation, we investigate the amplitudes of the geopotential height (GPH) waves in the troposphere and distinguish between planetary (wave numbers 1–3) and smaller-scale (wave numbers >3) waves. Figure 3 shows the amplitude of these waves for the NATURAL simulation (first row) averaged over December and January, i.e., up to 1 month before the largest differences between the CESM sensitivity simulations in major warming frequency occur (see Figure 1). The second to fourth rows in Figure 3 show differences in wave amplitudes between the GHG, the Fixed SSTs, and the NOQBO simulation with respect to the NATURAL simulation.

The amplitudes of planetary waves (left column) are significantly reduced in the Fixed SSTs experiment poleward of around 40°N throughout the middle to upper troposphere and lower stratosphere. This is according to our expectations, since planetary waves are, e.g., generated due to SST variabilities which are reduced in this experiment. The NOQBO simulation shows a similar response as the Fixed SSTs run in midlatitudes, though the negative signal is less statistically significant. Increasing GHGs lead to an upward shift of the wave amplitude maximum with a significant reduction of planetary wave amplitudes in the troposphere but a significant increase in the upper troposphere and lower stratosphere.

The strongest influence on smaller-scale waves (right column in Figure 3) is seen in the GHG experiment, where a significant amplitude increase centered around 50°N, 200 hPa occurs. The responses in both the Fixed SSTs and the NOQBO experiments are smaller compared to the GHG simulation and confined to the middle troposphere.

In summary, the effects of fixing the SSTs and switching off the QBO on wave generation are similar. Differences between both experiments which occur in the stratosphere might therefore be dominated by differences in the background winds and therefore wave propagation and wave-mean flow interactions. This will be further investigated in the following section.

4.2.3. Wave Propagation and Wave-Mean Flow Interaction

To analyze the strength and propagation direction of planetary waves, we use the Eliassen-Palm (EP) flux vector which is described in the Transformed Eulerian Mean (TEM) framework [*Andrews et al.*, 1987]. The divergence of the EP flux vector describes the interaction of resolved waves with the mean flow: in a region of EP flux divergence (convergence), the mean flow is accelerated to the east (west), e.g., prevailing westerly winds are accelerated (decelerated).

We compare the PNJ strength (represented by the zonal mean zonal wind), the EP flux vector, and its divergence averaged over January-February (JF), as the influence of the different factors on SSW frequency was found to be largest in these months. Figure 4a shows these three parameters for the NATURAL simulation. To highlight differences due to the different factors, Figures 4b–4d show these parameters for the GHG, the Fixed SSTs, and the NOQBO simulations as differences with respect to the NATURAL experiment. In JF, upward propagation of planetary waves from the troposphere into the stratospheric PNJ region occurs

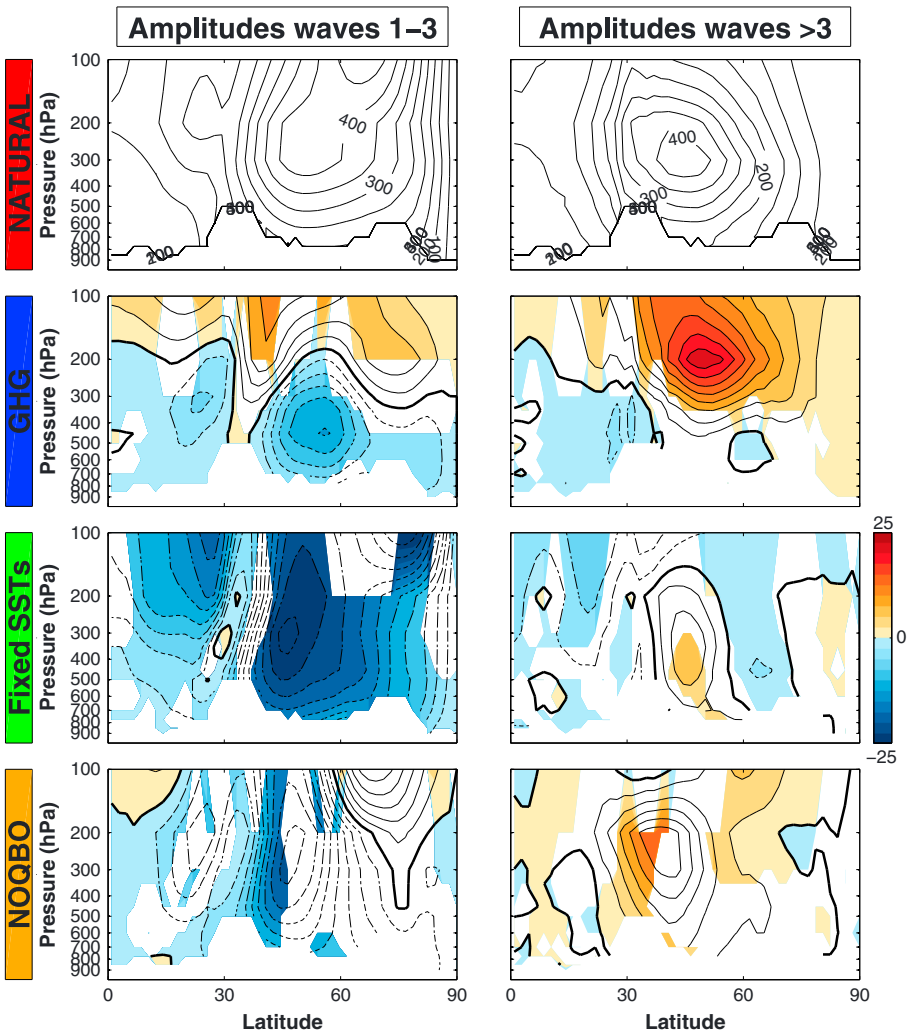

Figure 3. (first row) GPH wave amplitudes (contour interval: 50 m) in the NATURAL simulation; (left) planetary-scale waves (wave numbers 1–3), (right) smaller-scale waves (wave numbers >3). (second to fourth rows) Differences of planetary and smaller-scale wave amplitudes (contour interval: 2.5 m) between (second row) the GHG, (third row) the Fixed SSTs, (fourth row) the NOQBO simulation, and the NATURAL simulation, respectively, for the mean over December and January; shading indicates 95% statistical significance.

poleward of 50°N (Figure 4a). A large EP flux convergence region around 300 hPa poleward of 40°N indicates a deceleration of prevailing westerlies by wave-mean flow interactions.

As seen before in Figure 2, the PNJ strength (indicated by black contours in Figure 4) only shows very small differences between the GHG and the NATURAL experiments (Figure 4b), while larger differences are seen throughout the vortex region for the Fixed SSTs and NOQBO experiments (black contours in Figures 4c and 4d, respectively). In addition to the stronger PNJ, a downward and equatorward anomaly of the EP flux vector occurs between 40 and 60°N along the tropopause in the Fixed SSTs run, together with a downward anomaly in the lower to middle stratosphere northward of 70°N and a divergence anomaly in the lower PNJ region. Together with the significantly reduced planetary wave generation seen before (Figure 3), this suggests a weaker planetary wave propagation into the region of the stratospheric polar vortex and weaker deceleration of the westerlies in the lower polar stratosphere. This creates conditions which allow a stable, strong, and cold polar vortex and hence, as found before, a relatively lower number of major warmings when SSTs are kept fixed.

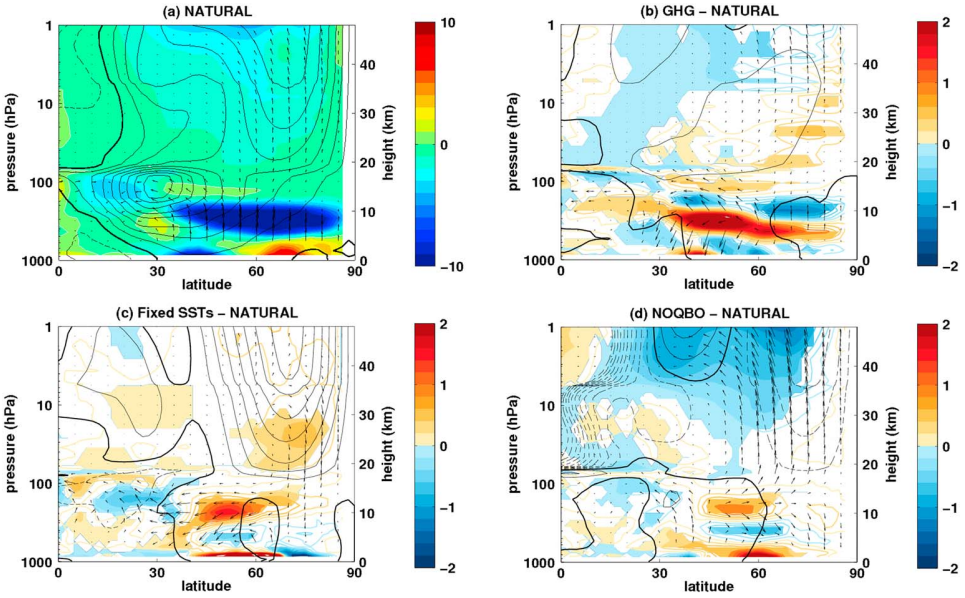

Figure 4. (a) January-February climatological zonal mean zonal wind (contours; contour interval 5 m/s, dashed lines indicate easterly winds, bold black line is the zero wind line), EP flux vector (arrows; scaled with the square root of pressure), and its divergence (colors; in $ms^{-1}d^{-1}$, positive values indicate divergence, white line is the zero line) for the NATURAL simulation. Differences of the zonal mean zonal wind (black contours; contour interval 1 m/s, dashed lines indicate easterly winds, bold line is the zero wind line), EP flux vector (arrows; scaled with the square root of pressure), and its divergence (colored contours and color shading; in $ms^{-1}d^{-1}$, shading indicates 95% statistical significance) between (b) the GHG and the NATURAL simulation, (c) the Fixed SSTs and the NATURAL simulation, and (d) the NOQBO simulation and the NATURAL simulation for January-February.

In contrast, in addition to the weakened PNJ in the NOQBO compared to the NATURAL experiment, the poleward and upward propagation of planetary waves into the polar vortex region is enhanced northward of 50°N above 200 hPa throughout the stratosphere. Together with enhanced convergence (and therefore PNJ deceleration) on the equatorward flank of the polar vortex, all this results in a weak, more disturbed and warmer vortex and is therefore consistent with the previous finding of an increased major warming frequency in this simulation.

The GHG experiment shows the largest changes of all simulations in EP flux divergence in the mid-latitude to high-latitude troposphere. These changes might result from the statistically significant changes in smaller-scale wave amplitudes in these regions, which are considerably smaller in the other experiments (Figure 3).

In summary, the differences in SSW frequency can be explained by differences in PNJ strength, resulting mainly from differences in wave propagation and wave-mean flow interaction and less from differences in wave generation: fewest SSWs occur without SST variability, where we find the strongest PNJ and reduced wave (generation and) propagation into the vortex region, and most SSWs occur without QBO nudging, where the PNJ is weakest of all experiments and where wave propagation into the PNJ region is enhanced. The interannual variability in PNJ strength is not changed significantly by the respective factors.

5. Major Warming Life Cycles

In the previous section we have compared the occurrence frequency of SSWs for different forcing factors and saw that removing SST and QBO variability has the largest effect on the number of SSWs, because it has the strongest influence on the polar stratospheric basic state due to changes in planetary wave propagation and in the mean flow. Here we will focus on the warming event itself to examine whether and how the different factors affect the life cycle of SSWs. We will start with the preconditioning phase, then investigate the phase around the central date, and finally study the coupling to the troposphere afterward.

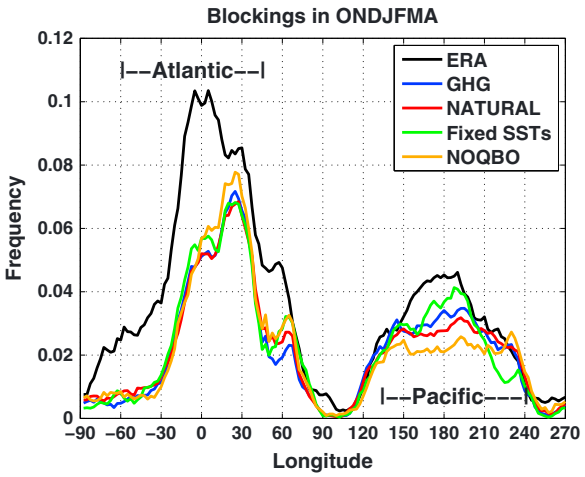

Figure 5. Frequency of days with tropospheric blocking between October and April at each longitude, for ERA and CESM sensitivity simulations. See text for details.

5.1. Preconditioning

Figure 5 shows the frequency of days with a tropospheric blocking in the NH extended winter season (October through April) over longitude, comparing ERA and the four CESM sensitivity experiments. Two frequency maxima can be detected in all data sets: one in the Euro-Atlantic (60°W–45°E) and a second one in the Pacific (135°E–120°W). Both maxima are remarkably reduced in CESM by about 20%, and the maximum in the Atlantic is shifted eastward by about 30°. An underestimation of blockings in climate models is a common model bias and well documented, e.g., in *Scaife et al.* [2010] and *Anstey et al.* [2013]. For CESM, the reduced frequency of blocking occurrence seen over the whole extended winter season has been shown in *Marsh et al.* [2013]. Blocking is reduced in all months but particularly in December and January (not shown) which is congruent with the reduced SSW frequency in these months (Figure 1). For the Pacific, the blocking frequency is too low for all months.

In GHG, NATURAL, and NOQBO, 40% of all SSWs are preceded by a blocking in at least one of the two regions, which is mainly the Euro-Atlantic area (see Table 2, fourth column). Comparing all CESM experiments, most blockings in the context of SSWs occur in the Fixed SSTs experiment where in 58% of all cases SSWs are preceded by at least one blocking and 16% by a blocking in both the Atlantic and Pacific regions. However, this is still less than in ERA, where around 80% of all SSWs are preceded by at least one blocking. The occurrence thereby refers to the period of up to 10 days prior to the central date. If we consider a period of 20 days before the major warming, around 55% (78%) of all events are preceded by at least one blocking in GHG, NATURAL, and NOQBO (Fixed SSTs). Because the number of major warmings preceded or not preceded by blocking is about the same, we cannot detect a general statistical relationship between the occurrence of blockings and SSWs.

Bancala et al. [2012] showed, for observational and model data, that blockings in the Euro-Atlantic are related to wave number-1 major warmings and blockings in the Pacific to wave number-2 major warmings. To investigate that for our CESM sensitivity experiments, we classified all major warmings as wave number-1 (W1), 2 (W2), or 3 (W3) events. This is done by comparing the amplitudes of geopotential height waves 1, 2, and 3 at 60°N at 10 and 50 hPa as well as the waves 1 and 2 components of the heatflux at 60°N, 100 hPa, computed as described by *Pawson and Kubitz* [1996], during the phase of strongest intensification. While in ERA about 25% of all major warmings are W2 events (and the remaining 75% are W1 events), we find only very few W2 events in our CESM experiments: three (of 60 events) in GHG, one in NATURAL, and two in the Fixed SSTs simulation (Table 2, fifth column). This may be related to the reduced frequency of tropospheric blockings discussed above, since especially blockings in the Pacific have been mentioned to be able to induce W2 events [*Martius et al.*, 2009; *Castanheira and Barriopedro*, 2010; *Bancala et al.*, 2012]. In our simulations, three of the six W2 events are preceded by a blocking in at least one of the two regions, Euro-Atlantic or Pacific. Interestingly, two W3 events occur in the NATURAL experiment which, at least to our knowledge, has not been reported before. These events are very weak in terms of easterly winds and temperature anomaly at the central date. However, these W3 events could also be a model artifact and need further investigation.

To further investigate the planetary wave behavior prior to the central date, we computed composites of daily anomalies of heat flux wave components 1 and 2 at 60°N, 100 hPa, over all SSWs following *Pawson and Kubitz* [1996], as well as daily anomalies of GPH wave 1 and 2 amplitudes at 60°N, 10 hPa. This is shown in Figure 6 for the period of 40 days prior to the SSW to 40 days after. For ERA, we see an increase in both the

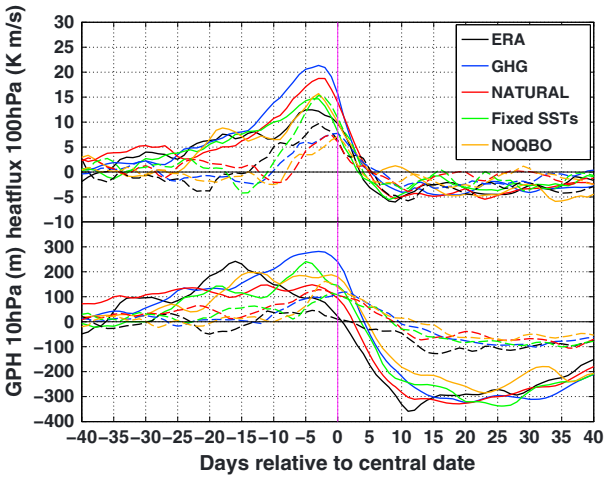

Figure 6. Composite of (top) heatflux anomalies at 60°N, 100 hPa (in K m/s) and (bottom) GPH wave anomalies at 60°N, 10 hPa (in m), wave 1 (solid lines) and wave 2 component (dashed lines) during major SSWs, for ERA and CESM sensitivity simulations.

heatflux wave 1 and wave 2 components before the major warming, with a maximum around 5 to 3 days before the central date. The GPH wave 1 at 10 hPa shows a maximum around 17 days before the central date. The figure reveals some similarities and differences between ERA and CESM and between the forcing experiments: all simulations show a peak in the heatflux wave 1 component around 3 days before the central date which is slightly overestimated but otherwise comparable to the observed peak in ERA. However, only in the Fixed SSTs simulation, the heatflux wave 1 and wave 2 components are about the same magnitude (solid and dashed green lines, upper part), whereas in the other CESM sensitivity experiments, the wave 1 component clearly dominates. In the NATURAL experiment, major warmings are preceded by an anomalous increase of heatflux and GPH wave 1 (red solid lines) which starts more than 5 weeks before the warming. Although the anomalies in the heatflux wave 1 component increase from 15 days before the warming on, the GPH wave 1 anomalies do not increase any further. This indicates a strong wave forcing from the troposphere which does not reach the 10 hPa level, which is shown in Figure 6, but propagates only up to around 30 hPa (not shown). This is especially different from the GHG experiment where the largest anomalies of all simulations occur in both heatflux and GPH wave 1 components (blue solid lines) from around 12 days before the warming on, suggesting that the tropospheric wave forcing prior to major warmings induces wave 1 propagation up to higher levels.

In the previous section we have seen a strong influence on the SSW frequency by the SST variability and the QBO; in this section we found that for the GPH planetary wave behavior during the preconditioning phase of major warmings, anthropogenic GHGs and ODSs play an important role by influencing the propagation and stratospheric influence of the tropospheric wave 1 forcing.

5.2. Around the Central Date

To examine some characteristics of major warmings around the central date, we first analyze the development of zonal wind and temperature in the vortex region. For this we computed composites over all SSWs of height-time sections of zonal mean zonal wind at 60°N and anomalies of polar cap (60–90°N) zonal mean temperature, shown in Figure 7. Values which are statistically significant at the 95% level are color shaded. Following *de la Torre et al.* [2012] or *Kolstad and Charlton-Perez* [2011], statistical significance of the composites is checked via a Monte Carlo method, where the "real" composite is tested against a 1000-member ensemble of random composites, each containing the same number of elements as the real composite and taking into account the months of the SSWs.

Directly around the central date, we see easterly winds in ERA and all simulations (left column in Figure 7), one criterion to define the major warmings. While these easterlies extend roughly between 15 and 0.02 hPa in the GHG, Fixed SSTs, and NOQBO experiment, they are bounded between 15 and 0.2 hPa in NATURAL, i.e., the easterlies do not reach as high as in the other experiments. The strongest easterlies which fall below −20 m/s can be found in the GHG experiment.

Already 5 weeks before the central date, statistically significant strong westerlies in the upper stratosphere precede the upcoming warming event in the NATURAL simulation. These wind anomalies are accompanied by positive anomalies of zonal mean polar cap temperature (right column in Figure 7) which are also statistically significant from 35 days before the major warming on and show a distinct maximum around 3 hPa at 25 days before the central date. This anomaly maximum in the prewarming phase was already described in the previous section as a maximum in wave activity starting 35 days before the central date. We find that this

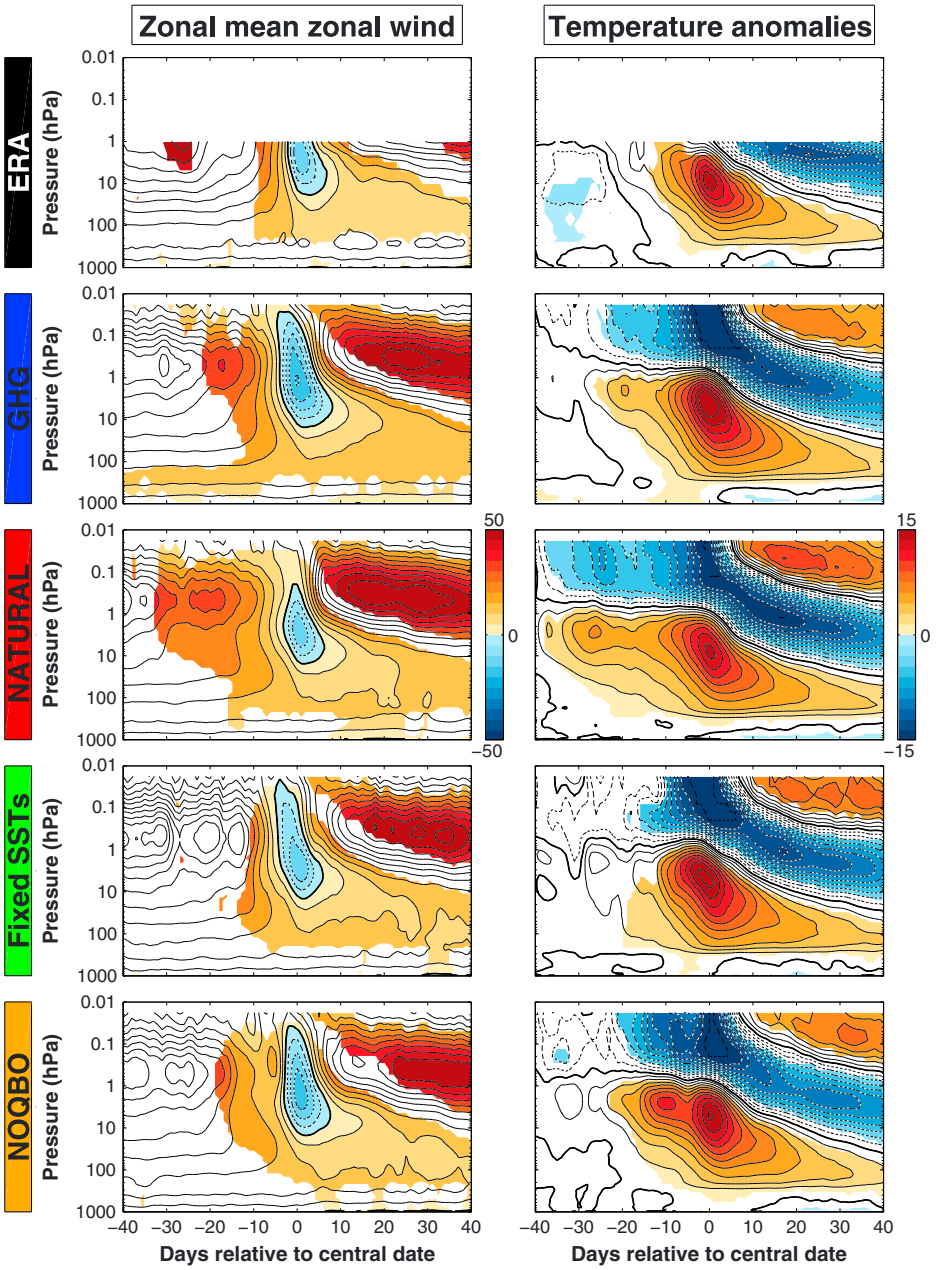

Figure 7. Height-time sections of (left column) zonal mean zonal wind at 60°N (contour interval: 5 m/s) and (right column) polar cap temperature anomalies (contour interval: 1.5°C) around central date; composite over all major SSWs; for ERA and CESM sensitivity experiments. Colors denote 95% statistical significance.

maximum is not due to the multiple occurrence of two SSWs at intervals of 25 days in a winter. Instead, we see that in several cases in NATURAL the zonal wind reverses in the upper stratosphere around 30–20 days before the central date of a warming which involves the warming anomaly seen at these lead times. As the wind reversal does not reach down to 10 hPa, no major but a minor SSW is defined in these cases. In the NOQBO simulation a "prewarming" seems to occur around 10 days before the major warming, which is seen as a maximum in positive temperature anomalies around 2 hPa. No comparable, statistically significant prewarming occurs in the Fixed SSTs simulation and in ERA, where the onset of the warmings occurs quite abruptly.

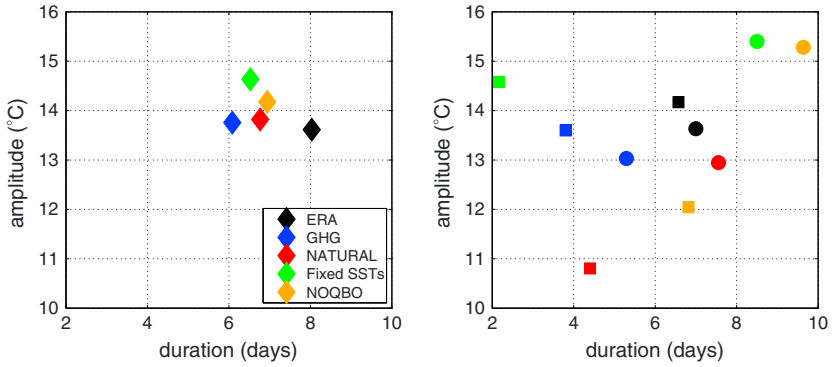

Figure 8. (left) Average amplitude and duration of all SSWs; (right) average amplitude and duration of SSWs preceded by an Atlantic (circles) or a Pacific (squares) blocking; in ERA and CESM sensitivity experiments.

After the central date, the warming anomaly propagates downward and then slowly fades out around 100 hPa in ERA and the CESM sensitivity runs. The downward propagation and surface impact after the warming will be further investigated in the next section.

To give another measure for the SSWs in the different CESM experiments, we calculated the duration and the amplitude of all events similar to *de la Torre et al.* [2012]. The duration of a SSW is defined as the number of consecutive days with easterlies at 60°N, 10 hPa; the amplitude is computed as the mean polar cap (60–90°N) temperature anomaly at 10 hPa within ±2 days around the central date. The average duration and amplitude of major warmings for the sensitivity experiments are shown in the left part of Figure 8 and listed in Table 2 in the sixth and seventh columns, with the numbers in brackets denoting the minimum and maximum values. For both duration and amplitude the differences are not statistically significant between any experiments or ERA, as tested with a two-sided *t* test. We also investigated if there are any differences in duration or amplitude between events that are preceded by Euro-Atlantic or Pacific blockings (see previous section) and found that SSWs which follow a Euro-Atlantic blocking are generally (in all simulations and ERA) longer than those preceded by a Pacific blocking (Figure 8, right part).

To distinguish between vortex split and displacement events, a distinction which refers to the wave number directly around the central date, we did a subjective analysis (like in *de la Torre et al.* [2012]) of the GPH fields at 10 hPa around the central date of the major warmings. The number of vortex split and displacement events is given in Table 2 in the eighth column. We found a few split SSWs in the CESM simulations, but compared to ERA, where more than 40% of all SSWs are classified as these events, their number is highly underestimated in CESM. This makes it difficult to do any further analysis with the distinction between displacement and split events or to draw any conclusions on this point. For the duration and amplitude of displacement and (the very few) split events, we did not find any significant differences.

5.3. After the Major Warming: Surface Impact

Strong major warmings have been shown to couple down from the stratosphere to the troposphere and have a significant influence on the surface circulation [e.g., *Baldwin and Dunkerton*, 2001; *Mitchell et al.*, 2013]. The most common method to investigate stratosphere-troposphere coupling is to analyze indices of the Northern and Southern Annular Modes (NAM and SAM) [*Baldwin and Dunkerton*, 2001]. We also use the NAM index to see whether any differences in the downward coupling occur in our CESM sensitivity experiments.

The NAM index is computed as the principal component (PC) of the first empirical orthogonal function (EOF) of daily, year-round GPH fields between 20 and 90°N. As suggested by *Baldwin and Thompson* [2009], we calculate the EOFs and PCs separately for each pressure level from zonal mean GPH anomalies. A positive (negative) NAM index implies an enhancement (diminishment) of the typical NAM pattern, corresponding with negative (positive) anomalies of GPH in the polar regions and positive (negative) anomalies in midlatitudes.

In Figure 9, composites of the time-height development of the NAM index are shown for all SSWs in ERA and all CESM experiments. During major warmings, the NAM index is negative (red colors in Figure 9) at almost

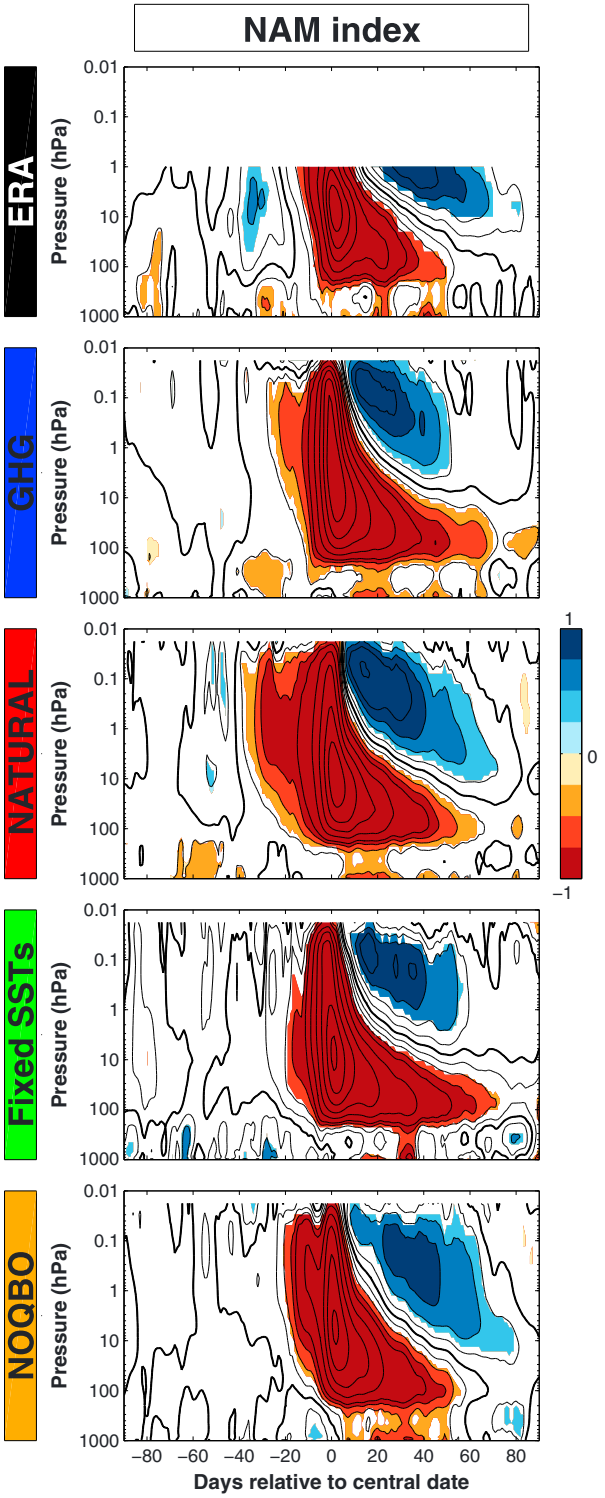

Figure 9. Height-time sections of NAM index around central date; contour interval 0.25 standard deviations for values between −1 and 1, 0.5 standard deviations for values below −1 and above 1; red (blue) colors denote 95% statistically significant negative (positive) values; composite over all major SSWs; for ERA and CESM sensitivity experiments.

all heights, with a minimum at the central date. In all simulations and in ERA we see a coupling to the troposphere indicated by the "dripping paint"-like negative NAM index in different periods after the central date. In ERA, the two most pronounced periods of coupling to the troposphere occur around 20 and 40 days after the central date, accompanied by an almost continuous statistically significant surface signal. In the GHG experiment, a significant influence on the surface occurs almost continuously between 7 and 50 days after the central date. The NATURAL simulation shows a similar behavior, especially in the significant downward coupling and surface imprint signals in the period 1–4 weeks after the central date. A very persistent statistically significant coupling of about 50 days to the troposphere and impact on the surface occurs in the NOQBO run. In contrast to the other experiments and ERA, only one short remarkable period of coupling to the troposphere can be found in the Fixed SSTs simulation, namely, after day 30, lasting about a week. This suggests that varying SSTs are needed to transport the signal of major warmings from the stratosphere to the troposphere.

In a last step, we examine the resulting surface impact pattern in the different simulations in more detail. For this we compute composites of all major warmings for sea level pressure (SLP) anomalies as 10 day averages in the periods before and after the central date of the warming. In Figure 10 these composites are shown exemplarily for the periods 20–10 days before, 5 days before to 5 days after, and 10–20 days after the major warming. In ERA and in the CESM sensitivity experiments the SLP anomalies before the central date resemble the positive phase of the Pacific-North American pattern (PNA) [*Wallace and Gutzler*, 1981], which was also described by *Charlton and Polvani* [2007]. Additionally, a positive SLP anomaly occurs above the Eurasian continent; however, not all

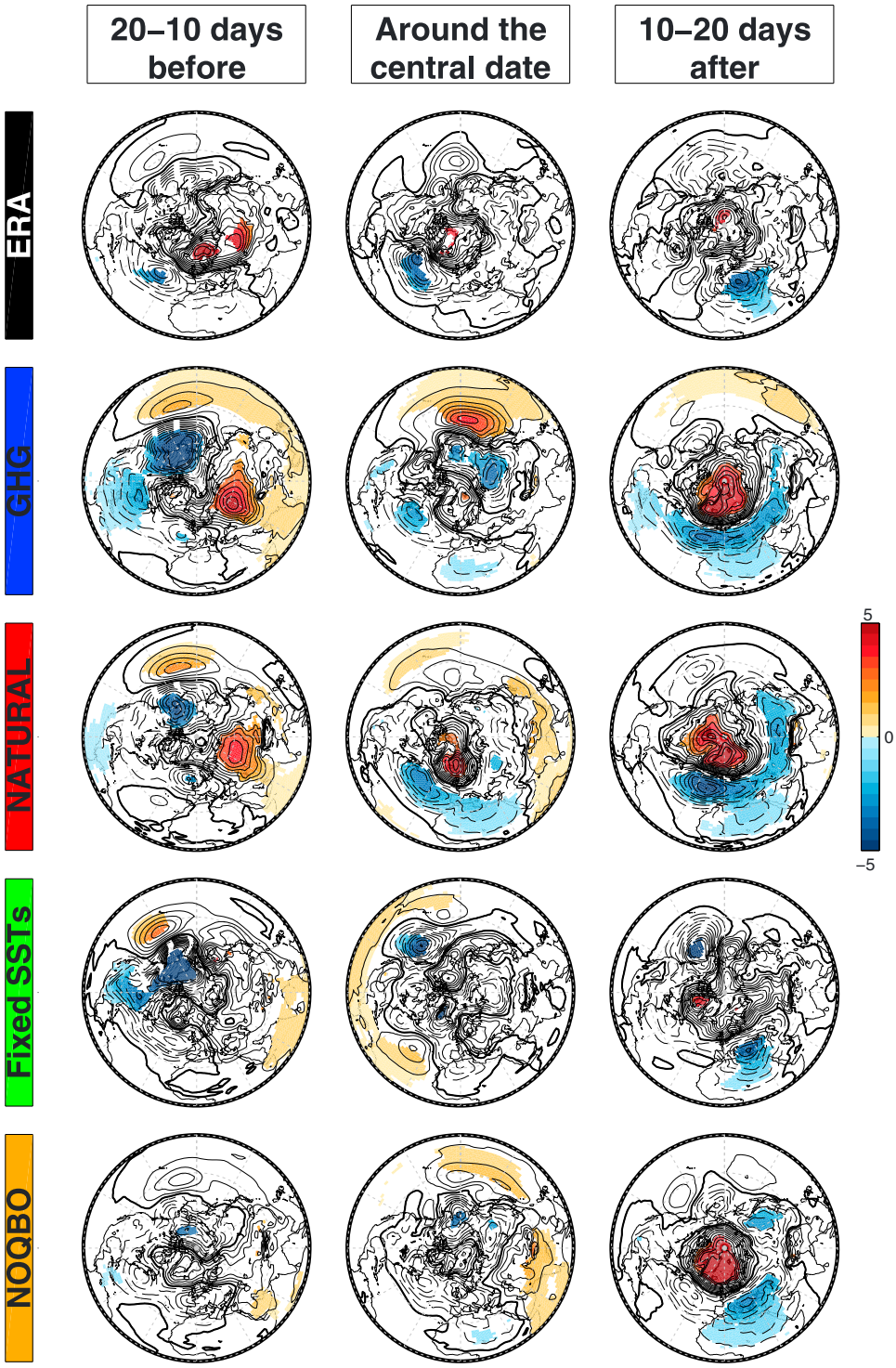

Figure 10. Composite of sea level pressure anomalies (in 0.5 hPa intervals), averaged over (from left to right) 20–10 days before, 5 days before to 5 days after, and 10–20 days after the central date, for ERA and CESM sensitivity simulations. Colors denote 95% statistical significance.

these signals are statistically significant in all simulations. The positive SLP anomaly above the Pacific persists through the central date and is still visible after the major warming in the GHG simulation.

Around and after the central date, the statistically significant SLP anomaly signals in ERA resemble a negative NAO pattern. The negative anomalies in the midlatitudes move from the central North Atlantic to the Mediterranean after the central date. In the GHG, NATURAL, and NOQBO simulation, the positive polar SLP anomaly is surrounded by a circular negative anomaly after the central date, making the signal resemble a negative AO (the "surface NAM") [*Thompson and Wallace*, 1998] pattern. However, the regions with statistically significant anomalies can mainly be found in the lower to midlatitudes between 30°W and 120°E, i.e., over the North Atlantic, Europe, North Africa and the Asian continent.

As found before for the coupling to the troposphere shown with the NAM index, only small differences occur between the GHG and the NATURAL simulation in the SLP surface response after the central date. In the NOQBO simulations, the negative AO pattern following major warmings has its maximum around 20–30 days after the central date (not shown), i.e., 10 days later than in the other simulations. In the Fixed SSTs experiment, the surface influence of major warmings does not only occur over a shorter period of time as seen before but potentially also over a smaller region, with the negative anomalies in the midlatitudes reduced to south Europe and north Africa. However, the latter finding might also be misinterpreted from a signal where the statistical significance is lower than in the other signals because of the small number of major warmings in the Fixed SSTs experiment. It therefore has to be confirmed, e.g., in longer simulations, if the ocean is really, as it seems here, influencing the stratosphere-troposphere coupling after major warmings and the persistence of the warmings's surface signal.

The surface impact of the major warmings can also be seen in anomalous SST signals both in the Atlantic and in the Pacific region (not shown) and is preserved longer in the CESM experiments with interactive ocean. According to *Barsugli and Battisti* [1998], this could be explained with the internal damping of anomalies due to surface heat fluxes which is enhanced when ocean and atmosphere are not coupled interactively, as in the Fixed SSTs simulation. Without an interactive but with a prescribed ocean, the enhanced damping reduces the variance in the atmosphere [*Barsugli and Battisti*, 1998].

In summary we find that for the tropospheric impact of major SSWs—a pattern which strongly projects on the NAO or AO and which lasts around 4 weeks—removing interannual SST variability and two-way ocean/atmosphere coupling seems to reduce the tropospheric signature in space and time. Removing the QBO seems to shift the period of significant influence by about 10 days.

6. Conclusions

In this study, we have investigated the influence of different natural and anthropogenic factors, namely, anthropogenic GHGs and ODSs, interannual SST variability, and the QBO, on major stratospheric warmings. For this, we have performed a set of sensitivity simulations with NCAR's CESM-WACCM model where we systematically switched on and off these factors, as summarized in Table 1. We analyzed differences in the frequency and distribution of major warmings and if these differences result from climatological differences in planetary wave generation, wave propagation, and wave-mean flow interaction. Afterward, we investigated the warming event itself, from its preconditioning phase until the downward coupling and surface impact afterward.

We found the following:

1. The frequency of major warmings is significantly increased by removing stratospheric variability provoked by the equatorial QBO, while it is significantly decreased when interannual SST variability and two-way atmosphere-ocean interaction is removed. These changes are consistent with differences in the climatological strength of the stratospheric polar night jet (PNJ) together with differences in climatological wave propagation and wave-mean flow interaction which, in turn, are all influenced by the QBO and SST variability. When QBO nudging is switched off and equatorial winds are in permanent easterly phase, planetary wave propagation from the troposphere into the PNJ region is enhanced, which leads to stronger deceleration of the PNJ through wave-mean flow interaction and, thus, to a weaker vortex that allows more major warmings to occur. Without SST variability, in contrast, the wave forcing from the troposphere is reduced, which means that the vortex is stronger and hence less easily disturbed.

Although the QBO and SST variability already have an influence on the generation of planetary waves in the troposphere, this does not seem to be the decisive factor for the differences in SSWs.

2. Anthropogenic GHGs and ODSs have some influence on the prewarming phase of the major warming events, i.e., the weeks before the central date. The GHG simulation shows an anomalous increase of the geopotential height wave 1 component starting several weeks before the warming, which does not occur in the other simulations where the GHGs are kept fixed at the 1960s level. In the simulation without anthropogenic forcing, a minor warming occurs in many cases around 5 weeks before the major warming, leading to a polar vortex which is already weakened before SSW occurrence.
3. In the phase following the central date, all experiments show a significant downward coupling to the troposphere and surface signature, which strongly projects on the negative NAO or AO pattern. It lasts around 4 weeks, probably due to the persistence of the signal in the ocean, but seems to be altered by the QBO and SST variability. Without the QBO, the 30 day period of significant surface influence is shifted by about 10 days. When the SSTs do not vary from year to year, the tropospheric signature seems to be confined to a smaller area (above the pole and the eastern North Atlantic) and a shorter period of time (between days 30 and 40 after the central date). This could be due to enhanced internal damping, which occurs when the ocean and atmosphere are not coupled interactively [*Barsugli and Battisti*, 1998]; however, this hypothesis has to be confirmed by future studies investigating more SSW cases, as the relatively low number of major warmings in the Fixed SSTs experiment does not allow final conclusions. The surface impact of major warmings in CESM-WACCM will not change significantly even under extreme (RCP8.5) global warming conditions.

Although many studies have reported a relationship between tropospheric blocking and the occurrence of major warmings, we can neither confirm nor negate this connection from our analysis, and we did not find any differences due to the different factors. However, this might be due to the inherent underestimation of Atlantic and Pacific blockings in the CESM model which has been documented for several models, e.g., in CMIP3 and CMIP5 [*Scaife et al.*, 2010; *Anstey et al.*, 2013], and which might be due to the relatively coarse horizontal resolution used in these models [*Jung et al.*, 2012]. Although the average amplitude and duration of major warmings does not seem to be influenced by the different factors, we found that SSWs preceded by a Euro-Atlantic blocking are on average longer than those which follow a Pacific blocking.

None of our simulations were able to reproduce the observed frequency of W2 and vortex split events; instead, almost all major warmings are W1 and vortex displacement warmings. This might also be due to the underestimation of blockings, as they (mainly the Pacific blockings) have been shown to often precede wave number 2 events.

With our study we confirm that all of the investigated factors influence several aspects of stratospheric warmings as described above; however, it is in general not easy to compare the effect of different factors directly, as they all influence atmospheric dynamics in different ways: the GHGs primarily act on the radiation budget, the QBO influences the dynamical stratospheric state, and the SSTs affect the lower to middle atmosphere from the lower boundary of the system. A subject of future studies is to deal with the quantification of the influence of the individual factors, e.g., by applying statistical methods. Knowledge about the absolute importance of the respective factors is crucial for the prediction of stratospheric polar vortex conditions and hence would increase the prediction skill for tropospheric weather.

Acknowledgments

This work has been performed within the Helmholtz-University Young Investigators Group NATHAN funded by the Helmholtz-Association through the President's Initiative and Networking Fund, the Helmholtz Centre for Ocean Research Kiel (GEOMAR), the German Centre for Geosciences Potsdam (GFZ), and the Freie Universität Berlin. The CESM simulations have been performed at the Deutsche Klimarechenzentrum (DKRZ) Hamburg, Germany. The authors thank D. Marsh, M. Mills, and the CESM development group at NCAR for help in setting up the coupled model at the DKRZ. Special thanks go to N.-E. Omrani, R. Thieblemont, and L. Neef for intensive discussions on the manuscript and to Shigeo Yoden and two anonymous reviewers for very helpful comments.

References

Andrews, D. G., J. Holton, and C. Leovy (1987), *Middle Atmosphere Dynamics*, Academic Press, San Diego, Calif.

Anstey, J. A., P. Davini, L. J. Gray, T. Woollings, N. Butchart, C. Cagnazzo, B. Christiansen, S. C. Hardiman, S. M. Osprey, and S. Yang (2013), Multi-model analysis of Northern Hemisphere winter blocking: Model biases and the role of resolution, *J. Geophys. Res. Atmos.*, *118*, 3956–3971, doi:10.1002/jgrd.50231.

Ayarzagüena, B., U. Langematz, S. Meul, S. Oberlander, J. Abalichin, and A. Kubin (2013), The role of climate change and ozone recovery for the future timing of major stratospheric warmings, *Geophys. Res. Lett.*, *40*, 2460–2465, doi:10.1002/grl.50477.

Baldwin, M., and T. Dunkerton (2001), Stratospheric harbingers of anomalous weather regimes, *Science*, *294*, 581–584.

Baldwin, M. P., and D. W. J. Thompson (2009), A critical comparison of stratosphere-troposphere coupling indices, *Q. J. R. Meteorol. Soc.*, *135*(644), 1661–1672, doi:10.1002/qj.479.

Bancala, S., K. Kruger, and M. Giorgetta (2012), The preconditioning of major sudden stratospheric warmings, *J. Geophys. Res.*, *117*, D04101, doi:10.1029/2011JD016769.

Barsugli, J. J., and D. S. Battisti (1998), The basic effects of atmosphere-ocean thermal coupling on midlatitude variability, *J. Atmos. Sci.*, *55*(4), 477–493, doi:10.1175/1520-0469(1998)055<0477:TBEOAO>2.0.CO;2.

Bell, C. J., L. J. Gray, A. J. Charlton-Perez, M. M. Joshi, and A. A. Scaife (2009), Stratospheric communication of El Nino teleconnections to European winter, *J. Clim.*, *22*(15), 4083–4096, doi:10.1175/2009JCLI2717.1.

Black, R. X., and B. A. McDaniel (2004), Diagnostic case studies of the northern annular mode, *J. Clim.*, *17*(20), 3990–4004, doi:10.1175/1520-0442(2004)017<3990:DCSOTN>2.0.CO;2.
Blume, C., K. Matthes, and I. Horenko (2012), Supervised learning approaches to classify sudden stratospheric warming events, *J. Atmos. Sci.*, *69*(6), 1824–1840, doi:10.1175/JAS-D-11-0194.1.
Butchart, N., J. Austin, J. R. Knight, A. A. Scaife, and M. L. Gallani (2000), The response of the stratospheric climate to projected changes in the concentrations of well-mixed greenhouse gases from 1992 to 2051, *J. Clim.*, *13*(13), 2142–2159, doi:10.1175/1520-0442(2000)013<2142:TROTSC>2.0.CO;2.
Butler, A. H., and L. M. Polvani (2011), El Niño, La Niña, and stratospheric sudden warmings: A reevaluation in light of the observational record, *Geophys. Res. Lett.*, *38*, L13807, doi:10.1029/2011GL048084.
Camp, C. D., and K. K. Tung (2007), Stratospheric polar warming by ENSO in winter: A statistical study, *Geophys. Res. Lett.*, *34*, L04809, doi:10.1029/2006GL028521.
Castanheira, J. M., and D. Barriopedro (2010), Dynamical connection between tropospheric blockings and stratospheric polar vortex, *Geophys. Res. Lett.*, *37*, L13809, doi:10.1029/2010GL043819.
Charlton, A. J., and L. M. Polvani (2007), A new look at stratospheric sudden warmings. Part I: Climatology and modeling benchmarks, *J. Clim.*, *20*(3), 449–469, doi:10.1175/JCLI3996.1.
Charlton, A. J., L. M. Polvani, J. Perlwitz, F. Sassi, E. Manzini, K. Shibata, S. Pawson, J. E. Nielsen, and D. Rind (2007), A new look at stratospheric sudden warmings. Part II: Evaluation of numerical model simulations, *J. Clim.*, *20*(3), 470–488, doi:10.1175/JCLI3994.1.
Charlton-Perez, A. J., L. M. Polvani, J. Austin, and F. Li (2008), The frequency and dynamics of stratospheric sudden warmings in the 21st century, *J. Geophys. Res.*, *113*, D16116, doi:10.1029/2007JD009571.
Danabasoglu, G., S. C. Bates, B. P. Briegleb, S. R. Jayne, M. Jochum, W. G. Large, S. Peacock, and S. G. Yeager (2012), The CCSM4 ocean component, *J. Clim.*, *25*(5), 1361–1389, doi:10.1175/JCLI-D-11-00091.1.
de la Torre, L., R. R. Garcia, D. Barriopedro, and A. Chandran (2012), Climatology and characteristics of stratospheric sudden warmings in the Whole Atmosphere Community Climate Model, *J. Geophys. Res.*, *117*, D04110, doi:10.1029/2011JD016840.
Erlebach, P., U. Langematz, and S. Pawson (1996), Simulations of stratospheric sudden warmings in the Berlin troposphere stratosphere mesosphere GCM, *Ann. Geophys.*, *14*(4), 443–463, doi:10.1007/s00585-996-0443-6.
Garcia, R. R., D. R. Marsh, D. E. Kinnison, B. A. Boville, and F. Sassi (2007), Simulation of secular trends in the middle atmosphere, 1950–2003, *J. Geophys. Res.*, *112*, D09301, doi:10.1029/2006JD007485.
Garcia, R. R., W. J. Randel, and D. E. Kinnison (2011), On the determination of age of air trends from atmospheric trace species, *J. Atmos. Sci.*, *68*(1), 139–154, doi:10.1175/2010JAS3527.1.
Garfinkel, C. I., A. H. Butler, D. W. Waugh, M. M. Hurwitz, and L. M. Polvani (2012), Why might stratospheric sudden warmings occur with similar frequency in El Nino and La Nina winters?, *J. Geophys. Res.*, *117*, D19106, doi:10.1029/2012JD017777.
Gent, P. R., et al. (2011), The Community Climate System Model Version 4, *J. Clim.*, *24*(19), 4973–4991, doi:10.1175/2011JCLI4083.1.
Gray, L. J., et al. (2010), Solar influences on climate, *Rev. Geophys.*, *48*, RG4001, doi:10.1029/2009RG000282.
Hansen, F., K. Matthes, and L. J. Gray (2013), Sensitivity of stratospheric dynamics and chemistry to QBO nudging width in the chemistry-climate model WACCM, *J. Geophys. Res. Atmos.*, *118*, 10,464–10,474, doi:10.1002/jgrd.50812.
Holland, M. M., D. A. Bailey, B. P. Briegleb, B. Light, and E. Hunke (2012), Improved sea ice shortwave radiation physics in CCSM4: The impact of melt ponds and aerosols on Arctic Sea ice, *J. Clim.*, *25*(5), 1413–1430, doi:10.1175/JCLI-D-11-00078.1.
Holton, J. R., and H.-C. Tan (1980), The influence of the equatorial quasi-biennial oscillation on the global circulation at 50 mb, *J. Atmos. Sci.*, *37*, 2200–2208.
Holton, J. R., and H.-C. Tan (1982), The quasi-biennial oscillation in the Northern Hemisphere lower stratosphere, *J. Meteorol. Soc. Jpn.*, *60*, 140–148.
Huebener, H., U. Cubasch, U. Langematz, T. Spangehl, F. Niehorster, I. Fast, and M. Kunze (2007), Ensemble climate simulations using a fully coupled ocean-troposphere-stratosphere general circulation model, *Philos. Trans. R. Soc. A*, *365*(1857), 2089–2101, doi:10.1098/rsta.2007.2078.
Hurrell, J. W., et al. (2013), The Community Earth System Model: A framework for collaborative research, *Bull. Am. Meteorol. Soc.*, *94*(9), 1339–1360, doi:10.1175/BAMS-D-12-00121.1.
Jung, T., et al. (2012), High-resolution global climate simulations with the ECMWF Model in Project Athena: Experimental design, model climate, and seasonal forecast skill, *J. Clim.*, *25*(9), 3155–3172, doi:10.1175/JCLI-D-11-00265.1.
Kinnison, D. E., et al. (2007), Sensitivity of chemical tracers to meteorological parameters in the MOZART-3 chemical transport model, *J. Geophys. Res.*, *112*, D20302, doi:10.1029/2006JD007879.
Kodera, K., and M. Chiba (1995), Tropospheric circulation changes associated with stratospheric sudden warmings—A case study, *J. Geophys. Res.*, *100*(D6), 11,055–11,068, doi:10.1029/95JD00771.
Kolstad, E. W., and A. J. Charlton-Perez (2011), Observed and simulated precursors of stratospheric polar vortex anomalies in the Northern Hemisphere, *Clim. Dyn.*, *37*(7–8), 1443–1456, doi:10.1007/s00382-010-0919-7.
Labitzke, K. (1977), Interannual variability of the winter stratosphere in Northern Hemisphere, *Mon. Weather Rev.*, *105*, 762–770.
Labitzke, K., and B. Naujokat (2000), The lower Arctic stratosphere in winter since 1952, *SPARC Newsletter*, *15*, 11–14.
Lean, J. L., G. Rottman, J. Harder, and G. Kopp (2005), Source contributions to new understanding of global change and solar variability, *Sol. Phys.*, *230*, 27–53.
Limpasuvan, V., D. W. J. Thompson, and D. L. Hartmann (2004), The life cycle of the Northern Hemisphere sudden stratospheric warmings, *J. Clim.*, *17*(13), 2584–2596, doi:10.1175/1520-0442(2004)017<2584:TLCOTN>2.0.CO;2.
Limpasuvan, V., J. H. Richter, Y. J. Orsolini, F. Stordal, and O. K. Kvissel (2012), The roles of planetary and gravity waves during a major stratospheric sudden warming as characterized in WACCM, *J. Atmos. Sol. Terr. Phys.*, *78-79*, 84–98, doi:10.1016/j.jastp.2011.03.004.
Manzini, E., M. A. Giorgetta, M. Esch, L. Kornblueh, and E. Roeckner (2006), The influence of sea surface temperatures on the northern winter stratosphere: Ensemble simulations with the MAECHAM5 model, *J. Clim.*, *19*(16), 3863–3881, doi:10.1175/JCLI3826.1.
Marsh, D., M. J. Mills, D. E. Kinnison, J.-F. Lamarque, N. Calvo, and L. M. Polvani (2013), Climate change from 1850 to 2005 simulated in CESM1(WACCM), *J. Clim.*, *26*, 7372–7391, doi:10.1175/JCLI-D-12-00558.1.
Martius, O., L. M. Polvani, and H. C. Davies (2009), Blocking precursors to stratospheric sudden warming events, *Geophys. Res. Lett.*, *36*, L14806, doi:10.1029/2009GL038776.
Matsuno, T. (1971), Dynamical model of stratospheric sudden warming, *J. Atmos. Sci.*, *28*(8), 1479–1494, doi:10.1175/1520-0469(1971)028<1479:ADMOTS>2.0.CO;2.
Matthes, K., D. R. Marsh, R. R. Garcia, D. E. Kinnison, F. Sassi, and S. Walters (2010), Role of the QBO in modulating the influence of the 11 year solar cycle on the atmosphere using constant forcings, *J. Geophys. Res.*, *115*, D18110, doi:10.1029/2009JD013020.

Matthes, K., K. Kodera, R. R. Garcia, Y. Kuroda, D. R. Marsh, and K. Labitzke (2013), The importance of time-varying forcing for QBO modulation of the atmospheric 11 year solar cycle signal, *J. Geophys. Res. Atmos.*, *118*, 4435–4447, doi:10.1002/jgrd.50424.
McLandress, C., and T. G. Shepherd (2009), Impact of climate change on stratospheric sudden warmings as simulated by the Canadian Middle Atmosphere Model, *J. Clim.*, *22*(20), 5449–5463, doi:10.1175/2009JCLI3069.1.
Meinshausen, M., et al. (2011), The RCP greenhouse gas concentrations and their extensions from 1765 to 2300, *Clim. Change*, *109*(1–2), 213–241, doi:10.1007/s10584-011-0156-z.
Mitchell, D. M., A. J. Charlton-Perez, and L. J. Gray (2011), Characterizing the variability and extremes of the stratospheric polar vortices using 2D moment analysis, *J. Atmos. Sci.*, *68*(6), 1194–1213, doi:10.1175/2010JAS3555.1.
Mitchell, D. M., S. M. Osprey, L. J. Gray, N. Butchart, S. C. Hardiman, A. J. Ciarlton-Perez, and P. Watson (2012), The effect of climate change on the variability of the Northern Hemisphere stratospheric polar vortex, *J. Atmos. Sci.*, *69*(8), 2608–2618, doi:10.1175/JAS-D-12-021.1.
Mitchell, D. M., L. J. Gray, J. Anstey, M. P. Baldwin, and A. J. Charlton-Perez (2013), The influence of stratospheric vortex displacements and splits on surface climate, *J. Clim.*, *26*(8), 2668–2682, doi:10.1175/JCLI-D-12-00030.1.
Naoe, H., and K. Shibata (2010), Equatorial quasi-biennial oscillation influence on northern winter extratropical circulation, *J. Geophys. Res.*, *115*, D19102, doi:10.1029/2009JD012952.
Nishii, K., H. Nakamura, and Y. J. Orsolini (2011), Geographical dependence observed in blocking high influence on the stratospheric variability through enhancement and suppression of upward planetary-wave propagation, *J. Clim.*, *24*(24), 6408–6423, doi:10.1175/JCLI-D-10-05021.1.
Omrani, N. E., N. S. Keenlyside, J. Bader, and E. Manzini (2014), Stratosphere key for wintertime atmospheric response to warm Atlantic decadal conditions, *Clim. Dyn.*, *42*(3–4), 649–663, doi:10.1007/s00382-013-1860-3.
Pawson, S., and T. Kubitz (1996), Climatology of planetary waves in the northern stratosphere, *J. Geophys. Res.*, *101*(D12), 16,987–16,996, doi:10.1029/96JD01226.
Quiroz, R. S. (1977), Tropospheric-stratospheric polar vortex breakdown of January 1977, *Geophys. Res. Lett.*, *4*(4), 151–154, doi:10.1029/GL004i004p00151.
Quiroz, R. S. (1986), The association of stratospheric warmings with tropospheric blocking, *J. Geophys. Res.*, *91*(D4), 5277–5285, doi:10.1029/JD091iD04p05277.
Richter, J. H., F. Sassi, and R. R. Garcia (2010), Toward a physically based gravity wave source parameterization in a general circulation model, *J. Atmos. Sci.*, *67*(1), 136–156, doi:10.1175/2009JAS3112.1.
Richter, J. H., K. Matthes, N. Calvo, and L. J. Gray (2011), Influence of the quasi-biennial oscillation and El Niño-Southern Oscillation on the frequency of sudden stratospheric warmings, *J. Geophys. Res.*, *116*, D20111, doi:10.1029/2011JD015757.
Rind, D., D. Shindell, P. Lonergan, and N. K. Balachandran (1998), Climate change and the middle atmosphere. Part III: The doubled CO_2 climate revisited, *J. Clim.*, *11*(5), 876–894, doi:10.1175/1520-0442(1998)011<0876:CCATMA>2.0.CO;2.
Robock, A. (2000), Volcanic eruptions and climate, *Rev. Geophys.*, *38*(2), 191–219, doi:10.1029/1998RG000054.
Sassi, F., D. Kinnison, B. A. Boville, R. R. Garcia, and R. Roble (2004), Effect of El Niño-Southern Oscillation on the dynamical, thermal, and chemical structure of the middle atmosphere, *J. Geophys. Res.*, *109*, D17108, doi:10.1029/2003JD004434.
Scaife, A. A., T. Woollings, J. Knight, G. Martin, and T. Hinton (2010), Atmospheric blocking and mean biases in climate models, *J. Clim.*, *23*(23), 6143–6152, doi:10.1175/2010JCLI3728.1.
Scherhag, R. (1952), Die explosionsartigen Stratosphärenerwärmungen des Spätwinters, 1951-1952, *Ber. Deut. Wetterdienst*, *38*, 51–63.
Schimanke, S., J. Korper, T. Spangehl, and U. Cubasch (2011), Multi-decadal variability of sudden stratospheric warmings in an AOGCM, *Geophys. Res. Lett.*, *38*, L01801, doi:10.1029/2010GL045756.
Schimanke, S., T. Spangehl, H. Huebener, and U. Cubasch (2013), Variability and trends of major stratospheric warmings in simulations under constant and increasing GHG concentrations, *Clim. Dyn.*, *40*(7-8), 1733–1747, doi:10.1007/s00382-012-1530-x.
Shepherd, T. G., and C. Mclandress (2011), A robust mechanism for strengthening of the Brewer-Dobson circulation in response to climate change: Critical-layer control of subtropical wave breaking, *J. Atmos. Sci.*, *68*(4), 784–797, doi:10.1175/2010JAS3608.1.
Simmons, A. J., S. M. Uppala, D. Dee, and S. Kobayashi (2006), ERA-Interim: New ECMWF reanalysis products from 1989 onwards, *ECMWF Newsletter*, *110*, 26–35.
Smith, A. K., R. R. Garcia, D. R. Marsh, and J. H. Richter (2011), WACCM simulations of the mean circulation and trace species transport in the winter mesosphere, *J. Geophys. Res.*, *116*, D20115, doi:10.1029/2011JD016083.
SPARC CCMVal, (2010), SPARC report on the evaluation of chemistry-climate models, *SPARC-Report No. 5, WCRP-132,WMO/TD-No. 1526*, SPARC CCMVal.
Taguchi, M. (2008), Interannual variations of the stratosphere and troposphere during northern winter as simulated by WACCM, *J. Clim.*, *21*(10), 2326–2331, doi:10.1175/2007JCLI1744.1.
Taguchi, M., and D. L. Hartmann (2006), Increased occurrence of stratospheric sudden warmings during El Niño as simulated by WACCM, *J. Clim.*, *19*(3), 324–332, doi:10.1175/JCLI3655.1.
Taylor, K., R. J. Stouffer, and G. A. Meehl (2012), An overview of CMIP5 and the experiment design, *Bull. Am. Meteorol. Soc.*, *93*, 485–498.
Thompson, D., and J. Wallace (1998), The Arctic Oscillation signature in the wintertime geopotential height and temperature fields, *Geophys. Res. Lett.*, *25*(9), 1297–1300, doi:10.1029/98GL00950.
Thompson, D. W. J., M. P. Baldwin, and J. M. Wallace (2002), Stratospheric connection to Northern Hemisphere wintertime weather: Implications for prediction, *J. Clim.*, *15*(12), 1421–1428, doi:10.1175/1520-0442(2002)015<1421:SCTNHW>2.0.CO;2.
Tibaldi, S., and F. Molteni (1990), On the operational predictability of blocking, *Tellus Ser. A*, *42*, 343–365.
Uppala, S., P. Kallberg, P. Hernandez, S. Saarinen, M. Fiorino, X. Li, K. Onogi, N. Sokka, U. Andrae, and V. D. C. Bechtold (2004), ERA-40: ECMWF 45-year reanalysis of the global atmosphere and surface conditions 1957–2002, *ECMWF Newsletter*, *101*, 2–21.
Van Loon, H., and K. Labitzke (1987), The Southern Oscillation .5. The anomalies in the lower stratosphere of the Northern-Hemisphere in winter and a comparison with the Quasi-biennial Oscillation, *Mon. Weather Rev.*, *115*(2), 357–369, doi:10.1175/1520-0493(1987)115<0357:TSOPVT>2.0.CO;2.
Wallace, J. M., and D. S. Gutzler (1981), Teleconnections in the geopotential height field during the Northern Hemisphere winter, *Mon. Weather Rev.*, *109*(4), 784–812, doi:10.1175/1520-0493(1981)109<0784:TITGHF>2.0.CO;2.
Watson, P. A. G., and L. J. Gray (2014), How does the quasi-biennial oscillation affect the stratospheric polar vortex?, *J. Atmos. Sci.*, *71*(1), 391–409, doi:10.1175/JAS-D-13-096.1.
Woollings, T., A. Charlton-Perez, S. Ineson, A. G. Marshall, and G. Masato (2010), Associations between stratospheric variability and tropospheric blocking, *J. Geophys. Res.*, *115*, D06108, doi:10.1029/2009JD012742.
Yoden, S., T. Yamaga, S. Pawson, and U. Langematz (1999), A composite analysis of the stratospheric sudden warmings simulated in a perpetual January integration of the Berlin TSM GCM, *J. Meteorol. Soc. Jpn.*, *77*(2), 431–445.

3 Sensitivity of stratospheric dynamics and chemistry to QBO nudging width in the chemistry-climate model WACCM

As was shown in the previous chapter, the QBO has a strong influence on the NH polar stratosphere. In this chapter, which is a reprint of an article of the same title published in *Journal of Geophysical Research - Atmospheres*, a more detailed analysis on the representation of this fascinating phenomenon in the stand-alone atmospheric chemistry-climate model WACCM is performed. Since WACCM, like most other models of comparable capability, is not able to generate the QBO internally (at least at the time when this study was done), this equatorial stratospheric oscillation has to be prescribed ("nudged") in the model in order to get a realistic representation of the dynamics between low and middle to higher latitudes and the appearing chemical processes. The influence of a varying equatorial QBO nudging width on the dynamics and chemistry is analyzed here.

Citation: **Hansen, F., K. Matthes, and L. J. Gray, 2013: Sensitivity of stratospheric dynamics and chemistry to QBO nudging width in the chemistry-climate model WACCM. J. Geophys. Res.-Atmos., 118, 10 464–10 474, doi:** $10.1002/\mathrm{jgrd}.50812$**.**

The authors' contributions to this publication are as follows:

- *F. Hansen did all the analyses, produced all figures and wrote the manuscript.*
- *K. Matthes initiated the study and contributed with ideas and discussions on the analysis and with comments on the manuscript.*
- *L. J. Gray provided the reanalysis data and commented the manuscript.*

JOURNAL OF GEOPHYSICAL RESEARCH: ATMOSPHERES, VOL. 118, 10,464–10,474, doi:10.1002/jgrd.50812, 2013

Sensitivity of stratospheric dynamics and chemistry to QBO nudging width in the chemistry-climate model WACCM

F. Hansen,[1] K. Matthes,[1] and L. J. Gray[2]

Received 8 April 2013; revised 3 September 2013; accepted 4 September 2013; published 20 September 2013.

[1] The consequences of different quasi-biennial oscillation (QBO) nudging widths on stratospheric dynamics and chemistry are analyzed by comparing two model simulations with the National Center for Atmospheric Research's Whole Atmosphere Community Climate Model (WACCM) where the width of the QBO is varied between 22° and 8.5° north and south. The sensitivity to the nudging width is strongest in Northern Hemisphere (NH) winter where the Holton-Tan effect in the polar stratosphere, i.e., stronger zonal mean winds during QBO west phases, is enhanced for the wider compared to the narrower nudging case. The differences between QBO west and east conditions for the two model experiments can be explained with differences in wave propagation, wave-mean flow interaction, and the residual circulation. In the wider nudging case, a divergence anomaly in the midlatitude upper stratosphere/lower mesosphere occurs together with an equatorward anomaly of the residual circulation. This seems to result in a strengthening of the meridional temperature gradient and hence a significant strengthening of the polar night jet (PNJ). In the narrower nudging case, these circulation changes are weaker and not statistically significant, consistent with a weaker and less significant impact on the PNJ. Chemical tracers like ozone, water vapor, and methane react accordingly. From a comparison of westerly minus easterly phase composite differences in the model to reanalysis and satellite data, we conclude that the standard WACCM configuration (QBO22) generates more realistic QBO effects in stratospheric dynamics and chemistry during NH winter. Our study also confirms the importance of the secondary mean meridional circulation associated with the QBO for the Holton-Tan effect.

Citation: Hansen, F., K. Matthes, and L. J. Gray (2013), Sensitivity of stratospheric dynamics and chemistry to QBO nudging width in the chemistry-climate model WACCM, *J. Geophys. Res. Atmos.*, *118*, 10,464–10,474, doi:10.1002/jgrd.50812.

1. Introduction

[2] The quasi-biennial oscillation (QBO) is the dominant mode of variability in the equatorial lower to upper stratosphere [*Baldwin et al.*, 2001]. It appears as downward propagating easterly and westerly wind regimes that alternate with a variable period around 28 months. The amplitude of the QBO is asymmetric in the westerly and easterly phases with around 20 m/s in maximum for QBO west and –30 m/s for QBO east and approximately symmetric and Gaussian about the equator with a half width of approximately 12° [*Baldwin et al.*, 2001; *Pascoe et al.*, 2005]. A secondary QBO circulation is induced in order to maintain thermal wind balance. This produces a wind anomaly in the subtropics of opposite sign to that at the equator [*Plumb and Bell*, 1982; *Gray*, 2010].

[3] Influenced by this secondary circulation, the QBO is clearly evident in the distribution of chemical constituents and trace gasses like water vapor, methane, CO, or N_2O in the tropical stratosphere. The structure of the QBO in these trace gasses is approximately symmetric about the equator but with a larger subtropical anomaly in the Northern Hemisphere [*Dunkerton*, 2001; *Schoeberl et al.*, 2008].

[4] The interannual variability of ozone is also dominated by the QBO. The respective roles of the ozone QBO in different heights have been investigated in several analyses of satellite and ground-based measurements of the ozone column [e.g., *Randel and Wu*, 1996; *Choi et al.*, 1998] and model studies [e.g., *Gray*, 2000; *Butchart et al.*, 2003; *Steinbrecht et al.*, 2006; *Tian et al.*, 2006; *Punge and Giorgetta*, 2008]. In particular, recent fully coupled chemistry models confirm the existence of a transition between the direct dynamic control of ozone below approximately 28 km and the indirect chemical control above that height. The QBO influences ozone in both of these regions [*Chipperfield et al.*, 1994].

[5] Although the QBO is defined in the tropics, it does not only influence the dynamics along the equator but also

[1]GEOMAR Helmholtz Centre for Ocean Research Kiel, Kiel, Germany.
[2]Centre for Atmospheric Sciences, Department of Atmospheric, Oceanic and Planetary Physics, University of Oxford, Oxford, UK.

Corresponding author: F. Hansen, GEOMAR Helmholtz Centre for Ocean Research Kiel, Düsternbrooker Weg 20, 24105 Kiel, Germany. (fhansen@geomar.de)

2169-897X/13/10.1002/jgrd.50812

in the extratropics and especially in the polar stratosphere. On average, the polar stratospheric vortex is colder and less disturbed in QBO west winters, while winters during QBO east phase tend to be warmer and more disturbed [*Holton and Tan*, 1980, 1982]. Holton and Tan proposed a mechanism to explain this equator-to-pole connection in winter. The so-called "Holton-Tan" mechanism involves planetary waves that can propagate into the tropical lower stratosphere during the westerly phase of the QBO since the zero wind line in the lower stratosphere, which acts as a critical surface for stationary planetary wave propagation, is positioned in the summer hemisphere. In contrast, during the QBO easterly phase, the planetary waves are guided further poleward because the zero wind line is positioned in the subtropics of the winter hemisphere and they can therefore disrupt the vortex more effectively.

[6] However, *Naoe and Shibata* [2010] and *Garfinkel et al.* [2012] have recently questioned the importance of this mechanism. In their studies they found no direct evidence for the Holton-Tan mechanism and suggested that the effect of the secondary QBO circulation may be more important for the polar QBO signal than the effect of the zero wind line. It introduces a barrier for planetary wave propagation in the middle to upper stratosphere during the easterly phase, resulting in enhanced planetary wave convergence in the polar region and therefore a more disturbed polar vortex. More recently, Watson, P. A. G. and L. J. Gray [How does the quasi-biennial oscillation affect the stratospheric polar vortex?, submitted to *Journal of Atmospheric Sciences*, 2013] noted that the typical response of the polar vortex to any sort of anomalous forcing is annular mode-like, and this makes it difficult to determine cause and effect. In reality, it is likely that the position of the zero wind line and also the secondary meridional circulation will both influence planetary wave propagation, but it is not clear which is the dominant mechanism. We try to address this question with this study.

[7] Simulating the QBO is a well-known shortcoming and one of the major challenges in modeling the middle atmosphere [e.g., *SPARC CCMVal*, 2010 report]. A growing number of climate models are able to successfully generate a spontaneous QBO [*Scaife et al.*, 2000; *Giorgetta et al.*, 2002; *Shibata and Deushi*, 2005; *Kulyamin et al.*, 2009; *Kawatani et al.*, 2010; *Anstey et al.*, 2010; *Xue et al.*, 2012]. However, there are still many general circulation models (GCMs) and chemistry-climate models (CCMs) that are not able to generate a spontaneous QBO. General reasons for this deficiency can be found in insufficient spatial resolution or problems in realistically simulating small-scale processes like tropical convection [*Scaife et al.*, 2000; *Giorgetta et al.*, 2002; *Shibata and Deushi*, 2005].

[8] In order to achieve a QBO in their simulations, models without a spontaneously generated QBO employ a "nudging" technique to relax the modeled zonal wind along the equator toward observations. However, it is not clear over what latitudinal range the nudging should be applied in order to achieve the optimum representation of the QBO impact on circulation and on tracer distributions, both of which are important factors for a good representation of stratospheric climate and chemistry. In the *SPARC CCMVal* [2010] report, the QBO nudging width ranged between 7° north and south in the ECHAM/MESSY Atmospheric Chemistry (EMAC) model to between 22° north and south in the National Center for Atmospheric Research's (NCAR) Whole Atmosphere Community Climate Model (WACCM) and even 23° north and south in the Universita degli Studi L'Aquila model. A large spread was also found between the models' representation of the QBO influence on both ozone and polar variability. For example, the EMAC model with a very narrow QBO nudging width reproduced best the tropical ozone variability, while WACCM, which nudged over a much wider latitudinal range, performed comparatively poorly in this aspect (compare with *SPARC CCMVal* [2010], Figure 8.14) but performed better in polar regions, especially in simulating the Northern Hemisphere (NH) winter jet strength [*SPARC CCMVal*, 2010, Figure 4.3] and frequency of Stratospheric Sudden Warmings. Because the different models differed not only in their nudging widths but in many other respects, it was not possible to obtain a clear understanding of whether these differences in performance of the models were directly related to the chosen width of the nudging employed.

[9] The goal of this study is therefore to investigate the impact of different QBO nudging widths on the representation of QBO temperature and circulation anomalies and their impact on trace gas distributions. The studies described above have shown that the QBO affects the stratosphere in multiple ways, through its direct control of dynamical variability in the tropics, its indirect effect on the high-latitude variability, and its influence on the distribution of ozone and other radiatively active trace gasses. It is therefore an important requirement for climate models to be able to represent its impact accurately. With our analysis, we also address the question of the mechanisms behind the polar QBO influence.

[10] *Hurwitz et al.* [2011] analyzed the sensitivity of the midwinter Arctic stratosphere to the variability of the QBO width with a simplified chemistry-climate model (version 4.5.1 of the UK Met Office Unified Model). They found that a wider QBO acts like a preferential shift toward the easterly phase of the QBO, i.e., a weaker NH polar vortex. In this study we extend their analysis using a fully coupled chemistry-climate model (WACCM) and place special emphasis on the representation of the Holton-Tan mechanism in the NH polar stratosphere.

[11] The outline of this paper is as follows: Section 2 describes the model, the QBO relaxation procedure, and the simulations. Section 3 compares the QBO in the model with reanalysis data. The QBO effects on NH stratospheric dynamics and chemistry are then tested for their sensitivity to the two different QBO relaxation widths in sections 4 and 5. Final conclusions are given and discussed in section 6.

2. Model Description

[12] The model used in this study is the National Center for Atmospheric Research (NCAR) Whole Atmosphere Community Climate Model, version 3.5 (WACCM3.5). WACCM is a fully interactive CCM extending from the Earth's surface to ∼145 km. It uses the physical parametrizations from the Community Atmospheric Model, version 3.5 and the finite volume dynamical core of *Lin* [2004] with

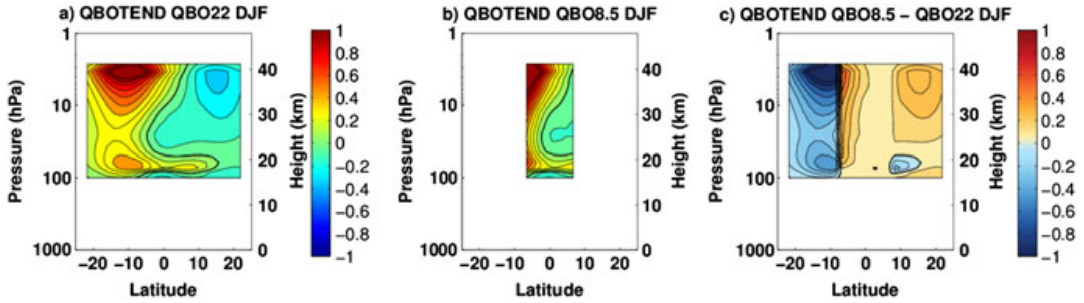

Figure 1. Wind tendency from QBO relaxation (1e-05 m/s/s) for (a) the QBO22 simulation, (b) the QBO8.5 simulation, and (c) differences between the QBO8.5 and QBO22 simulation. Contour interval 0.1 × 1e-05 m/s/s.

66 vertical levels. A detailed description of model physics specific to WACCM3 can be found in *Garcia et al.* [2007]. The changes in physical parametrization from WACCM3.1 to WACCM3.5 are described by *Richter et al.* [2010]. They mainly include changes in parametrization of convection and gravity wave drag which influences, e.g., the occurrence of sudden stratospheric warmings which are more realistic in the version used here.

[13] The horizontal resolution for the WACCM3.5 runs presented here is 1.9° × 2.5° (latitude × longitude). WACCM3.5 includes a detailed neutral chemistry scheme for the middle atmosphere based on the Model for Ozone and Related Tracers, version 3. The species included in this mechanism are contained within the O_x, NO_x, HO_x, ClO_x, and BrO_x chemical families, along with CH_4 and its degradation products [*Kinnison et al.*, 2007].

[14] Like many recent GCMs, WACCM3.5 is not able to generate a realistic QBO internally but shows weak easterlies above the equator instead. Therefore, a nudging technique based on *Balachandran and Rind* [1995] is used to relax the modeled tropical winds to observations [*Matthes et al.*, 2010]. The nudging is applied using a Gaussian weighting function decaying latitudinally from the equator with a half width of 10° which is close to the observed half width of the QBO of 10°–12° [*Baldwin et al.*, 2001]. Full vertical relaxation extends from 86 to 4 hPa, which is half that strong in one model level below and above this range (100 and 2.7 hPa, respectively) and zero for all other levels. The time constant for the relaxation of the zonal mean wind is 10 days [*Matthes et al.*, 2010]. Different from the nudging procedure described in *Matthes et al.* [2010], the semiannual oscillation (SAO) is not filtered out from the observed winds in our study before the model winds are nudged toward these winds.

[15] In the following, we will focus on extratropical feedbacks to equatorial changes because our experimental design does not allow the analysis of feedback processes in the opposite direction.

[16] *Richter et al.* [2008] found that WACCM generally exhibits a realistic middle atmosphere mean state and variability compared to observations. The most prominent model bias is an overestimation in the Southern Hemisphere (SH) polar stratospheric jet strength, which is also a common bias in other models [*SPARC CCMVal*, 2010]. Note that the frequency of stratospheric sudden warmings in the NH, an indicator of the stratospheric polar vortex variability, compares now well to ERA-40 in the model version used here (WACCM3.5) compared to WACCM version 3.1 [*Richter et al.*, 2010].

2.1. Experimental Design

[17] For this study we performed two simulations with WACCM3.5. In the first one, WACCM3.5 was run in the configuration which was also used in the SPARC CCMVal report [*SPARC CCMVal*, 2010] with the model's standard QBO nudging width extending from 22°S to 22°N and a height range of 86 to 4 hPa [*Matthes et al.*, 2010], called QBO22 hereafter. For the second simulation, called QBO8.5 hereafter, the QBO nudging width was reduced in latitudinal extend from 8.5°S to 8.5°N while the vertical range remained unchanged. The narrower nudging width of 8.5° was chosen as the closest poleward model latitude to 7°, the nudging width for the EMAC model (the model with the narrowest QBO nudging) in *SPARC CCMVal* [2010].

[18] Both simulations follow the SPARC CCMVal REF-B1 scenario [*SPARC CCMVal*, 2010] which includes the daily variations of the 11 year solar cycle and monthly variations of the QBO, Sea Surface Temperatures, greenhouse gasses, and ozone-depleting substances. Volcanic eruptions were prescribed as well. In these transient simulations, all forcings are taken from observations. The experiments cover a period from the recent past (1958–2006), of which the first 2 years of spin-up have been neglected for analysis.

[19] Figure 1 shows the wind tendency from the QBO relaxation for the QBO22 and QBO8.5 experiments in their respective nudging regions for NH winter. The strongest intervention on the modeled wind takes place in the summer hemisphere, where the prevailing easterlies are forced toward smaller amplitudes. This has also been described as the "net effect of the QBO" in *Punge and Giorgetta* [2008]. The largest differences between the forcings in QBO22 and QBO8.5 occur poleward from 8.5° in the SH (or rather in the summer hemisphere in general), where the nudging is only applied in QBO22, and equatorward of 8.5° where a stronger intervention is done in QBO8.5 (Figure 1c). Within the shared nudging region in the SH, the forcing is stronger in QBO8.5 as the prevailing easterlies are stronger in this simulation, i.e., the differences to the observed winds are larger. In the winter hemisphere, the wind tendency differences between the two simulations are smaller. So we note that the two experiments are not expected to be identical

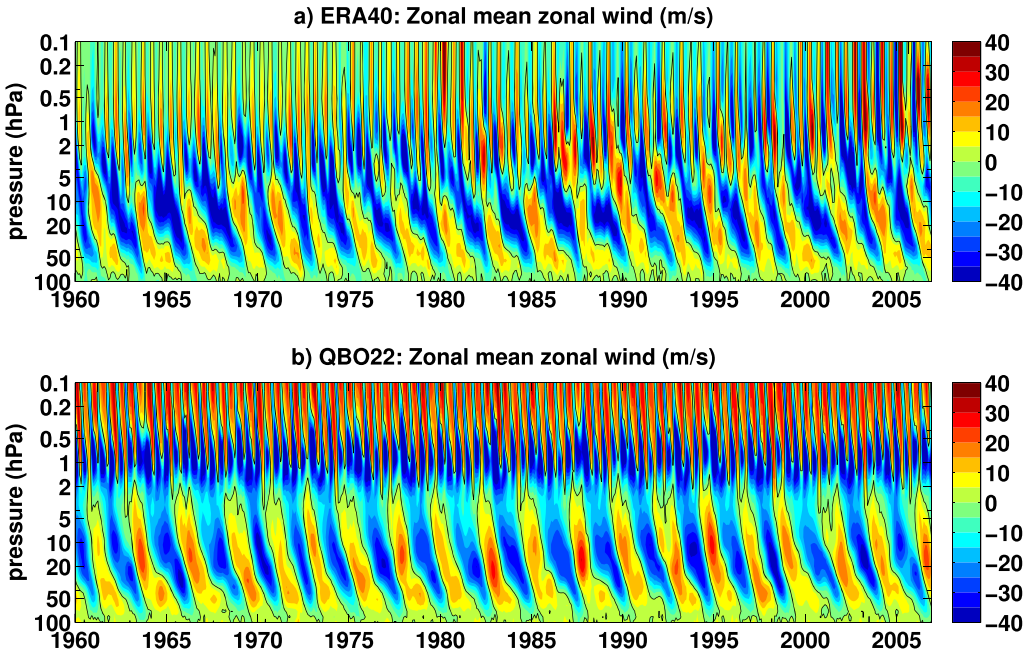

Figure 2. Zonal mean zonal wind (m/s) in the equatorial stratosphere, averaged between 2.8°S and 2.8°N, for (a) ERA-40 and (b) the QBO22 simulation, with black contour indicating the zero wind line.

above the equator, not even in the shared nudging region between 8.5° south and north.

3. QBO: Definition and Comparison Between WACCM and ERA-40

[20] As the goal of this study is to investigate WACCM's sensitivity to the width of the QBO, the next step is to compare the QBO in the model to reanalysis data. For that, the extended ERA-40 reanalysis data (abbreviated "ERA-40" in the following) are used, which means the 40 year European Centre for Medium-Range Weather Forecasts (ECMWF) Re-Analysis (ERA-40) data set [*Uppala et al.*, 2004] extended to 2008 by using the ECMWF operational analysis [*Frame and Gray*, 2010]. Different studies use different definitions for the QBO, e.g., the equatorial wind at 40 [*Baldwin et al.*, 2001; *Gray*, 2000; *Baldwin and Dunkerton*, 1998], at 44 [*Gray et al.*, 2004], or at 50 hPa and averaged over 10°S–10°N [*Yamashita et al.*, 2011] with the phases defined as positive or negative wind velocities at that level or as amplitudes more than +/– 5 m/s [*Gray*, 2000; *Gray et al.*, 2004].

[21] To differentiate between the westerly and easterly phase of the QBO, we define a QBO time series as the zonal mean zonal wind averaged between 2.8°S and 2.8°N and 43 and 51 hPa. With the resolution of WACCM3.5, this is an average over 4×2 grid points. We label a time step as QBO west phase (QBOW) when the average exceeds 5 m/s and QBO east phase (QBOE) when it falls below –2.5 m/s. The motivation for picking these particular wind thresholds is that this QBO definition turned out to be most suitable for WACCM as it leads to QBO west and east phases with approximately equal lengths.

[22] Figures 2a and 2b display the zonal mean zonal wind averaged along the equator between 2.8°S and 2.8°N for ERA-40 reanalysis data and the QBO22 simulation, respectively, for the simulated period of our experiment from 1960 to 2006. We see the expected agreement between the simulation and ERA-40 in the structure of the QBO below 10 hPa where direct wind observations exist and are assimilated in the ERA-40 data. We do not expect a perfect match between WACCM and ERA-40 for several reasons: (i) the model levels are not the same as the levels of the observations, so there might be some interpolation differences, (ii) the nudging is applied with a time constant of 10 days; this leaves some freedom to the model's resolved small-scale waves which can influence the zonal mean flow, (iii) especially in the upper part of the nudging region, the modeled SAO, which is shifted upward in WACCM as discussed in *Matthes et al.* [2010] and as can be observed in Figure 2, interacts with the SAO from the observed winds; this leads to especially QBO westerly phases reaching into higher levels compared to ERA-40, and (iv) further away from the equator, the nudging weights decay with a Gaussian function.

4. QBO Effects on Stratospheric Winter Dynamics

[23] In order to examine the effect of the QBO on tropical and extratropical dynamics in the two runs, composite differences, where QBOE composites of quantities such as zonal mean zonal wind, temperature, Eliassen-Palm (EP) flux, and residual mean meridional circulation are subtracted from QBOW composites, are computed. "Composite" thereby means the average of the quantity over all months being in the same QBO phase, e.g., QBO westerly phase for the QBOW composite. We focus the following analysis on the representation of the Holton-Tan mechanism in the northern polar winter stratosphere.

4.1. Polar Night Jet

[24] Figure 3 shows the zonal mean zonal wind differences between QBO westerly and easterly phase for Northern Hemisphere (NH) winter (December, January and February (DJF)) for the QBO22 and the QBO8.5 simulation and for ERA-40. The significance of the differences has been tested with a two-tailed Student's *t* test, and colors in Figure 3 (as in the following figures) denote that differences are statistically significant at the 95% confidence level. All figures reveal the prominent features of the equatorial QBO which is a statistically significant sandwich structure of the zonal mean zonal wind in the tropical stratosphere with a westerly wind speed anomaly of more than 20 m/s at about 40 hPa, an easterly anomaly of about 30 m/s above at about 5 hPa, and a smaller westerly anomaly of about 12 m/s above at 1 hPa. This feature is broader in QBO22 than in QBO8.5 which is a direct effect of the broader nudging along the equator in this run. Notable is also the broader extent of the easterly anomaly in height.

[25] In the extratropics, both WACCM simulations show a QBO response in the zonal mean wind which agrees with *Holton and Tan*, [1980, 1982] who showed that the polar vortex (and therefore the polar night jet (PNJ)) is stronger during QBOW phase and weaker during QBOE phase. The wind differences in the QBO22 experiment reach up to 14 m/s. That means that they are stronger and more significant at high latitudes than the wind differences in the QBO8.5 experiment which are 8 m/s at their maximum. We have also tested the statistical significance of the differences between the QBO22 and QBO8.5 responses in Figures 3a and 3b and note that the difference in response of the strength of the PNJ is significant at the 95% level, confirming that the high-latitude response is stronger in QBO22 than in QBO8.5.

[26] In ERA-40 (Figure 3c), the anomalies in the polar night reach up to 12 m/s and are statistically significant almost throughout the jet region. The PNJ anomalies in QBO8.5 are significantly weaker than in ERA-40 data, and hence, the Holton and Tan effect is more realistically reproduced in QBO22 than in QBO8.5.

4.2. Wave-Mean Flow Interactions

[27] The reasons for the nudging-dependent different responses in the PNJ can be related to differences in the propagation of planetary waves and/or its interactions with the mean flow. To analyze the origin of the zonal mean wind differences, we use the Transformed Eulerian Mean (TEM) equations [*Andrews et al.*, 1987] which describe the EP flux vector, its divergence, and the residual mean meridional circulation (meaning the meridional circulation in the TEM formalism, with v^* and w^* as its meridional and vertical components). While the EP flux vector describes the strength and propagation direction of planetary waves, its divergence describes the interaction of planetary waves with the mean flow: In a region of divergence of the EP flux vector, the mean flow is accelerated to the east, while in convergent regions, acceleration to the west occurs. Depending on the respective mean flow, this leads to a strengthening or a weakening of the circulation. During NH winter conditions with prevailing westerly background winds, a divergence (convergence) leads to acceleration (deceleration) of the flow.

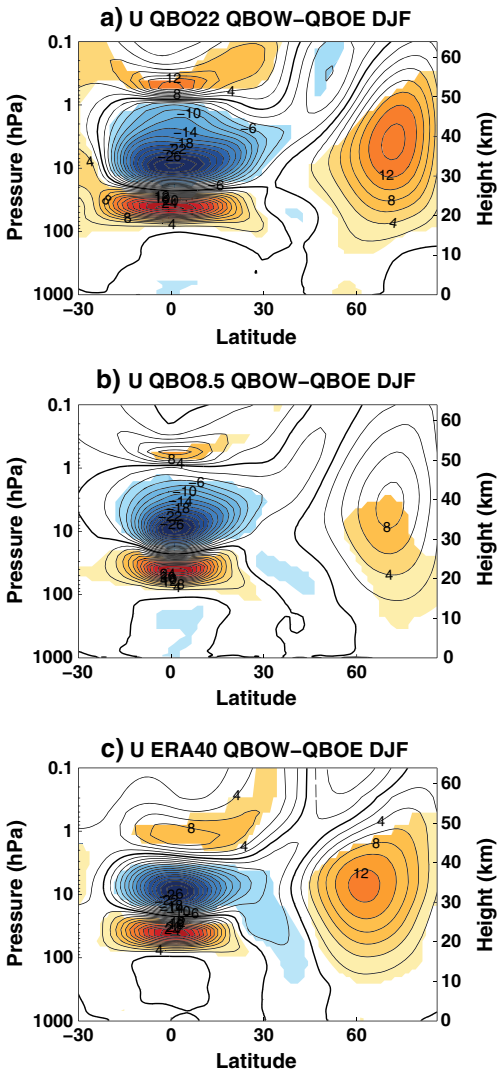

Figure 3. Differences of the zonal mean zonal wind (in m/s) between QBOW and QBOE years for (a) the QBO22, (b) the QBO8.5 experiment, and (c) ERA-40 in DJF. Contour interval: 2 m/s; color shading indicates 95% statistically significant differences.

[28] In Figure 4, vectors indicate the magnitude and direction of the EP flux vector differences between QBOW and QBOE conditions while anomalies of the EP flux vector divergence are depicted by contours. Red colors (contours and shading) mean positive (divergent) EP flux vector anomalies, and blue colors stand for negative (convergent) EP flux vector anomalies. Shaded areas highlight statistically significant differences.

[29] In Figure 4a (showing QBO22), positive EP flux divergence anomalies appear around 60°N and 0.3 hPa, i.e., exactly where we have seen the pronounced positive zonal mean wind differences in Figure 3 which indicate a strengthening of the PNJ during QBO west conditions.

[30] The zonal momentum TEM equation reveals that changes in the divergence of the EP flux vector are linked to anomalies of the residual mean circulation in the way that

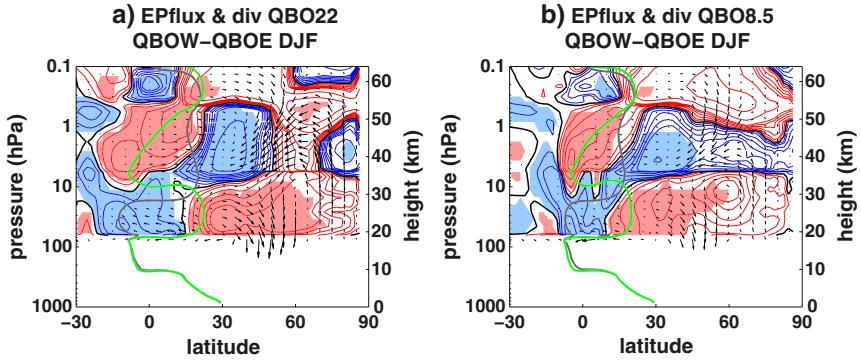

Figure 4. Differences of the EP Flux vector (arrows; scaled with the square root of pressure) and its divergence (contours; in $ms^{-1}d^{-1}$) between QBOW and QBOE years for (a) the QBO22 and (b) the QBO8.5 experiment. Contour lines: +/– 0, 0.05, 0.1, 0.2, 0.3, 0.4, 0.5, 1.0, 2.0, and 5.0 $ms^{-1}d^{-1}$; shading indicates 95% statistically significant divergence differences. The grey (green) line indicates the zero line of the zonal mean zonal wind during QBOW (QBOE) phase.

divergence leads to an equatorward anomaly of the residual circulation. This enhanced equatorward circulation can indeed be seen at around 60°N above 1 hPa in Figure 5a (for QBO22) where the QBOW–QBOE differences of the residual mean circulation are shown by vectors; the contours indicate temperature anomalies. Related to the equatorward anomaly of the residual circulation is the upward anomaly (i.e., a weakening of the prevailing net downwelling) in polar regions, especially in the upper stratosphere, together with the downward motion anomaly around 60°N, which is strongest around 1 hPa but reaches down to 10 hPa (Figure 5a for QBO22). The upward anomaly causes adiabatic cooling, while the downward anomaly leads to adiabatic warming. This together results in a strengthening of the meridional temperature gradient poleward of 60°N during QBOW as can be seen in the temperature anomaly contours in Figure 5a. The meridional temperature gradient is linked to the zonal wind by the thermal wind equation and thus is consistent with the statistically significant strengthening of the PNJ in Figure 3a.

[31] Most of the discussed features and relations can be seen in both simulations (QBO22 and QBO8.5, Figures 5a and 5b, respectively), though the response in QBO8.5 tends to be generally weaker. However, we find a major difference: In QBO8.5, there is no significant divergence anomaly in the midlatitude upper stratosphere/lower mesosphere (Figure 4b) and hence no significant effect on the residual mean circulation (Figure 5b). This is consistent with temperature anomalies that are not statistically significant throughout the PNJ region (especially not in the region of cold anomalies north of 60°N), i.e., we do not find the significant strengthening of the meridional temperature gradient which would support the significant strengthening of the jet. This implies a weaker and less statistically significant stratospheric polar vortex in QBO8.5 compared to QBO22 (Figure 3).

[32] In the tropics and NH subtropics, differences in the QBO anomalies of the EP flux vector, its divergence (Figure 4), and the residual circulation (Figure 5) between the QBO22 and QBO8.5 simulation appear only in the strength but not in the pattern of the signal. Here the anomaly patterns of the EP flux vector and its divergence involve the latitudinal position of the zero wind line which is related to the QBO (grey (QBOW) and green (QBOE) line in Figure 4). This line plays an important role for the propagation of planetary waves since these waves can

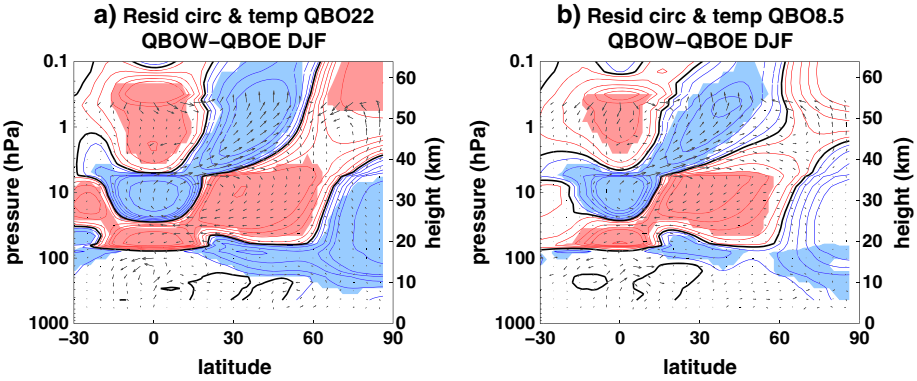

Figure 5. Same as Figure 4 but for the mean residual circulation (arrows) and temperature (contours; in °C). Contour lines: +/– 0°C, 0.2°C, 0.5°C, 1°C, 1.5°C, 2°C, 4°C, and 8°C; shading indicates 95% statistically significant temperature differences.

only propagate in (not too strong) westerly wind regimes [*Charney and Drazin*, 1961]. In the lower stratosphere around 50 hPa during QBOW, the zero wind line shifts equatorward (grey line). Planetary waves that propagate from the extratropics toward the equator can reach the equatorial lower stratosphere, whereas they are reflected to higher latitudes during QBOE (green line). Higher up in the equatorial stratosphere above 10 hPa the opposite occurs: Planetary waves propagating from the NH midlatitude troposphere toward the low-latitude upper stratosphere are restricted to the extratropics during QBOW, whereas these waves can reach the equator during QBOE, when the zero wind line is located in the Southern Hemisphere. A poleward anomaly of the EP flux vector consistent with that can be found here – in a region of consistent easterly wind anomalies seen in Figure 3 – with a divergence anomaly at the equator and a convergence anomaly around 30°N (Figure 4). The poleward anomaly of the residual mean meridional circulation (Figure 5) in the convergence anomaly region is consistent because here the converged waves lead to an enhanced wave-mean flow interaction, meaning stronger wave-induced transfer of energy and momentum to the mean flow. This reduces the mean westerly flow and, due to the disturbance of the quasi-geostrophic balance, can lead to an intensification of the poleward residual circulation in this region.

[33] In summary, our analysis suggests that the QBO nudging width in WACCM significantly influences the propagation of planetary waves as seen in the EP flux vector and its divergence as well as the residual circulation between QBO west and east years. Especially in the midlatitude upper stratosphere, differences in the divergence of the EP flux vector and hence in the residual circulation occur between QBO west and east conditions which could significantly impact meridional temperature gradient and are consistent with wind signals in the PNJ. Clear differences are seen between QBO22 and QBO8.5 reflecting the impact of the QBO nudging width on extratropical circulation.

5. QBO Effects on Chemistry

[34] Since dynamical changes like those induced by the QBO have an influence on the distribution of chemical tracers, the influence of the QBO nudging width on stratospheric chemical constituents, namely ozone and water vapor, is investigated.

[35] To see which of the WACCM simulations behaves more realistically compared to observational data, the differences between QBOW and QBOE conditions for ozone and water vapor obtained from the Global Ozone Chemistry And Related trace gas Data records for the Stratosphere (GOZCARDS) project are analyzed. GOZCARDS products are merged data sets based primarily on measurements from satellite-borne instruments and from National Aeronautics and Space Administration missions studying the Earth's stratosphere since the late 1970s. The data products used here are the ozone data set [*Wang et al.*, 2013], available from 1979 to 2012 (with the years 1981–1983 missing) in 10° latitude bins and the water vapor data set [*Anderson et al.*, 2013], available for the period 1991–2012. Since the GOZCARDS data contain fewer QBO cycles than the model data, less statistically significant results can be obtained.

5.1. Ozone

[36] The concentration of ozone in the stratosphere is a result of a combination of transport and photochemical processes. The direct impact of transport decreases with height in favor of the importance of chemical processes where the boundary between transport dominated and chemically dominated regions is often mentioned to be at 28 km (e.g., *Brasseur et al.* [1999]). While for the transport of trace species into, within, and out of the stratosphere, both the large-scale circulation and mixing processes associated with waves play a role, chemical ozone depletion not only depends on the available amount of ozone-depleting substances, but also on temperature.

[37] Figure 6 shows the differences in ozone between the QBOW and QBOE phases for the QBO22 and the QBO8.5 simulations (Figures 6a and 6b). Like for the wind anomalies, a sandwich structure is evident above the equator but only in a height range between 100 and 5 hPa in a region where the nudging has been applied, and around and below the maximum of stratospheric ozone mixing ratio at 10 hPa where the ozone concentration is dominated by transport processes. The signal peaks around 70 hPa, with an up to 30% higher ozone mixing ratio during QBOW compared to QBOE, and is quite symmetric around the equator. Additionally, a statistically significant negative ozone signal can be found in the NH polar regions around 100 hPa that extends into midlatitudes.

[38] Like for zonal wind (see previous section), the ozone differences between QBOW and QBOE conditions appear differently in the QBO22 and the QBO8.5 simulation. First, the response above the equator, i.e., the described sandwich structure, is much stronger in QBO22 than in QBO8.5, with maximum ozone differences of up to 30% compared to 20%. This is consistent with the differences between the two QBO runs in circulation (i.e., transport), concerning both strength and significance. During QBOW, the mean Brewer-Dobson circulation tropical upwelling is suppressed (Figure 4). This relative downwelling is stronger in QBO22 than in QBO8.5 which can be particularly seen in the tropical QBOW–QBOE temperature signal (Figure 5) that reaches up to 4°C in QBO22 compared to 2°C in QBO8.5.

[39] The negative polar ozone signal is strong and significant in QBO22 but very weak in the QBO8.5 run. The negative signal itself can be explained with the significantly lower temperatures during QBOW in these regions (Figure 5) which slow down the ozone production rates and also lead to more efficient ozone depletion. In addition, because of the weakened downwelling seen in the mean residual circulation signal in the polar region (Figure 5), less ozone is transported into this region. On the other hand, the negative ozone anomaly itself can also be partly responsible for the negative temperature anomaly, since ozone absorbs solar radiation and outgoing infrared radiation. Less ozone therefore means less radiation absorption and therefore lower temperatures. Both responses, in temperature and in ozone, feed back to each other. The negative temperature anomaly has been shown to be much weaker and less significant in QBO8.5 (Figure 5) which is consistent with the weaker response in ozone in this run.

[40] Differences above 5 hPa are less prominent since they are determined by the available amount of reaction

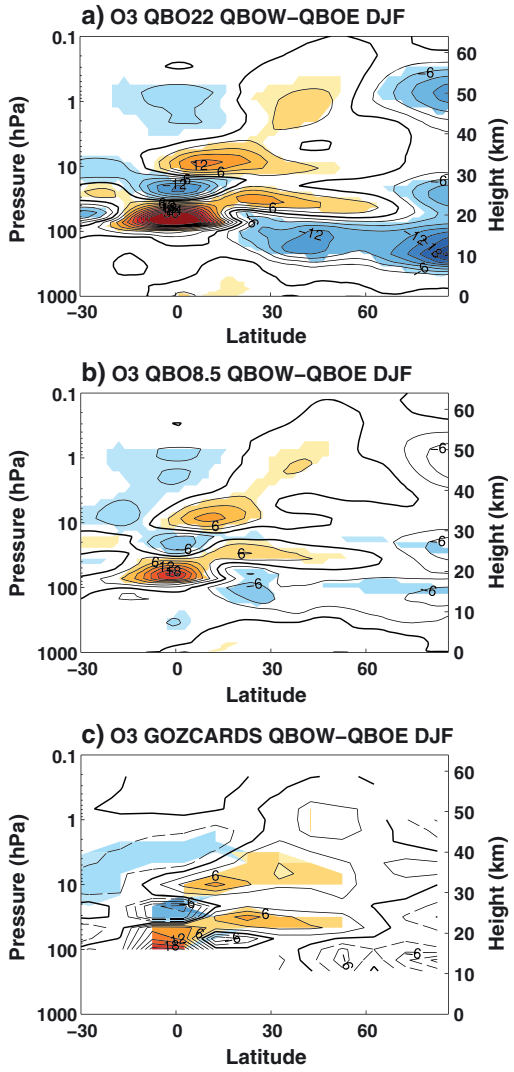

Figure 6. Differences of ozone (in %) between QBOW and QBOE years for (a) the QBO22, (b) the QBO8.5 experiment, and (c) for GOZCARDS data (1979–2012). Contour interval: 3%; color shading indicates 95% statistically significant differences.

partners for photochemical reactions (primarily NO_y (the total reactive nitrogen reservoir) [*Brasseur and Solomon*, 2005]) which are similar in both runs.

[41] Comparing our two WACCM simulations with the observed QBOW–QBOE differences from GOZCARDS (Figure 6c) reveals that the QBOW–QBOE differences above the equator are well represented in QBO8.5, while QBO22 slightly overestimates the response. In the lower stratosphere polar regions, however, it is the QBO22 experiment which outperforms the QBO8.5 simulation again, as the strength of the negative QBO signal is captured much better here. Note that due to the shorter time period of the GOZCARDS data, less statistical significances are achieved.

5.2. Water Vapor and Methane

[42] The long-lived trace gasses methane and water vapor (where "long-lived" refers to stratospheric water vapor) are transported into the lower tropical stratosphere by upwelling from the troposphere and are then transported poleward and downward by the Brewer-Dobson circulation [*Brasseur and Solomon*, 2005]. In the stratosphere, water vapor increases with height due to production via methane oxidation in this altitude [*Brasseur and Solomon*, 2005]. Therefore, the QBO response of methane and water vapor mimic each other but with opposite sign (water vapor gain = methane loss) which is why we show only the results for water vapor and discuss it where they differ from the results for methane.

[43] Figure 7 shows the difference in water vapor between the westerly and easterly QBO phase for the two WACCM experiments. In the region of the tropopause, strong positive QBO anomalies occur. These anomalies have their maximum above the equator, decrease with latitudes, and can only be seen in water vapor but not in methane. This signal can be explained with the QBO response in temperature that shows positive anomalies, i.e., higher temperatures during QBOW than QBOE, around the tropical tropopause (compare contours in Figure 5). With anomalous high temperatures, more water vapor can enter the equatorial lower stratosphere leading to the positive H_2O response at the tropical tropopause (Figure 7).

[44] Comparing now our two simulations QBO22 and QBO8.5, we mainly find differences in the strength of the signals. Especially the QBO signal of water vapor in the equatorial tropopause region is weaker in QBO8.5 than in QBO22 and restricted to a smaller latitudinal width. Furthermore, the negative anomaly above the equator around 50 hPa is almost twice as strong in QBO22 compared to QBO8.5.

[45] As it has already been observed for ozone, we find a strong QBOW–QBOE anomaly in water vapor in the NH polar lower stratosphere. It changes sign from negative (below) to positive (above) around 25 km, i.e., lies within the altitudes where water vapor concentration is dominated by transport processes. In the polar region above the tropopause, a weakened downwelling (upward anomalies) occurs in the mean residual circulation in QBOW compared to QBOE (see Figure 5) which leads to a weaker downward transport of water vapor and therefore the negative water vapor anomaly above the tropopause and the positive anomaly above. The change of sign of the signal at the pole in the stratosphere occurs exactly around the altitude of the maximum polar temperature response (also in Figure 5). The anomaly is, like for ozone, both stronger and significant in a larger region in the simulation with the wider QBO nudging.

[46] Comparing now the QBO response in WACCMs water vapor to the observed QBOW–QBOE response in GOZCARDS, we find that the structure of the signal in both constituents compares well with observations, although none of the simulations captures the strong positive anomaly above the equator around 3hPa seen in the observations. However, GOZCARDS in general shows a slightly stronger response above 50 hPa which is better represented in QBO22 than in QBO8.5.

[47] In summary for the water vapor and methane differences between the westerly and the easterly QBO phase, we find that the QBO22 run slightly better reproduces the strength of the signal but uncertainties in the observations [*Anderson et al.*, 2013] prevent firm final conclusions. The differences in water vapor and methane between the two runs are smaller than the differences seen for ozone.

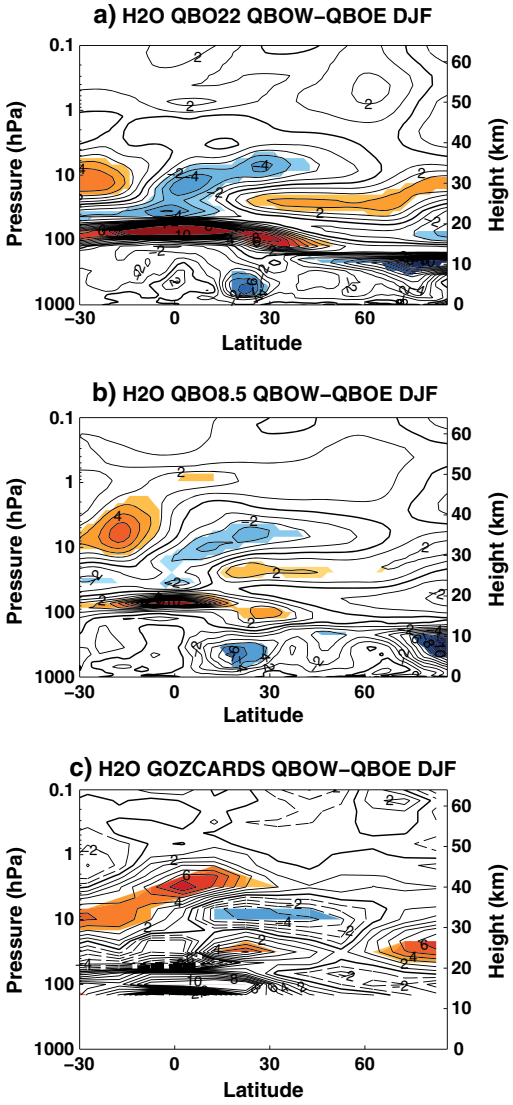

Figure 7. Same as Figure 6 but for water vapor; GOZCARDS data for 1991–2012. Contour interval: 1%; color shading indicates 95% statistically significant differences.

This confirms the findings of the SPARC CCMVal report [*SPARC CCMVal*, 2010] where WACCM was mentioned to perform very well in the stratospheric chemistry intercomparison with the exception of some deficits in representing H_2O in the polar regions.

6. Conclusions and Discussion

[48] Two 47 year simulations with the fully interactive chemistry-climate model WACCM version 3.5 were used to study the influence of the QBO nudging width on stratospheric dynamics and chemistry. For the control run, WACCM's standard QBO nudging width extending from 22°S to 22°N was used; for the second run, the latitudinal range of the wind relaxation was reduced to 8.5° south and north.

[49] The analysis of the atmospheric response to differences between QBOW and QBOE conditions in both model simulations revealed that differences in the QBO responses between the two simulations arise especially in the region of the stratospheric PNJ during NH winter (DJF). In QBO22, the zonal mean wind in the PNJ was found to be up to 14 m/s stronger during the westerly phase of the QBO than during QBOE, while the QBO response in QBO8.5 reached values only up to 8 m/s and showed less statistical significance in particular in the upper stratosphere and lower mesosphere.

[50] The connection between the equatorial QBO and the higher latitudes is consistent with the Holton-Tan mechanism, yet there are different theories on the importance of different effects: the effect of the zero wind line in the lower stratosphere which is shifted away from the equator during QBOE leading to planetary waves being reflected poleward or the effect of the secondary QBO circulation in the middle to upper stratosphere where a "barrier" to planetary wave propagation is created during QBOE in midlatitudes so that these waves converge in the polar region. From our analysis, we cannot present clear proof of the causality of this mechanism. However, dynamical arguments lead to a consistent explanation of the chain of events: In the QBO22 experiment during QBO west years, a divergence anomaly of the EP flux vector occurs around 60°N in the upper stratosphere/lower mesosphere, together with enhanced equatorward wave propagation and an equatorward anomaly of the residual mean circulation. This is consistent with a strengthening of the meridional temperature gradient in higher latitudes and hence a significant strengthening of the PNJ during QBOW. In QBO8.5, these changes in wave propagation and dissipation as well as the residual circulation are weaker than in QBO22 and not statistically significant, consistent with a weaker and less significant impact on the PNJ. Thus, our study suggests that changes in wave propagation and dissipation in the midlatitude middle to upper stratosphere associated with the equatorial QBO play a role in the modulation of the stratospheric polar vortex, similar to the findings of *Naoe and Shibata* [2010] and *Garfinkel et al.* [2012], although we note that this does not exclude a direct contribution from wave reflection at the zero wind line, as proposed originally by *Holton and Tan* [1980, 1982] [see also Watson, P. A. G. and L. J. Gray, submitted to *Journal of Atmospheric Sciences*, 2013].

[51] Consistent with the Holton and Tan response in the dynamical parameters, WACCM shows a signal in chemical tracers such as ozone, water vapor, and methane. Again, the response in QBO22 is stronger and more significant than in QBO8.5 whereupon the differences between the two experiments were larger for ozone than for water vapor and methane. The concentration and composition of these chemical constituents below 10 hPa are determined mostly by transport, while temperature-dependent chemical reactions determine the concentration and composition above that height. Therefore, the differences in chemical tracers between QBO22 and QBO8.5 in the two QBO phases are entirely consistent with the differences in the circulation and the slowing down or acceleration of the reaction velocities through changes in temperature.

[52] As a result of our investigation, we find that the optimal nudging width for WACCM is close to the model's

standard nudging width, i.e., between 22° south and north, which was also used for the *SPARC CCMVal* [2010] report. A generalization for all models can not be given within this study. When using this nudging width, the response of planetary wave propagation and the residual circulation to the forcing from the equatorial QBO agrees well with ERA-40. The QBO zonal wind response in the QBO22 run does not differ significantly from the response in ERA-40 (overestimation by +2 m/s) which reaches up to 12 m/s significantly higher wind speeds in the PNJ during QBOW compared to QBOE, whereas QBO8.5 significantly underestimates the ERA-40 response by 4 m/s. For the QBO response in chemical tracers, a comparison with GOZCARDS-merged data products confirms that the QBO22 simulation performs better than the QBO8.5 simulation keeping in mind the uncertainties in the GOZCARDS data itself. With our study we confirm a role for the mean meridional circulation associated with the QBO in influencing the polar stratospheric QBO response, although we emphasize that this does not mean that the direct mechanism proposed by *Holton and Tan* [1980, 1982] via reflection at the zero wind line is not also operating. Future studies should focus on investigating QBO effects in the recently successfully generated internal QBO in WACCM [*Xue et al.*, 2012] in order to study feedback processes between the tropical and middle to high latitudes in both directions.

[53] **Acknowledgments.** This work has been performed within the Helmholtz-University Young Investigators Group NATHAN funded by the Helmholtz-Association through the President's Initiative and Networking Fund, the Helmholtz Centre for Ocean Research Kiel (GEOMAR), the German Centre for Geosciences Potsdam (GFZ), and the Freie Universität Berlin. We thank Christopher Kadow for performing the model calculations at the Deutsche Klimarechenzentrum (DKRZ) Hamburg, Germany, and the GOZCARDS team for providing the ozone and water vapor data sets. We would like to particularly thank Chaim Garfinkel and two anonymous reviewers for their comments which helped to improve the manuscript considerably.

References

Anderson, J., L. Froidevaux, R. A. Fuller, P. F. Bernath, N. J. Livesey, H. C. Pumphrey, W. G. Read, Russell J. M. III, and K. A. Walker (2013), GOZCARDS merged data for water vapor monthly zonal means on a geodetic latitude and pressure grid, version 1.01. Greenbelt, MD, USA: NASA Goddard Earth Science Data and Information Services Center. Accessed at doi:10.5067/MEASURES/GOZCARDS/DATA3004.

Andrews, D. G., J. Holton, and C. Leovy (1987), *Middle Atmosphere Dynamics*, Academic Press, San Diego, California.

Anstey, J. A., T. G. Shepherd, and J. F. Scinocca (2010), Influence of the quasi-biennial oscillation on the extratropical winter stratosphere in an atmospheric general circulation model and in reanalysis data, *J. Atmos. Sci.*, *67*(5), 1402–1419, doi:10.1175/2009JAS3292.1.

Balachandran, N. K., and D. Rind (1995), Modeling the effects of UV variability and the QBO on the troposphere–stratosphere system. 1. The middle atmosphere, *J. Clim.*, *8*(8), 2058–2079.

Baldwin, M. P., and T. J. Dunkerton (1998), Biennial, quasi-biennial, and decadal oscillations of potential vorticity in the northern stratosphere, *J. Geophys. Res.*, *103*(D4), 3919–3928, doi:10.1029/97JD02150.

Baldwin, M. P., et al. (2001), The quasi-biennial oscillation, *Rev. Geophys.*, *39*(2), 179–229.

Brasseur, G. P., J. J. Orlando, and G. S. Tyndall (1999), *Atmospheric Chemistry and Global Change*, Oxford University Press, New York, NY, USA.

Brasseur, G. P., and S. Solomon (2005), *Aeronomy of the Middle Atmosphere: Chemistry and Physics of the Stratosphere and Mesosphere*, 3rd ed., Springer, Dordrecht, The Netherland.

Butchart, N., A. A. Scaife, J. Austin, S. H. E. Hare, and J. R. Knight (2003), Quasi-biennial oscillation in ozone in a coupled chemistry-climate model, *J. Geophys. Res.*, *108*(D15), 4486, doi:10.1029/2002JD003004.

Charney, J. G., and P. G. Drazin (1961), Propagation of planetary-scale disturbances from the lower into the upper atmosphere, *J. Geophys. Res.*, *66*, 83–109.

Chipperfield, M. P., L. J. Gray, J. S. Kinnersley, and J. Zawodny (1994), A two-dimensional model study of the QBO signal in SAGE II NO_2 and O_3, *Geophys. Res. Lett.*, *21*(7), 589–592, doi:10.1029/94GL00211.

Choi, W., W. B. Grant, J. H. Park, K. M. Lee, H. Lee, and J. M. Russell (1998), Role of the quasi-biennial oscillation in the transport of aerosols from the tropical stratospheric reservoir to midlatitudes, *J. Geophys. Res.*, *103*(D6), 6033–6042, doi:10.1029/97JD03118.

Dunkerton, T. J. (2001), Quasi-biennial and subbiennial variations of stratospheric trace constituents derived from HALOE observations, *J. Atmos. Sci.*, *58*(1), 7–25, doi:10.1175/1520-0469(2001)058<0007:QBASVO>2.0.CO;2.

Frame, T. H. A., and L. J. Gray (2010), The 11-yr solar cycle in ERA-40 data: An update to 2008, *J. Clim.*, *23*(8), 2213–2222, doi:10.1175/2009JCLI3150.1.

Garcia, R. R., D. R. Marsh, D. E. Kinnison, B. A. Boville, and F. Sassi (2007), Simulation of secular trends in the middle atmosphere, 1950–2003, *J. Geophys. Res.*, *112*, D09301, doi:10.1029/2006JD007485.

Garfinkel, C. I., T. A. Shaw, D. L. Hartmann, and D. W. Waugh (2012), Does the Holton–Tan mechanism explain how the quasi-biennial oscillation modulates the arctic polar vortex? *J. Atmos. Sci.*, *69*(5), 1713–1733, doi:10.1175/JAS-D-11-0209.1.

Giorgetta, M. A., E. Manzini, and E. Roeckner (2002), Forcing of the quasi-biennial oscillation from a broad spectrum of atmospheric waves, *Geophys. Res. Lett.*, *29*(8), 1245, doi:10.1029/2002GL014756.

Gray, L. J. (2000), A model study of the influence of the quasi-biennial oscillation on trace gas distributions in the middle and upper stratosphere, *J. Geophys. Res.*, *105*(D4), 4539–4551, doi:10.1029/1999JD900320.

Gray, L. J., S. Crooks, C. Pascoe, S. Sparrow, and M. Palmer (2004), Solar and QBO influences on the timing of stratospheric sudden warmings, *J. Atmos. Sci.*, *61*(23), 2777–2796.

Gray, L. J. (2010), Stratospheric equatorial dynamics, in The Stratosphere: Dynamics, transport, and chemistry, *Geophys. Monogr. Ser.*, *190*, 93–107.

Holton, J. R., and H.-C. Tan (1980), The influence of the equatorial quasi-biennial oscillation on the global circulation at 50 mb, *J. Atmos. Sci.*, *37*, 2200–2208.

Holton, J. R., and H.-C. Tan (1982), The quasi-biennial oscillation in the Northern Hemisphere lower stratosphere, *J. Meteorol. Soc. Jpn.*, *60*, 140–148.

Hurwitz, M. M., P. Braesicke, and J. A. Pyle (2011), Sensitivity of the mid-winter Arctic stratosphere to QBO width in a simplified chemistry-climate model, *Atmos. Sci. Lett.*, *12*, 268–272.

Kawatani, Y., K. Sato, T. J. Dunkerton, S. Watanabe, S. Miyahara, and M. Takahashi (2010), The roles of equatorial trapped waves and internal inertia-gravity waves in driving the quasi-biennial oscillation. Part I: Zonal mean wave forcing, *J. Atmos. Sci.*, *67*(4), 963–980, doi:10.1175/2009JAS3222.1.

Kinnison, D. E., et al. (2007), Sensitivity of chemical tracers to meteorological parameters in the MOZART-3 chemical transport model, *J. Geophys. Res.*, *112*, D20302, doi:10.1029/2006JD007879.

Kulyamin, D. V., E. M. Volodin, and V. P. Dymnikov (2009), Simulation of the quasi-biennial oscillations of the zonal wind in the equatorial stratosphere: Part II. Atmospheric general circulation models, *Izv. Atmos. Oceanic Phys.*, *45*(1), 37–54, doi:10.1134/S0001433809010046.

Lin, S. J. (2004), A "vertically lagrangian" finite-volume dynamical core for global models, *Mon. Weather Rev.*, *132*(10), 2293–2307, doi:10.1175/1520-0493(2004)132<2293:AVLFDC>2.0.CO;2.

Matthes, K., D. R. Marsh, R. R. Garcia, D. E. Kinnison, F. Sassi, and S. Walters (2010), Role of the QBO in modulating the influence of the 11 year solar cycle on the atmosphere using constant forcings, *J. Geophys. Res.*, *115*, D18110, doi:10.1029/2009JD013020.

Naoe, H., and K. Shibata (2010), Equatorial quasi-biennial oscillation influence on northern winter extratropical circulation, *J. Geophys. Res.*, *115*, D19102, doi:10.1029/2009JD012952.

Pascoe, C. L., L. J. Gray, S. A. Crooks, M. N. Juckes, and M. P. Baldwin (2005), The quasi-biennial oscillation: Analysis using ERA-40 data, *J. Geophys. Res.*, *110*, D08105, doi:10.1029/2004JD004941.

Plumb, R. A., and R. C. Bell (1982), A model of the quasi-biennial oscillation on an equatorial beta-plane, *Q. J. R. Meteorolog. Soc.*, *108*, 335–352.

Punge, H. J., and M. A. Giorgetta (2008), Net effect of the QBO in a chemistry climate model, *Atmos. Chem. Phys.*, *8*(21), 6505–6525.

Randel, W., and F. Wu (1996), Isolation of the ozone QBO in SAGE II data by singular-value decomposition, *J. Atmos. Sci.*, *53*, 2546–2559.

Richter, J. H., F. Sassi, and R. R. Garcia (2010), Toward a physically based gravity wave source parameterization in a general circulation model, *J. Atmos. Sci.*, *67*, 1136–156, doi:10.1175/2009JAS3112.1.

Richter, J. H., F. Sassi, R. R. Garcia, K. Matthes, and C. A. Fischer (2008), Dynamics of the middle atmosphere as simulated by the Whole Atmosphere Community Climate Model, version 3 (WACCM3), *J. Geophys. Res.*, *113*, D08101, doi:10.1029/2007JD009269.

Scaife, A. A., N. Butchart, C. D. Warner, D. Stainforth, W. Norton, and J. Austin (2000), Realistic quasi-biennial oscillations in a simulation of the global climate, *Geophys. Res. Lett.*, *27*(21), 3481–3484.

Schoeberl, M. R., et al. (2008), QBO and annual cycle variations in tropical lower stratosphere trace gases from HALOE and AURA MLS observations, *J. Geophys. Res.*, *113*, D08101, doi:10.1029/2007JD008678.

Shibata, K., and M. Deushi (2005), Partitioning between resolved wave forcing and unresolved gravity wave forcing to the quasi-biennial oscillation as revealed with a coupled chemistry-climate model, *Geophys. Res. Lett.*, *32*, L12820, doi:10.1029/2005GL022885.

SPARC CCMVal, (2010), SPARC report on the evaluation of chemistry-climate models, *SPARC-Report No. 5*, WCRP-132,WMO/TD-No. 1526, SPARC CCMVal.

Steinbrecht, W., et al. (2006), Interannual variation patterns of total ozone and lower stratospheric temperature in observations and model simulations, *Atmos. Chem. Phys.*, *6*, 349–374.

Tian, W. S., M. P. Chipperfield, L. J. Gray, and J. M. Zawodny (2006), Quasi-biennial oscillation and tracer distributions in a coupled chemistry-climate model, *J. Geophys. Res.*, *111*, D20301, doi:10.1029/2005JD006871.

Uppala, S., et al. (2004), ERA-40: ECMWF 45-year reanalysis of the global atmosphere and surface conditions 1957–2002, *ECMWF Newsletter*, *101*, 2–21.

Wang, R., L. Froidevaux, J. Anderson, R. A. Fuller, P. F. Bernath, M. P. McCormick, N. J. Livesey, J. M. Russell III, K. A. Walker, and J. M. Zawodny (2013), GOZCARDS merged data for ozone monthly zonal means on a geodetic latitude and pressure grid, version 1.01. Greenbelt, MD, USA: NASA Goddard Earth Science Data and Information Services Center. Accessed at doi:10.5067/MEASURES/GOZCARDS/DATA3006.

Xue, X. H., H. L. Liu, and X. K. Dou (2012), Parameterization of the inertial gravity waves and generation of the quasi-biennial oscillation, *J. Geophys. Res.*, *117*, D06103, doi:10.1029/2011JD016778.

Yamashita, Y., H. Akiyoshi, and M. Takahashi (2011), Dynamical response in the Northern Hemisphere midlatitude and high-latitude winter to the QBO simulated by CCSR/NIES CCM, *J. Geophys. Res.*, *116*, D06118, doi:10.1029/2010JD015016.

4 Tropospheric QBO-ENSO interactions and differences between Atlantic and Pacific

This chapter, which is a reprint of an article of the same title submitted to *Journal of Climate*, presents analyses on the tropospheric influence of the stratospheric QBO. The analyses fill a gap of existing studies by taking into account the interaction with ENSO in the QBO's tropospheric response. As the signals turn out to be zonally asymmetric, a distinction is made between the North Atlantic and North Pacific sector. For this study, the CESM-WACCM "NATURAL", "FixedSSTs" and "NOQBO" simulations introduced in Chapter 2 are analyzed, but the "FixedSSTs" and "NOQBO" experiments have been extended from 2010 until 2099.

Citation: **Hansen, F., K. Matthes, and S. Wahl, 2015: Tropospheric QBO-ENSO interactions and differences between Atlantic and Pacific. Submitted to J. Climate.**

The authors' contributions to this publication are as follows:

- *F. Hansen initiated the study, performed one of the three model simulations, did all the analyses, produced all figures and wrote the manuscript.*
- *K. Matthes contributed with ideas and discussions on the analysis and with comments on the manuscript.*
- *S. Wahl extended two of the three model simulations.*

Tropospheric QBO-ENSO interactions and differences between Atlantic and Pacific

Felicitas Hansen*, Katja Matthes† and Sebastian Wahl

GEOMAR Helmholtz Centre for Ocean Research Kiel, Kiel, Germany

Corresponding author address: GEOMAR Helmholtz Centre for Ocean Research Kiel, Düsternbrooker Weg 20, 24105 Kiel, Germany.

E-mail: fhansen@geomar.de

†2nd affil.: Christian-Albrechts-Universität zu Kiel, Kiel, Germany

ABSTRACT

This study is the first which investigates the interaction of the Quasi-Biennial Oscillation (QBO) and the El Nino-Southern Oscillation (ENSO) in the troposphere. Furthermore, the combined tropospheric QBO-ENSO response is examined separately for the North Pacific and the North Atlantic region. Three 145-year model simulations with NCAR's Community Earth Sytem Model (CESM-WACCM) are analyzed where only natural and no anthropogenic forcings are considered. These long simulations allow to obtain statistically reliable results from an exceptional large number of cases for each combination of the QBO (westerly and easterly) and ENSO phases (El Niño and La Niña).

The analyses reveal that the stratospheric equatorial QBO anomalies extend down to the troposphere over the North Pacific during Northern hemisphere winter only during La Niña and not during El Niño events. The conditions for the genesis and intensification of synoptic-scale waves are improved during QBO west (QBOW) as compared to QBO east (QBOE) conditions by linear QBO-ENSO interactions. The Aleutian low is deepened, and the subtropical jet is strengthened and shifted northward.

In the North Atlantic, the non-linear interaction of QBOW with La Niña conditions (QBOE with El Niño) results in a positive (negative) North Atlantic Oscillation pattern. The other two combinations counteract the North Atlantic ENSO signal.

The results provide potential to enhance the skill of tropospheric seasonal predictions in the North Atlantic and North Pacific region. Predictions in the area of Northern hemisphere storm tracks have large socio-economic relevance.

1. Introduction

The Quasi-Biennial Oscillation (QBO) is the dominant mode of variability in the equatorial lower to upper stratosphere (Baldwin et al. 2001). It appears as alternating westerly and easterly wind regimes which propagate downward with an average period of 28 months. By influencing the propagation of planetary waves and their interaction with the mean flow at middle and high latitudes, the tropical QBO affects the mean state and variability in the extra-tropical and even polar stratosphere. A colder and more stable stratospheric polar vortex is observed during its westerly phase (QBOW) and a warmer, more disturbed polar vortex during its easterly phase (QBOE) (Holton and Tan 1980, 1982; Anstey and Shepherd 2014).

Although the QBO is primarily a stratospheric phenomenon, there are at least two ways in which it can affect the troposphere: 1) directly in the tropics and extra-tropics, by modifying, e.g., properties which are important for stratosphere-troposphere exchange in this region, or 2) indirectly through its effect on the stratospheric polar vortex; at the poles, anomalies can propagate down and affect extra-tropical surface weather and climate.

It might be natural to assume that the QBO has an effect on the tropical troposphere, bearing in mind the dominance of the oscillation for the variability in the overlying stratosphere. It has been shown that the tropical troposphere has its own biennial or quasi-biennial oscillation (Meehl 1987, 1993), which is often referred to as the tropical or tropospheric biennial oscillation (TBO) (Meehl (1997)). The TBO is irregular in time and asymmetric in longitude (Xu 1992; Chang and Li 2000; Baldwin et al. 2001). Several studies linked the TBO to the Southern Oscillation (e.g. Berlage 1955; van Loon and Madden 1981; Meehl 1987; Kiladis and Van Loon 1988; Ropelewski et al. 1992) and the Asian monsoon (e.g. Lau 1992; Meehl 1997; Loschnigg et al. 2003). However, no linear correlation exists with the stratospheric QBO (Barnett 1991; Xu 1992). Nonlinear or multi-

variate relationships between the two oscillations have been investigated, e.g., by Maruyama and Tsuneoka (1988); Kwan and Abu Samah (2003), but no consensus has been reached so far.

Aside from a QBO-TBO connection, the QBO has nevertheless been shown to influence the tropical and subtropical troposphere. Through the QBO modulation of temperature and vertical wind shear along the tropical tropopause (Gray et al. 1992; Huang et al. 2012), stronger tropical deep convection (Gray et al. 1992; Collimore et al. 2003) and a stronger Hadley circulation (Rind and Balachandran 1995; Hitchman and Huesmann 2009) is observed during QBOE compared to QBOW conditions. This strengthening of the Hadley circulation leads to a weakening of the tropospheric subtropical jet during QBOE compared to QBOW conditions, especially in the North Pacific region (Garfinkel and Hartmann 2011a,b). Other tropical and subtropical phenomena are thereby affected as well: Strong hurricanes in the tropical Atlantic occur significantly more often during QBOW conditions and vice versa (e.g., Shapiro 1989). In the western North Pacific, the tracks (though not the number) of tropical cyclones depend on the QBO phase (Ho et al. 2009). The boreal summer monsoon is also influenced significantly by the phase of the QBO (e.g., Giorgetta et al. (1999)). Fadnavis et al. (2011) found a dependance of cyclones in the Bay of Bengal on the QBO, which occur more often during QBOE conditions and change their tracks depending on the QBO and monsoon phases. Seo et al. (2013) reports that the spring rainband over eastern China and the Japanese islands is located further south during QBOW than during QBOE conditions.

At high latitudes, the QBO signal in the stratospheric polar vortex can be seen as a clear AO/NAO response at the surface. The tropospheric anomalies follow the stratospheric anomalies by 2–3 weeks (Baldwin and Dunkerton 1999). This has some implications for mid-latitude surface weather, e.g., over Europe. During QBOE conditions, the mean surface temperatures are below normal and the frequency of winter cold spells increases (Marshall and Scaife 2009).

In this study, we investigate the influence of the stratospheric QBO on the troposphere, and how the tropospheric QBO signal interacts with the El Niño-Southern Oscillation (ENSO). ENSO is the dominant mode of global sea surface temperature (SST) variability (Trenberth 1997). It consists of a seesaw between warm and cold SST anomalies in the equatorial Pacific, but influences both the regional and global weather and climate via a number of teleconnections. The strongest ENSO effects can be observed in the troposphere, but its effects on the stratosphere, especially on the polar regions during winter, are also well-pronounced. During the ENSO warm phase (El Niño), a significantly warmer stratospheric polar vortex occurs, as shown in observational studies, e.g., by van Loon and Labitzke (1987); Camp and Tung (2007); Mitchell et al. (2011) and confirmed in model studies, e.g., by Sassi et al. (2004); Manzini et al. (2006); Taguchi and Hartmann (2006); Ayarzagüena et al. (2013). Manzini et al. (2006) and Ayarzagüena et al. (2013) suggested that the Aleutian low is deepened during El Niño events which enhances the forcing and vertical propagation of planetary waves from the troposphere into the stratosphere, resulting in a weaker and warmer stratospheric polar vortex. This in turn influences the frequency of stratospheric sudden warmings (SSWs) which are extreme events of an anomalously weak stratospheric polar vortex. Altogether, there seems to be a tropospheric (via tropospheric teleconnections) and a stratospheric (via SSWs) pathway of ENSO influencing the troposphere as recently suggested from reanalysis data by Butler et al. (2014).

By influencing the same regions as described for the QBO above, it is likely that ENSO also has an effect on the QBO signals in both the stratosphere and the troposphere. Taguchi (2010) used radiosonde data to investigate the dependence of the QBO amplitude and period at the equator on ENSO warm and cold phases. He observed that the QBO amplitude is significantly weaker during El Niño than during La Niña events, and that the QBO period is longer during La Niña and shorter during El Niño. Yuan et al. (2014) recently confirmed these results, also using radiosonde

data, and demonstrated the zonal symmetry of ENSO's influence on the equatorial QBO along the tropopause.

Some studies investigated the ENSO influence on the QBO signal and vice versa with a focus on the stratospheric polar night jet region. Wei et al. (2007) analyzed reanalysis atmospheric data and reconstructed ocean data and found that the QBO response in the Northern Hemisphere (NH) wintertime stratospheric polar vortex is significant during La Niña, but much weaker during El Niño, because the QBO modulation of planetary wave propagation is only significant during La Niña. Garfinkel and Hartmann (2007) investigated different combinations of both ENSO with both QBO phases in reanalysis data and found that ENSO only has an effect on NH polar stratospheric temperatures during QBOW, but not during QBOE conditions. Another outcome of their study is that during either El Niño or QBOE, the influence of the other factor on the polar vortex is weakened, suggesting a nonlinear interaction of both phenomena. Calvo et al. (2009) confirmed this nonlinear behaviour between QBOE and El Niño conditions in their model study. They also suggested that El Niño intensifies (weakens) the QBO polar vortex response in early (late) winter. This has direct implications for the duration of the QBO signal in the NH polar stratosphere and the speed of the downward propagation of the signal.

Most of the studies which investigate the QBO influence on the troposphere do not take into account ENSO as an additional altering factor, mainly because the observational data used in these studies are too short to distinguish in a statistically reasonable way between all the different combinations of QBO and ENSO phases. However, knowledge about the interaction between QBO and ENSO signals in the troposphere is important, e.g., for improved tropospheric weather predictions. The QBO itself has been shown to be predictable up to three years in advance (Scaife et al. 2014) and can potentially add skill to forecasts on different timescales (Boer and Hamilton 2008; Tripathi et al. 2014).

In this study, we use three long (145 years) simulations of NCAR's Community Earth Sytem Model (CESM-WACCM) where anthropogenic greenhouse gas forcings were set to constant 1960 conditions. We investigate the combined QBO-ENSO effect in the troposphere without any anthropogenic factors. We focus on the NH winter and examine the tropospheric QBO-ENSO interaction separately for the North Pacific and the North Atlantic since the tropospheric QBO signal has been shown to be hidden when global zonally averaged fields are investigated (Garfinkel and Hartmann 2011a). Switching off the anthropogenic influence in the model simulations neglects one of the factors which could conceal the QBO or ENSO signals and allows us to investigate pure natural and internal variability. The length of the model simulations allows us to analyze composites of each of the QBO-ENSO combinations with enough cases to obtain statistically robust signals. By comparing CESM-WACCM simulations where either the QBO or ENSO has been switched off, we shortly address the question of the nonlinearity of the QBO-ENSO interaction.

This paper is organized as follows: Section 2 briefly describes NCAR's CESM-WACCM model and the simulations analyzed in this study. Section 3 explains how the composites for QBO and ENSO phases are computed. Section 4 deals with the identification of a QBO signal in zonal mean zonal wind and how this interacts with ENSO, followed by the analysis of the combined QBO-ENSO signals in some tropospheric and surface parameters in Section 5. A brief investigation on the (non-)linearity of the QBO-ENSO interaction follows in Section 6. Finally, the main outcomes are summarized and discussed in section 7.

2. Model Simulations

The model simulations analyzed in this study were performed with the National Center for Atmospheric Research (NCAR) Community Earth System Model (CESM-WACCM) version 1.0.2. CESM is a state-of-the-art coupled model system, containing an interactive ocean, land, sea ice

and atmosphere component. The atmosphere component used here is the Whole Atmosphere Community Climate Model (WACCM) version 4, a fully interactive chemistry-climate model, extending on 66 vertical levels from the Earth's surface to ∼140 km altitude (Garcia et al. 2007; Richter et al. 2010). WACCM is run on a horizontal grid of 1.9 x 2.5° (latitude x longitude); the interactive ocean and sea ice components are run on a 1 x 1° triangular horizontal grid and are described in Holland et al. (2012) and Danabasoglu et al. (2012).

The experiments analyzed in this study correspond to the "NATURAL", "Fixed SSTs" and "NOQBO" experiments described in Hansen et al. (2014). Unless otherwise stated, the results presented in the following are obtained from the "NATURAL" simulation, a 145 year model run (1955–2099) where only natural but no anthropogenic factors are considered.

The "Fixed SSTs" and "NOQBO" simulations are used to give an estimate of how much of a combined tropospheric QBO-ENSO signal comes from either linear or non-linear interactions. Both simulations have been extended since Hansen et al. (2014) and now span the period 1955–2099. The "Fixed SSTs" experiment uses the climatological annual cycle from the "NATURAL" experiment for the underlying SST and sea ice forcing, and repeats this forcing for each of the simulated years. For the "NOQBO" simulation, the equatorial QBO nudging is switched off, which leads to relatively constant but weak easterlies in the equatorial stratosphere of about -10 m/s. All other settings in these two experiments are equivalent to the "NATURAL" simulation.

3. Method: Composites of QBO and ENSO phases

In the following analysis, we compute composites of anomalies of different parameters for QBO and ENSO phases separately, as well as for combinations of QBO and ENSO phases together. Anomalies are computed with respect to the climatology. A month is defined as being in the westerly QBO phase (QBOW), when the zonal mean zonal wind averaged along the equator between

2.8°S and N and between 40 and 50hPa exceeds 5 m/s during that month. An easterly QBO phase (QBOE) occurs, when this wind average falls below -2.5 m/s. The ENSO phases are defined via the Nino3.4 index like in Trenberth (1997): if the 5-months running mean of SST anomalies in the Niño3.4 region (5°N – 5°S, 170° – 120°W) exceeds 0.4°C (falls below -0.4°C) for at least 6 consecutive months, an El Niño (La Niña) phase occurs.

The anomalies investigated here are strongest during the NH winter season from November through February (NDJF), and therefore we show four-months averages in the following. The NDJF average is representative for the NH winter signal. Including several months increases the number of cases for the respective phases in the composites, leading to statistically more reliable signals. Statistical significance has been tested with a two-sided t-test, and colours in the following composite figures denote that the anomalies are significantly different from the climatology at the 90% confidence interval.

Some of the following composites show zonally averaged anomalies; however, as some of the investigated signals are zonally asymmetric, we distinguish between different longitudinal sectors as well. The Atlantic sector is defined between 10 and 50°W, and the Pacific sector between 160°E and 160°W.

4. QBO and ENSO signals in zonal mean zonal wind

a. Separate effects

We first investigate how the two QBO phases (QBOW and QBOE) and the two ENSO phases (El Niño and La Niña) influence the NH zonal mean zonal wind alone. Therefore, we compute averages of zonal mean zonal wind anomalies during those months where the respective phases occur. Figure 1 shows composites of zonal mean zonal wind anomalies for QBOW (Fig. 1 a),

QBOE (Fig. 1 b), La Niña (Fig. 1 c) and El Niño (Fig. 1 d) averaged for the NH winter season from November to February (NDJF). The number of cases for each of the composites can be read from Table 1.

Figure 1 a) and b) show the prominent features of the QBO: a ”sandwich” structure of statistically significant zonal mean zonal wind anomalies of alternating sign in the tropical to subtropical stratosphere. In the polar stratosphere, the wind speeds in the stratospheric polar night jet are significantly increased during QBOW and significantly decreased during QBOE conditions.

The zonal mean zonal wind anomalies due to the two ENSO phases (Figure 1 c) and d)) show that the zonal mean zonal wind is stronger (weaker) than normal in the tropical to mid-latitude troposphere and lower stratosphere during El Niño (La Niña). Around 60 °N, the zonal mean wind speeds are decreased (increased) during El Niño (La Niña) from the surface to the middle stratosphere. Another significant ENSO signal of the same sign can be found in the mid-latitude upper stratosphere/lower mesosphere.

Except for this latter ENSO anomaly, the ENSO response in zonal mean zonal wind is confined to the troposphere, while the zonal mean QBO response is confined to the stratosphere. Garfinkel and Hartmann (2011a) showed in their model study that the tropospheric anomalies occurring in connection with the different QBO phases are hard to detect when globally zonally averaged fields are investigated, since the signals are zonally asymmetric and vary strongly between the North Atlantic and North Pacific. We confirm their findings, as can be seen in Figure 2 d), e) and f), where the composite differences of zonal mean zonal wind between QBOW and QBOE in NDJF are shown for a global average as well as the Pacific and the Atlantic separately. The climatologies of the zonal mean zonal wind in NDJF averaged over the respective sectors are shown in Figures 2 a), b) and c) for comparison. Only in the North Pacific, the equatorial QBO wind anomalies, which occur in the stratosphere around 50hPa, arch downward into the subtropical troposphere in

a horseshoe-shaped pattern, suggesting a significant influence of the QBO on the subtropical jet in this region (Figure 2 e)). No significant tropospheric QBO influence can be seen in the global mean (Figure 2 d)) or in the North Atlantic (Figure 2 f)).

b. Combined effects

The next step is to analyze the combined QBO-ENSO signal, i.e., the anomalies which occur when one of the QBO phases exists together with one of the ENSO phases. Figure 3 shows composites of zonal mean zonal wind anomalies during NDJF for the four possible combinations of QBO and ENSO phases. In Figure 3 a), the anomaly composite is built from months where the above mentioned criteria for QBOW and La Niña are met simultaneously, in Figure 3 b), the conditions for QBOE and El Niño are fulfilled at the same time, and so on. The number of cases for each of the four combinations can be obtained from Table 1.

From Figure 3 we can see that the strongest response in the stratospheric polar night jet occurs when either QBOW and La Niña (Figure 3 a) or QBOE and El Niño (Figure 3 b) happen simultaneously. During the other two combinations, the response in this region is very weak. In general, it seems that for the combinations of QBOW with La Niña as well as QBOE with El Niño the resulting anomalies in zonal mean zonal wind are nonlinearly enhanced compared to the separate signals shown in Figure 1. For example, during the combined occurrence of QBOW and La Niña (Figure 3 a), the polar night jet is significantly stronger than during QBOW (Figure 1 a)) or La Niña (Figure 1 c)) alone (more than 5 m/s higher than climatologically versus $\sim$3 plus $\sim$1 m/s higher than climatologically). On the contrary, for the combinations of QBOW with El Niño (Figure 3 c) and QBOE with La Niña (Figure 3 d), the response throughout the troposphere and the stratosphere is composed linearly as the sum of the separate anomalies.

These results partly confirm Calvo et al. (2009) who reported that the QBOE phase intensifies in

a nonlinear way the weak and warm El Niño polar vortex response. However, their finding that QBOW phases, too, have the same effect on the El Niño signal, cannot be confirmed here.

Distinguishing again between the Pacific and Atlantic sector (Figure 4) reveals that the statistically significant downward arching of the QBO wind signal (i.e., QBOW minus QBOE composite difference) from the equatorial stratosphere into the mid latitude troposphere in the North Pacific sector occurs only during La Niña events (Figure 4 b)), but is absent during El Niño events (Figure 2 e)). This combined QBO/La Niña effect can also be observed in the global average of zonal mean zonal wind (Figure 4 a)).

In the North Atlantic sector, it is also a La Niña phase which connects a stratospheric QBO signal with the troposphere (Figure 4 c)). Here this coupling happens at high latitudes, where a statistically significant negative QBOW–QBOE anomaly extends from the stratosphere down to the troposphere during La Niña phases, while El Niño phases change the general QBO signal only slightly (Figure 4 f)).

5. Combined QBO and ENSO signals in tropospheric fields

The former analysis of combined QBO/ENSO effects suggests that the QBO influence on the subtropical jet is only significant during La Niña phases. In this section we aim at analyzing in more detail the combined QBO-ENSO signal in several tropospheric variables. Figure 5, 1st column, shows the NH winter season (NDJF) climatology (1st row) and composite differences for zonal wind at 300hPa between QBOW and QBOE phases without separating into ENSO phases (2nd row), and considering La Niña (3rd row) and El Niño (4th row). The westerly subtropical jet is significantly stronger over the western North Pacific during QBOW compared to QBOE conditions, and its maximum is shifted northward (Figure 5 d)). Consistent with the previous findings of Figure 4, this tropospheric QBO signal is modified in different regions by the two ENSO phases:

while La Niña amplifies the significant signal and lets it extend further eastward over the central and eastern North Pacific (Figure 5 g)), no significant wind changes are seen in this region during El Niño (Figure 5 j)). Instead, during El Niño phases, the QBO signal shows statistically significant higher wind speeds during QBOW compared to QBOE conditions over the North Atlantic in the region of the North Atlantic storm track, and significantly lower wind speeds over the central North Atlantic and central Europe (Figure 5 j)).

The geopotential height (GPH) at 500 hPa (shown in Figure 5, 2nd column), is without ENSO influence significantly lower by up to 25 m during QBOW compared to QBOE conditions in the western North Pacific, extending over the eastern Eurasian continent around 60 °N (Figure 5 e)). As expected from the findings for the winds at 300 hPa, this significant signal is again extended towards the central and eastern North Pacific during La Niña, and more zonally oriented then (Figure 5 h)). In addition to the negative GPH anomaly over the North Pacific, a positive anomaly over the pole occurs. Again, the influence of El Niño phases appears as a statistically significant signal over the North Atlantic. The GPH is significantly increased by around 20 m south of the North Atlantic storm track region, while the significant QBO signal in the western North Pacific/eastern Eurasian continent is almost absent (Figure 5 k)). Altogether this combined QBO/El Niño signal resembles the positive phase of the Arctic Oscillation (AO) pattern.

At the surface, a combined QBO-ENSO signal can also be seen in sea level pressure (SLP) anomalies (Figure 5, 3rd column). The QBO signal without ENSO influence (Figure 5 f)) shows a significant SLP decrease of up to 2 hPa in the region of the climatological Aleutian low (compare Figure 5 c)) in the northern North Pacific during QBOW compared to QBOE conditions. Two centers of significant SLP increase during QBOW compared to QBOE conditions can be found over the Barents Sea and Northeastern Europe which extend the climatological high pressure system over Asia. During La Niña phases these regions of significant QBO anomalies are strengthend

(Figure 5 i)). During El Niño phases the QBO surface signal in the North Pacific is absent like at higher altitudes for the GPH and the zonal wind (Figure 5 l)). Instead, a new statistically significant combined QBO-ENSO signal establishes in the North Atlantic during El Niño phases which projects onto the positive phase of the North Atlantic Oscillation (NAO) (Figure 5 l)). Statistically significant positive SLP anomalies of more than 1.5hPa can be found southeast of Newfoundland and over Northeastern Europe.

Possible mechanisms

From Figure 6, we can obtain some additional information about the interaction of the single QBO phases with the single ENSO phases by looking exemplarily at GPH anomaly composites for the two QBO and ENSO phases, respectively, and their four combinations separately. Over the North Pacific and eastern Eurasian continent, the combined QBO-ENSO signal (Figure 6 e–h) seems to be a linear superposition of the single QBO (Figure 6 a and b) and ENSO (Figure 6 c and d) signals. The significant anomalous GPH decrease over the eastern Eurasian continent during QBOW is extended towards the whole North Pacific by the equally signed GPH anomaly in this region occurring during El Niño phases, while it is extinguished in combination with La Niña. The QBO alone does not have a significant influence on the North Atlantic GPH, while the ENSO phases have: during El Niño (La Niña) phases, the GPH is significantly increased (decreased) around Iceland, and significantly decreased (increased) in a broad band south of that extending over the North Atlantic and central Europe, hence it strongly projects onto the NAO. This North Atlantic signal changes when QBO and ENSO phases are combined: when a QBOW phase occurs together with an El Niño phase (Figure 6 e), the significant negative GPH anomaly band generated by El Niño is limited to the western North Atlantic and does not extend over Europe. The same is true when QBOE and La Niña phases act together (Figure 6 h). Only QBOW in combination

with La Niña (Figure 6 f) as well as QBOE in combination with El Niño (Figure 6 g) sustain and even increase the significant ENSO influence on the North Atlantic. Knowledge about this can be very useful for tropospheric weather prediction over the North Atlantic region and Europe where a significant influence on GPH has direct implications, e.g., for the strength and tracks of extra-tropical cyclones and hence for primary meteorological parameters like wind, temperature and precipitation.

To explore further the QBO-ENSO-interaction which lead to different effects in the North Pacific and North Atlantic region, the baroclinicity is investigated. As a parameter representing baroclinicity, the Eady Growth Rate (abbreviated "EADY" in the following) is chosen. EADY was developed by Eady (1949) from a two-layer model and is computed as $EADY = 0.31 \cdot \frac{f}{N} \cdot |\frac{\Delta \vec{v}}{\Delta z}|$, with f being the Coriolis parameter, N the Brunt-Väisälä frequency and $\frac{\Delta \vec{v}}{\Delta z}$ the vertical wind shear between two layers. Via thermal wind balance, the vertical wind shear is proportional to the meridional temperature gradient, and therefore EADY becomes large at frontal zones and is a measure for baroclinic instability.

Figure 7 a–c shows composite differences between QBOW and QBOE conditions with and without separation into ENSO phases (analogous to Figure 5) for EADY at 850 hPa. The QBO alone (Figure 7 a) increases baroclinic instability significantly over the western North Pacific during QBOW conditions. Then, conditions for genesis and intensification of synoptic-scale waves are improved in this region which is the favored track of North Pacific cyclones. During La Niña phases, this signal is even stronger, being consistent with the findings discussed in the previous section (Figure 7 b). In the North Atlantic, only the contemporaneous occurrence of El Niño phases lead to a significant signal which consists of an increase in baroclinicity south of Greenland and a decrease around 30 °N (Figure 7 c). This suggests a northward shift of the North Atlantic storm track. Coinciding with El Niño phases, the QBO signal over the North Pacific vanishes.

Baroclinic instability can increase where the meridional SST gradient is increased. Thus, the QBO signal in SSTs depending on the ENSO phases is additionally investigated (Figure 7 d–f). In the western North Pacific, a strengthening of the meridional SST gradient occurs during QBOW compared to QBOE conditions, consistent with the increase in baroclinic instability. The EADY changes due to the QBO in the North Atlantic which are observed only during El Niño phases also seem to be controlled by changes in the SST gradient.

Altogether, we find that the QBO alone does not have a significant influence on the troposphere over the Atlantic, but on the Pacific. Here, during QBOW compared to QBOE winters, conditions for the genesis and intensification of synoptic-scale waves are improved through a strengthening of the meridional SST gradient which leads to enhanced baroclinic instability. The Aleutian low is deepened, and the subtropical jet is stronger and shifted northward. This Pacific QBO signal is stronger and extended during La Niña and absent during El Niño. An Atlantic NAO signal establishes during the combinations QBOW/La Niña and QBOE/El Niño.

6. Non-linear signals

As a last point in this study, we want to briefly analyze how much of the signal interpreted as a combined QBO-ENSO signal might result from a linear or non-linear superposition of the two phenomena. For this, we use the ”NOQBO” and ”FixedSST” simulations where the QBO and SST variability are switched off, respectively, as described in section 2. We compute composite differences of the zonal mean zonal wind between QBOW and QBOE conditions. The sum of these QBO signals from the two simulations then represents the linear combination of QBO and ENSO signals. Its difference to the signal from the ”NATURAL” simulation can be interpreted as the residual signal, i.e., as a non-linear interaction of the QBO and the ENSO signals.

Figure 8 a) shows the sum of the QBO signals from the ”NOQBO” and ”FixedSST” experiments,

and Figure 8 b) the difference of this signal to the QBO signal of the "NATURAL" simulation (which is shown in Figure 2 d)). Throughout the stratospheric polar night jet region, most of the differences between QBOW and QBOE conditions can be attributed to a linear superposition of QBO and ENSO (no statistically significant signals in Figure 8 b) in this region). However, in both the tropics and mid-latitudes, there are regions where non-linear interactions seem to play a role. In the equatorial troposphere, where the upwelling branch of the Hadley circulation is located and where tropical deep convection plays an important role for troposphere-stratosphere exchange, significant differences appear between the "NATURAL" simulation and the wind signal coming solely from the linear superposition of the separated QBO and ENSO signals. This suggests non-linear interactions of the two phenomena in this region, as well as in the tropical stratosphere and lower mesosphere. Furthermore, Figure 8 b) reveals that non-linear interactions are also of importance for the downward arching wind signal in the subtropical jet region. Although the QBO is responsible for the largest part of it, some additional non-linear processes seem to favor this downward coupling of the stratospheric wind oscillation to the troposphere.

Other sources of variability might contribute to the residual signal in Figure 8 b) as well. Possible contributors could be the solar cycle, volcanic eruptions or the semi-annual oscillation. However, identifying these additional sources is beyond the scope of this paper.

7. Summary and Conclusions

In this study, we used three long (145 years) simulations of the coupled model system CESM-WACCM to investigate the influence of the stratospheric QBO on the troposphere, and how this interacts with tropospheric ENSO signals. For the simulations, only natural and no anthropogenic forcings were considered, allowing us to detect QBO and ENSO signals unmasked from any anthropogenic influence. QBO signals in several parameters were analyzed with and without consid-

ering ENSO phases. The length of our simulations allowed us to create enough cases for each of the QBO-ENSO combinations to obtain reliable results. In our analysis, we distinguished between global QBO-ENSO responses as well as separate responses in the North Pacific and the North Atlantic region. In a last step, we investigated in which regions non-linear QBO-ENSO interactions might play a role.

Our analysis revealed the following:

- In the stratospheric polar night jet, the combined occurrence of the westerly QBO phase (QBOW) with the cold ENSO phase (La Niña) as well as the combined occurrence of the easterly QBO phase (QBOE) with the warm ENSO phase (El Niño) amplify the effects which the respective QBO and ENSO phases alone have on this region. The stratospheric polar night jet is strengthened during QBOW and La Niña, and weakened during QBOE and El Niño conditions, but the QBO-ENSO interaction enhances these responses.

- The stratospheric equatorial QBO anomalies extend down to the troposphere over the North Pacific region, but only during La Niña and not during El Niño phases. During La Niña, the conditions for the genesis and intensification of synoptic-scale waves are improved during QBOW compared to QBOE conditions through a strengthening of the meridional SST gradient which leads to enhanced baroclinic instability. The Aleutian low is deepened, and the subtropical jet is stronger and shifted northward. The combined QBO-ENSO signal is a linear superposition of the anomaly signals coming from the QBO or ENSO alone.

- In the North Atlantic, the combination of QBOW with La Niña (QBOE with El Niño) establishes a positive (negative) NAO pattern. These NAO patterns are generated as a non-linear amplification of the respective QBO and ENSO phase responses. The other two combinations counteract the general North Atlantic ENSO signals.

- Non-linear QBO-ENSO interactions might play a role in the tropical troposphere, tropical to subtropical stratosphere and lower mesosphere, as well as in the region of the subtropical jet where the stratospheric equatorial QBO anomalies extend down to the troposphere.

Our findings highlight the importance of stratospheric processes, in this case the QBO, for a better understanding of tropospheric dynamics. Knowledge about how the individual QBO phases act together with the individual ENSO phases in different regions can enhance the skill of tropospheric seasonal predictions. The results obtained in our study can be applied to the prediction of meteorologically interesting regions: the North Pacific and North Atlantic storm tracks. Extra-tropical cyclones which travel along the North Atlantic storm track are important phenomena especially for Europe, as they transport heat, moisture and momentum and thus influence primary meteorological parameters like temperature and precipitation. Hence, improved predictions of these phenomena can be of great value.

Our study did not explicitly consider other factors which might contribute to or favor the non-linear QBO-ENSO signal. These other factors could be the solar cycle, volcanic eruptions or the semi-annual oscillation. Their identification and a more detailed analysis on the dynamics of the combined QBO-ENSO signals should be the focus of future studies.

Acknowledgments. This work has been performed within the Helmholtz-University Young Investigators Group NATHAN funded by the Helmholtz-Association through the Presidents Initiative and Networking Fund and the Helmholtz Centre for Ocean Research Kiel (GEOMAR). The CESM-WACCM simulations have been performed at the Deutsche Klimarechenzentrum (DKRZ) Hamburg, Germany. The authors thank S. Lubis for computing the Eady Growth Rate.

References

Anstey, J. A., and T. G. Shepherd, 2014: High-latitude influence of the quasi-biennial oscillation. *Quarterly Journal of the Royal Meteorological Society*, **140 (678)**, 1–21, doi:10.1002/qj.2132.

Ayarzagüena, B., U. Langematz, S. Meul, S. Oberlander, J. Abalichin, and A. Kubin, 2013: The role of climate change and ozone recovery for the future timing of Major Stratospheric Warmings. *Geophys. Res. Lett.*, **40**, 2460–2465, doi:10.1002/grl.50477.

Baldwin, M. P., and T. J. Dunkerton, 1999: Propagation of the arctic oscillation from the stratosphere to the troposphere. *J. Geophys. Res.-Atmos.*, **104 (D24)**, 30 937–30 946, doi:10.1029/1999JD900445.

Baldwin, M. P., and Coauthors, 2001: The quasi-biennial oscillation. *Rev. Geophys.*, **39 (2)**, 179–229.

Barnett, T. P., 1991: The Interaction of Multiple Time Scales In the Tropical Climate System. *Journal of Climate*, **4 (3)**, 269–285, doi:10.1175/1520-0442(1991)004⟨0269:TIOMTS⟩2.0.CO;2.

Berlage, H. P., 1955: The Southern Oscillation - A 2–3 year fundamental Oscillation of world-wide significance, I.U.G.G. 10th General Assembly, Rome. *Scientific Proc. of the International Association of Meteorology, London*, 336–345.

Boer, G. J., and K. Hamilton, 2008: QBO influence on extratropical predictive skill. *Climate Dyn.*, **31 (7-8)**, 987–1000, doi:10.1007/s00382-008-0379-5.

Butler, A. H., L. M. Polvani, and C. Deser, 2014: Separating the stratospheric and tropospheric pathways of El Nino-Southern Oscillation teleconnections. *Environmental Research Letters*, **9 (2)**, 024 014, doi:10.1088/1748-9326/9/2/024014.

Calvo, N., M. A. Giorgetta, R. Garcia-Herrera, and E. Manzini, 2009: Nonlinearity of the combined warm ENSO and QBO effects on the Northern Hemisphere polar vortex in MAECHAM5 simulations. *J. Geophys. Res.-Atmos.*, **114**, D13 109, doi:10.1029/2008JD011445.

Camp, C. D., and K. K. Tung, 2007: Stratospheric polar warming by ENSO in winter: A statistical study. *Geophys. Res. Lett.*, **34 (4)**, L04 809, doi:10.1029/2006GL028521.

Chang, C. P., and T. Li, 2000: A theory for the tropical tropospheric biennial oscillation. *Journal of the Atmospheric Sciences*, **57 (14)**, 2209–2224, doi:10.1175/1520-0469(2000)057⟨2209:ATFTTT⟩2.0.CO;2.

Collimore, C. C., D. W. Martin, M. H. Hitchman, A. Huesmann, and D. E. Waliser, 2003: On the relationship between the qbo and tropical deep convection. *J. Climate*, **16 (15)**, 2552–2568, doi:10.1175/1520-0442(2003)016⟨2552:OTRBTQ⟩2.0.CO;2.

Danabasoglu, G., S. C. Bates, B. P. Briegleb, S. R. Jayne, M. Jochum, W. G. Large, S. Peacock, and S. G. Yeager, 2012: The CCSM4 Ocean Component. *J. Climate*, **25 (5)**, 1361–1389, doi:10.1175/JCLI-D-11-00091.1.

Eady, E. T., 1949: Long waves and cyclone waves. *Tellus*, **1 (3)**, 33–52, doi:10.1111/j.9302153-3490.1949.tb01265.x.

Fadnavis, S., T. Chakraborty, S. D. Ghude, G. Beig, and P. E. Raj, 2011: Modulation of Cyclone tracks in the Bay of Bengal by QBO. *J. Atmos. Sol.-Terr. Phy.*, **73 (13)**, 1868–1875, doi:10.1016/j.jastp.2011.04.014.

Garcia, R. R., D. R. Marsh, D. E. Kinnison, B. A. Boville, and F. Sassi, 2007: Simulation of secular trends in the middle atmosphere, 1950-2003. *J. Geophys. Res.-Atmos.*, **112 (D9)**, D09 301, doi:10.1029/2006JD007485.

Garfinkel, C. I., and D. L. Hartmann, 2007: Effects of the El Nino-Southern Oscillation and the Quasi-Biennial Oscillation on polar temperatures in the stratosphere. *J. Geophys. Res.-Atmos.*, **112 (D19)**, D19 112, doi:10.1029/2007JD008481.

Garfinkel, C. I., and D. L. Hartmann, 2011a: The Influence of the Quasi-Biennial Oscillation on the Troposphere in Winter in a Hierarchy of Models. Part I: Simplified Dry GCMs. *J. Atmos. Sci.*, **68 (6)**, 1273–1289, doi:10.1175/2011JAS3665.1.

Garfinkel, C. I., and D. L. Hartmann, 2011b: The Influence of the Quasi-Biennial Oscillation on the Troposphere in Winter in a Hierarchy of Models. Part II: Perpetual Winter WACCM Runs. *J. Atmos. Sci.*, **68 (9)**, 2026–2041, doi:10.1175/2011JAS3702.1.

Giorgetta, M. A., L. Bengtsson, and K. Arpe, 1999: An investigation of QBO signals in the east Asian and Indian monsoon in GCM experiments. *Climate Dyn.*, **15 (6)**, 435–450, doi:10.1007/s003820050292.

Gray, W. M., J. D. Sheaffer, and J. A. Knaff, 1992: Influence of the Stratospheric QBO on ENSO Variability. *J. Meteor. Soc. Japan*, **70 (5)**, 975–995.

Hansen, F., K. Matthes, C. Petrick, and W. Wang, 2014: The influence of natural and anthropogenic factors on major Stratospheric Sudden Warmings. *J. Geophys. Res.-Atmos.*, **119**, 8117–8136, doi:10.1002/2013JD021397.

Hitchman, M. H., and A. S. Huesmann, 2009: Seasonal Influence of the Quasi-Biennial Oscillation on Stratospheric Jets and Rossby Wave Breaking. *J. Atmos. Sci.*, **66 (4)**, 935–946, doi:10.1175/2008JAS2631.1.

Ho, C. H., H. S. Kim, J. H. Jeong, and S. W. Son, 2009: Influence of stratospheric quasi-biennial oscillation on tropical cyclone tracks in the western North Pacific. *Geophys. Res. Lett.*, **36**, L06 702, doi:10.1029/2009GL037163.

Holland, M. M., D. A. Bailey, B. P. Briegleb, B. Light, and E. Hunke, 2012: Improved Sea Ice Shortwave Radiation Physics in CCSM4: The Impact of Melt Ponds and Aerosols on Arctic Sea Ice. *J. Climate*, **25 (5)**, 1413–1430, doi:10.1175/JCLI-D-11-00078.1.

Holton, J. R., and H.-C. Tan, 1980: The influence of the equatorial quasi-biennial oscillation on the global circulation at 50 mb. *J. Atmos. Sci.*, **37**, 2200–2208.

Holton, J. R., and H.-C. Tan, 1982: The quasi-biennial oscillation in the Northern Hemisphere lower stratosphere. *J. Meteor. Soc. Japan*, **60**, 140–148.

Huang, B. H., Z. Z. Hu, J. L. Kinter, Z. H. Wu, and A. Kumar, 2012: Connection of stratospheric qbo with global atmospheric general circulation and tropical sst. part i: methodology and composite life cycle. *Climate Dyn.*, **38 (1-2)**, 1–23, doi:10.1007/s00382-011-1250-7.

Kiladis, G. N., and H. Van Loon, 1988: The Southern Oscillation .7. Meteorological Anomalies Over the Indian and Pacific Sectors Associated With the Extremes of the Oscillation. *Monthly Weather Review*, **116 (1)**, 120–136, doi:10.1175/1520-0493(1988)116⟨0120:TSOPVM⟩2.0.CO;2.

Kwan, K. F., and A. Abu Samah, 2003: A conceptual model relating the quasi-biennial oscillation and the tropospheric biennial oscillation. *International Journal of Climatology*, **23 (3)**, 347–362, doi:10.1002/joc.876.

Lau, K. M., 1992: East-asian Summer Monsoon Rainfall Variability and Climate Teleconnection. *Journal of the Meteorological Society of Japan*, **70 (1B)**, 211–242.

513 Loschnigg, J., G. A. Meehl, P. J. Webster, J. M. Arblaster, and G. P. Compo, 2003: The
514 Asian monsoon, the tropospheric biennial oscillation, and the Indian Ocean zonal mode in the
515 NCAR CSM. *Journal of Climate*, **16 (11)**, 1617–1642, doi:10.1175/1520-0442(2003)016⟨1617:
516 TAMTTB⟩2.0.CO;2.

517 Manzini, E., M. A. Giorgetta, M. Esch, L. Kornblueh, and E. Roeckner, 2006: The influence of
518 sea surface temperatures on the northern winter stratosphere: Ensemble simulations with the
519 MAECHAM5 model. *J. Climate*, **19 (16)**, 3863–3881, doi:10.1175/JCLI3826.1.

520 Marshall, A. G., and A. A. Scaife, 2009: Impact of the QBO on surface winter climate. *J. Geophys.*
521 *Res.-Atmos.*, **114**, D18 110, doi:10.1029/2009JD011737.

522 Maruyama, T., and Y. Tsuneoka, 1988: Anomalously Short Duration of the Easterly Wind Phase
523 of the QBO at 50 hPa in 1987 and its Relationship to an El-Nino Event. *Journal of the Meteo-*
524 *rological Society of Japan*, **66 (4)**, 629–634.

525 Meehl, G. A., 1987: The annual Cycle and the Interannual Variability in the Tropical Pacific and
526 Indian Ocean regions. *Mon. Wea. Rev.*, **115**, 27–50.

527 Meehl, G. A., 1993: A Coupled Air-sea Biennial Mechanism In the Tropical Indian and Pacific
528 Regions - Role of the Ocean. *Journal of Climate*, **6 (1)**, 31–41, doi:10.1175/1520-0442(1993)
529 006⟨0031:ACASBM⟩2.0.CO;2.

530 Meehl, G. A., 1997: The south Asian monsoon and the tropospheric biennial oscillation. *Journal*
531 *of Climate*, **10 (8)**, 1921–1943, doi:10.1175/1520-0442(1997)010⟨1921:TSAMAT⟩2.0.CO;2.

532 Mitchell, D. M., L. J. Gray, and A. J. Charlton-Perez, 2011: The structure and evolution of the
533 stratospheric vortex in response to natural forcings. *J. Geophys. Res.-Atmos.*, **116**, D15 110,
534 doi:10.1029/2011JD015788.

Richter, J. H., F. Sassi, and R. R. Garcia, 2010: Toward a Physically Based Gravity Wave Source Parameterization in a General Circulation Model. *J. Atmos. Sci.*, **67 (1)**, 136–156, doi:10.1175/2009JAS3112.1.

Rind, D., and N. K. Balachandran, 1995: Modeling the Effects of UV Variability and the QBO on the Troposphere-Stratosphere System .2. The Troposphere. *J. Climate*, **8 (8)**, 2080–2095.

Ropelewski, C. F., M. S. Halpert, and X. L. Wang, 1992: Observed Tropospheric Biennial Variability and Its Relationship To the Southern Oscillation. *Journal of Climate*, **5 (6)**, 594–614, doi:10.1175/1520-0442(1992)005⟨0594:OTBVAI⟩2.0.CO;2.

Sassi, F., D. Kinnison, B. A. Boville, R. R. Garcia, and R. Roble, 2004: Effect of El Nino-Southern Oscillation on the dynamical, thermal, and chemical structure of the middle atmosphere. *J. Geophys. Res.-Atmos.*, **109 (D17)**, D17 108, doi:10.1029/2003JD004434.

Scaife, A. A., and Coauthors, 2014: Predictability of the quasi-biennial oscillation and its northern winter teleconnection on seasonal to decadal timescales. *Geophysical Research Letters*, **41 (5)**, 1752–1758, doi:10.1002/2013GL059160.

Seo, J., W. Choi, D. Youn, D. S. R. Park, and J. Y. Kim, 2013: Relationship between the stratospheric quasi-biennial oscillation and the spring rainfall in the western north pacific. *Geophys. Res. Lett.*, **40 (22)**, 5949–5953, doi:10.1002/2013GL058266.

Shapiro, L. J., 1989: The Relationship of the Quasi-biennial Oscillation to Atlantic Tropical Storm Activity. *Mon. Wea. Rev.*, **117 (7)**, 1545–1552, doi:10.1175/1520-0493(1989)117⟨1545:TROTQB⟩2.0.CO;2.

555 Taguchi, M., 2010: Observed connection of the stratospheric quasi-biennial oscillation with El
556 Nino-Southern Oscillation in radiosonde data. *J. Geophys. Res.-Atmos.*, **115**, D18 120, doi:10.
557 1029/2010JD014325.

558 Taguchi, M., and D. L. Hartmann, 2006: Increased occurrence of stratospheric sudden warmings
559 during El Nino as simulated by WACCM. *J. Climate*, **19 (3)**, 324–332, doi:10.1175/JCLI3655.1.

560 Trenberth, K. E., 1997: The definition of El Niño. *Bull. Amer. Meteor. Soc.*, **78**, 2771–2777.

561 Tripathi, O. P., and Coauthors, 2014: The predictability of the extratropical stratosphere on
562 monthly time-scales and its impact on the skill of tropospheric forecasts. *Q.J.R. Meteorol. Soc.*,
563 n/a–n/a, URL http://dx.doi.org/10.1002/qj.2432.

564 van Loon, H., and K. Labitzke, 1987: The Southern Oscillation .5. The Anomalies in
565 the Lower Stratosphere of the Northern-hemisphere in Winter and a Comparison with the
566 Quasi-Biennial Oscillation. *Mon. Wea. Rev.*, **115 (2)**, 357–369, doi:10.1175/1520-0493(1987)
567 115⟨0357:TSOPVT⟩2.0.CO;2.

568 van Loon, H., and R. A. Madden, 1981: The Southern Oscillation. Part I: Global Associa-
569 tions with Pressure and Temperature in Northern Winter. *Mon. Wea. Rev.*, **109 (6)**, 1150–
570 1162, doi:10.1175/1520-0493(1981)109⟨1150:TSOPIG⟩2.0.CO;2, URL http://dx.doi.org/10.
571 1175/1520-0493(1981)109⟨1150:TSOPIG⟩2.0.CO;2.

572 Wei, K., W. Chen, and R. H. Huang, 2007: Association of tropical Pacific sea surface temperatures
573 with the stratospheric Holton-Tan Oscillation in the Northern Hemisphere winter. *Geophys. Res.*
574 *Lett.*, **34 (16)**, L16 814, doi:10.1029/2007GL030478.

Xu, J. S., 1992: On the Relationship Between the Stratospheric Quasi-Biennial Oscillation and the Tropospheric Southern Oscillation. *Journal of the Atmospheric Sciences*, **49 (9)**, 725–734, doi:10.1175/1520-0469(1992)049⟨0725:OTRBTS⟩2.0.CO;2.

Yuan, W., M. A. Geller, and P. T. Love, 2014: ENSO influence on the QBO modulations of the tropical tropopause. *Q. J. R. Meteorol. Soc.*, **140**, 1670–1676, doi:10.1002/qj.2247.

LIST OF TABLES

584 TABLE 1. Number of NDJF seasons under QBOW, QBOE, El Niño and La Niña conditions and combinations
585 of QBO and ENSO phases in the NATURAL experiment.

number of cases		**QBOW**	**QBOE**
		69	58
El Niño	49	25	20
La Niña	55	26	22

LIST OF FIGURES

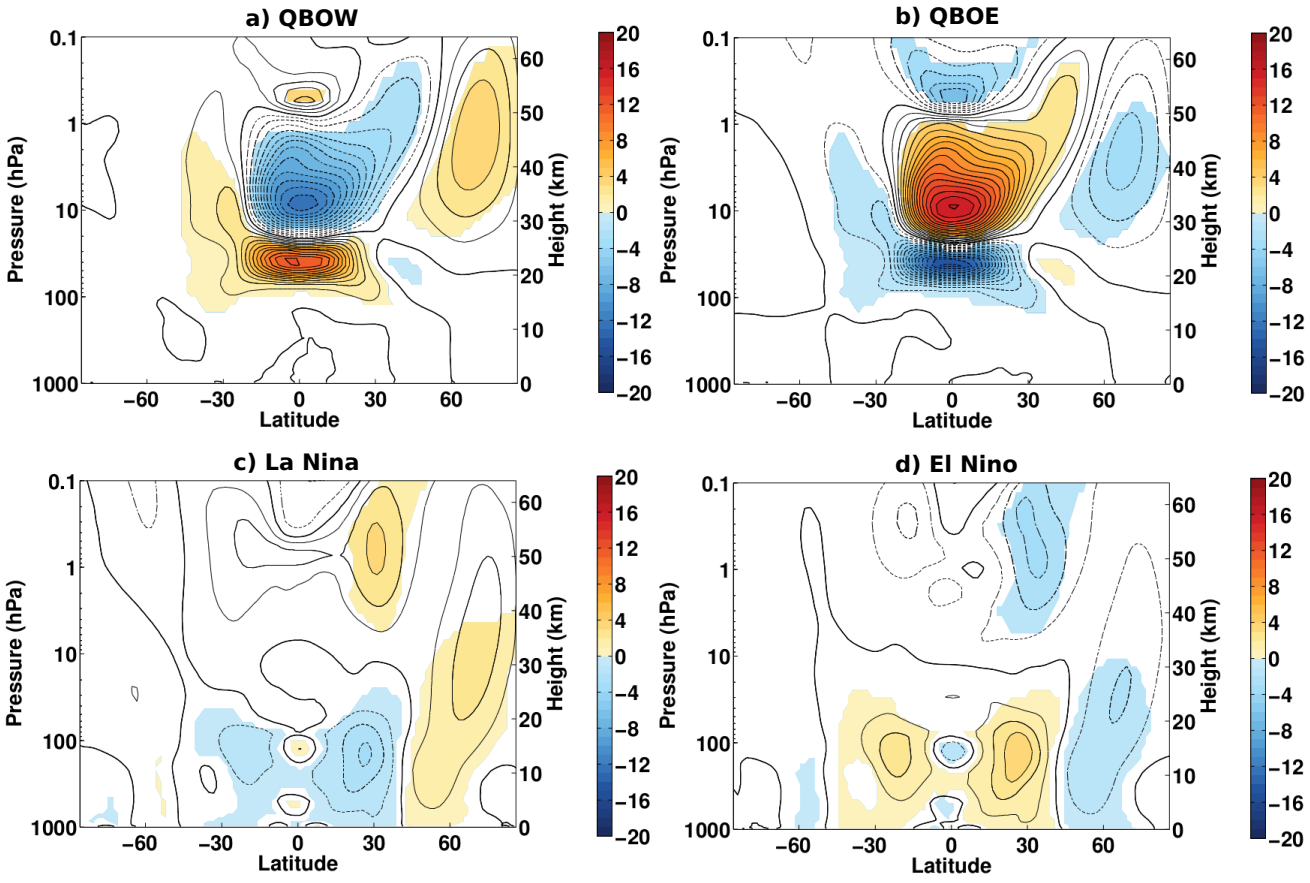

619 FIG. 1. Anomalies of the zonal mean zonal wind in NDJF with respect to the NDJF climatology for QBO and
620 ENSO phases in the CESM-WACCM NATURAL experiment. Contour interval 1 m/s, colour shading indicates
621 90% statistical significance.

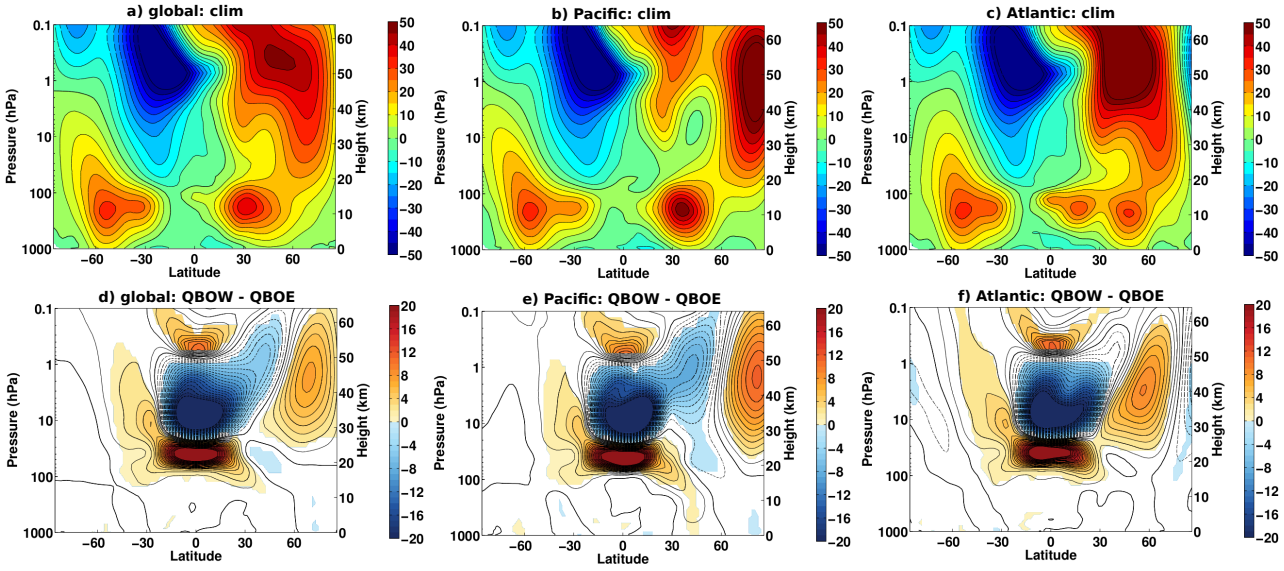

FIG. 2. Climatologies (1st row; contour interval 5 m/s) and composite differences of QBOW minus QBOE conditions (2nd row; contour interval 1 m/s; colour shading indicates 90% statistical significance) for the zonal mean zonal wind globally averaged (1st column), averaged over the Pacific (2nd column) and averaged over the Atlantic (3rd column) in NDJF in the NATURAL experiment.

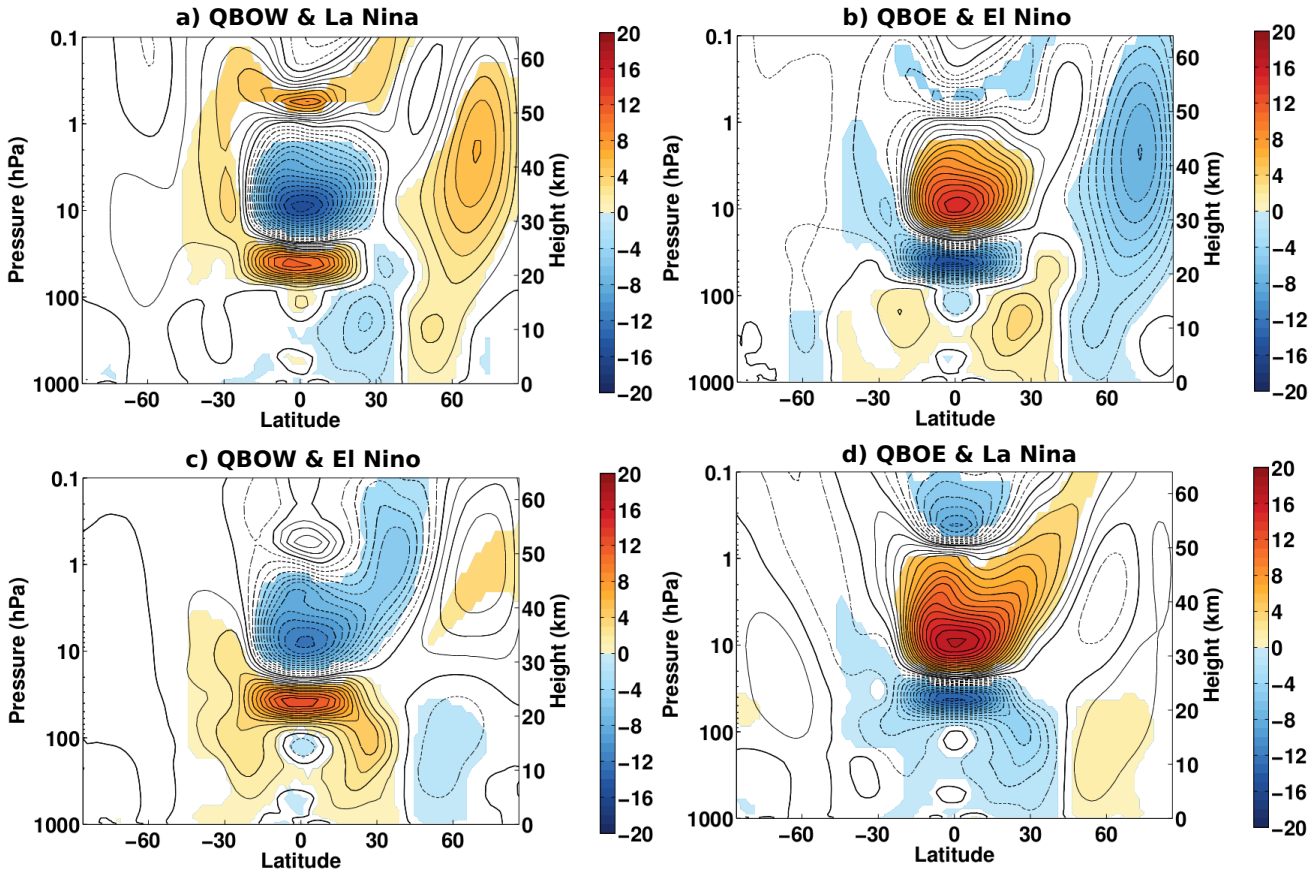

FIG. 3. Same as Figure 1 but for all combinations of QBO phases coinciding with ENSO phases.

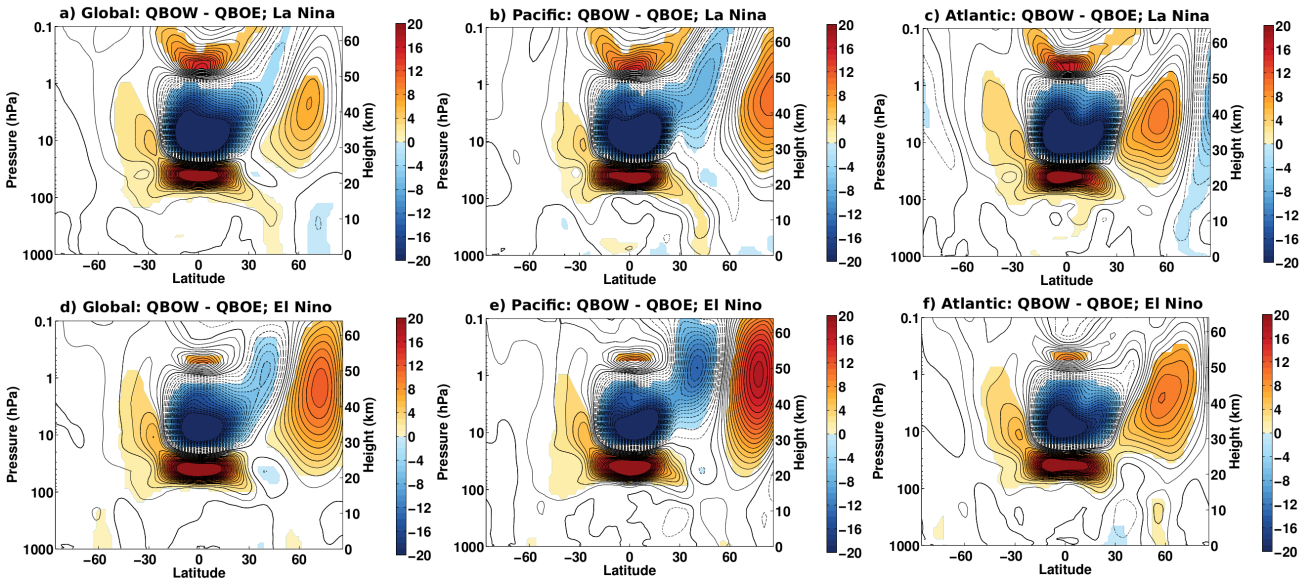

FIG. 4. Composite differences of QBOW minus QBOE conditions coinciding with La Niña (1st row) and El Niño (2nd row) for the zonal mean zonal wind globally averaged (1st column), averaged over the Pacific (2nd column) and averaged over the Atlantic (3rd column) in NDJF in the NATURAL experiment. Contour interval 1 m/s; colour shading indicates 90% statistical significance.

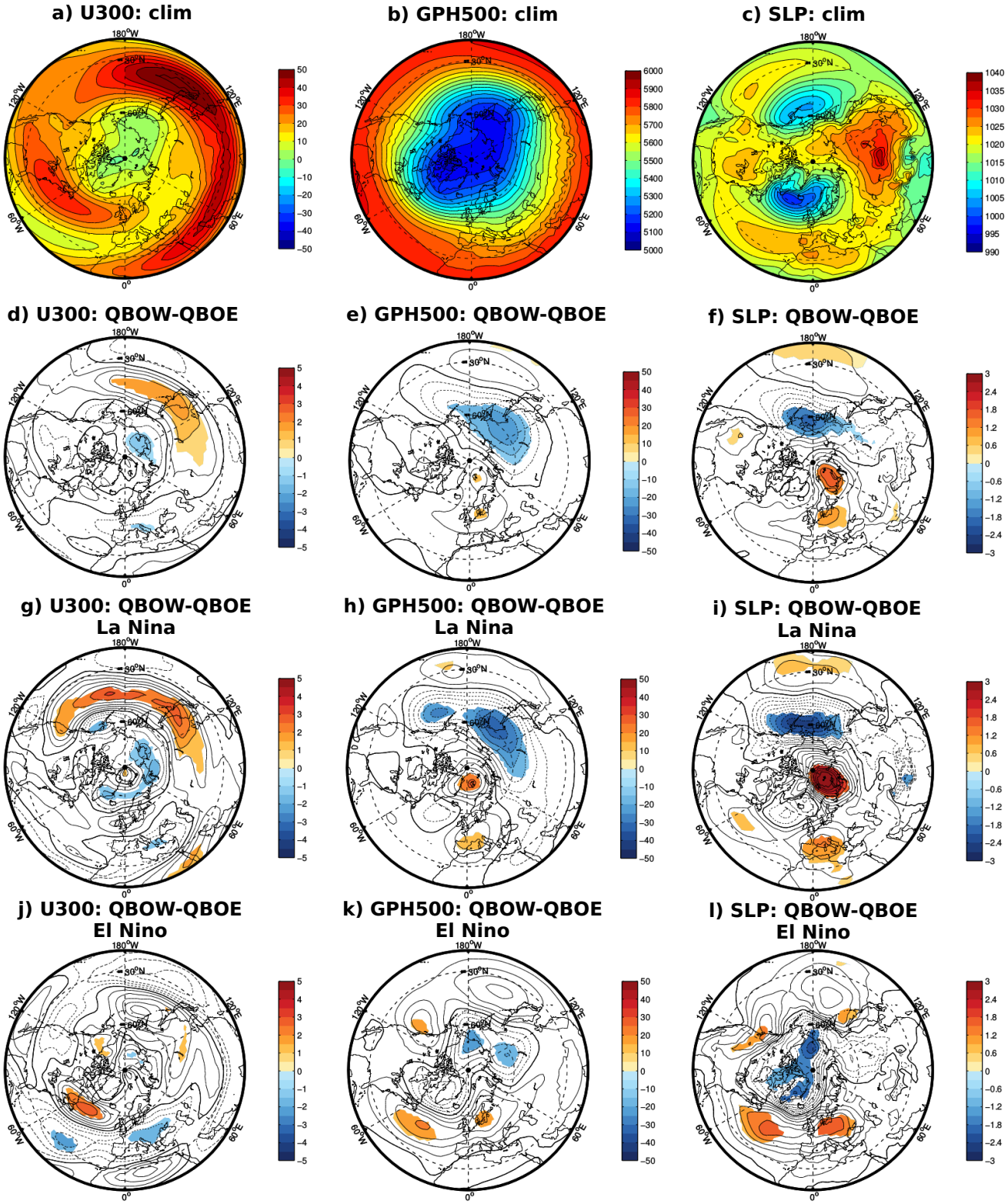

630 FIG. 5. Climatologies (1st row) and composite differences of QBOW minus QBOE conditions coinciding
631 with ENSO phases (2nd, 3rd and 4th row) for the zonal wind at 300 hPa (1st column; contour interval 5 m/s for
632 the climatology and 0.5 m/s for the composite differences), geopotential height at 500 hPa (2nd column; contour
633 interval 50 m / 5 m) and sea level pressure (3rd row; contour interval 5 hPa / 0.3 hPa) in NDJF in the NATURAL
634 experiment. 2nd, 3rd and 4th row: colour shading indicates 90% statistical significance.

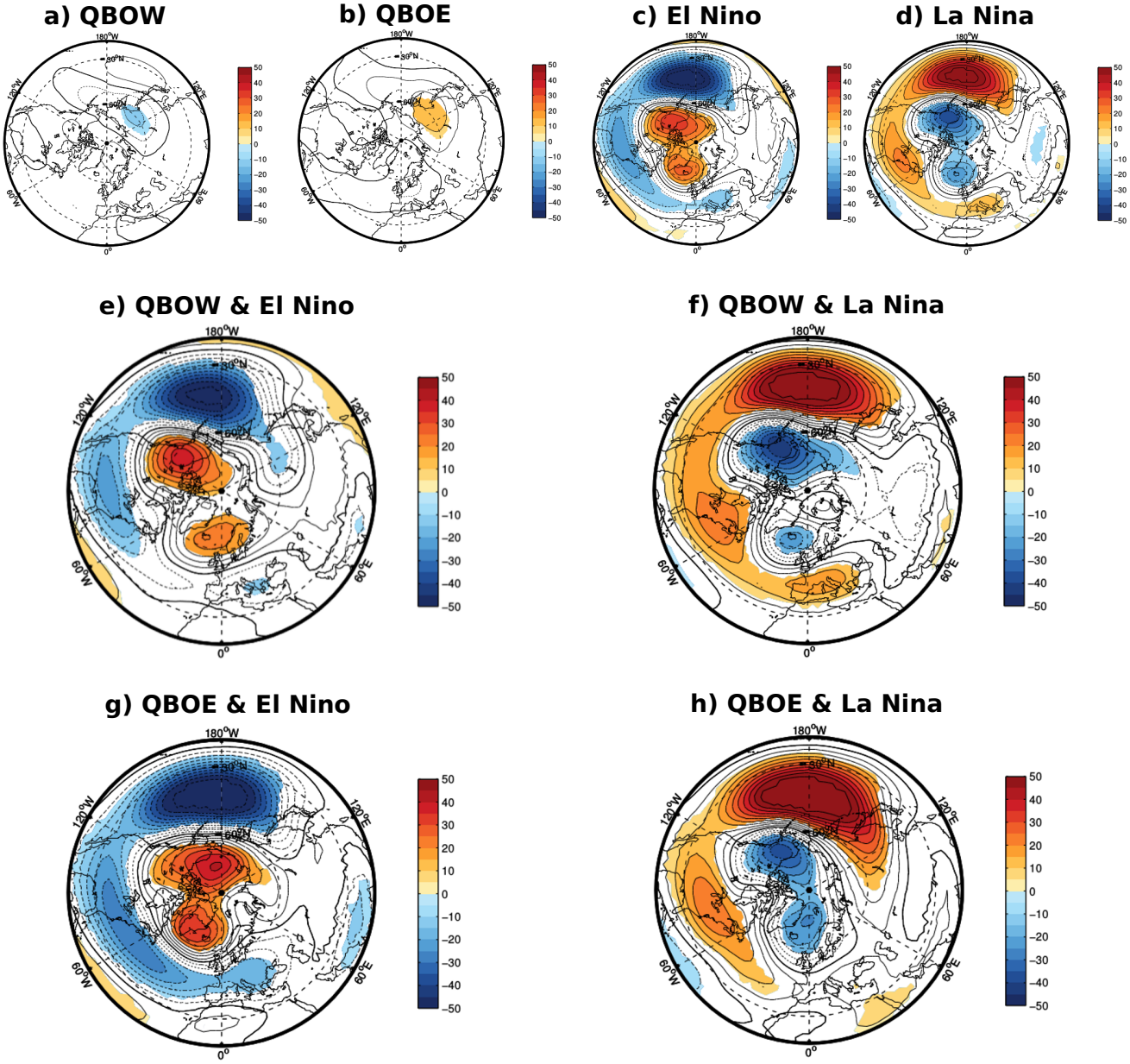

635 FIG. 6. Anomalies of geopotential height at 500 hPa in NDJF with respect to the NDJF climatology for
636 QBO and ENSO phases and combinations of them in the NATURAL experiment. Contour interval 5 m, colour
637 shading indicates 90% statistical significance.

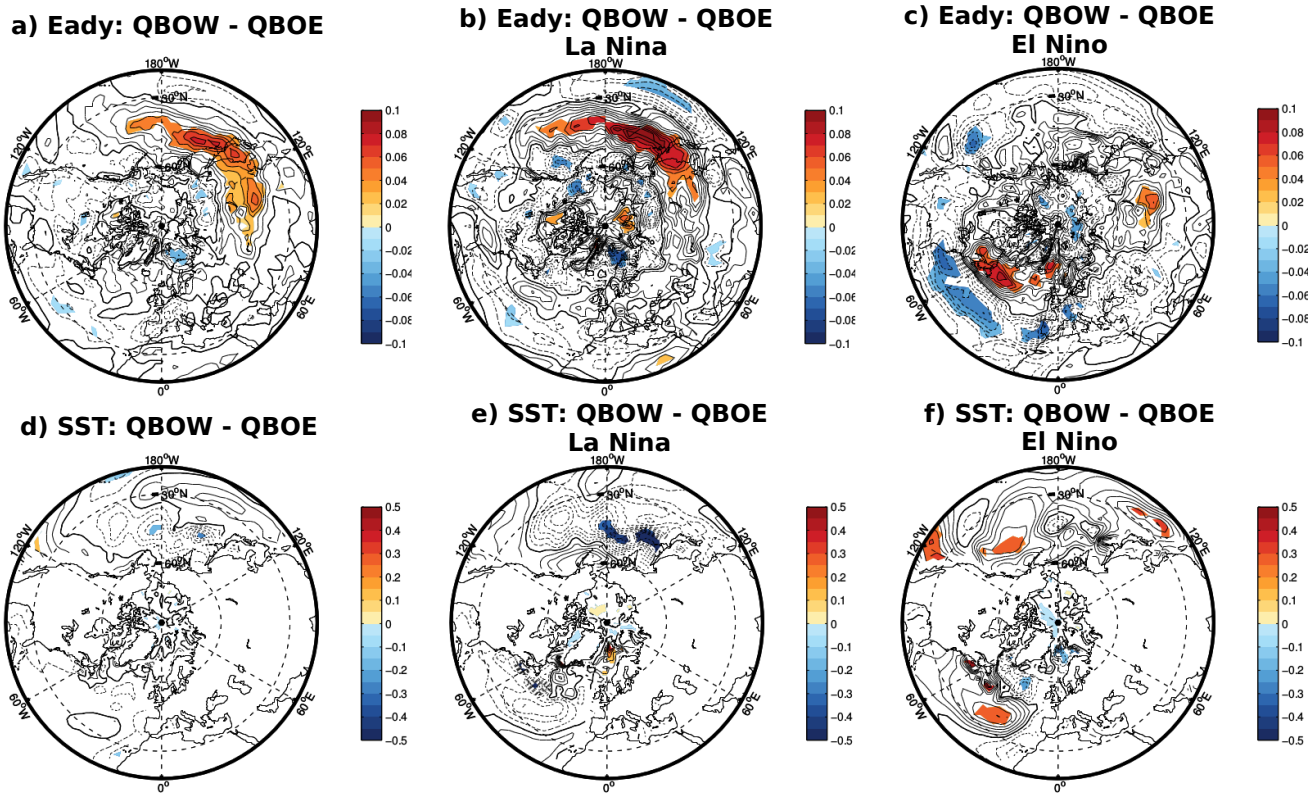

FIG. 7. Composite differences of the Eady Growth Rate at 850 hPa (first row; contour interval 0.01/day) and SSTs (second row; contour interval 0.05 °C) in NDJF for QBOW minus QBOE conditions coinciding with ENSO phases in the NATURAL experiment. Colour shading indicates 90% statistical significance.

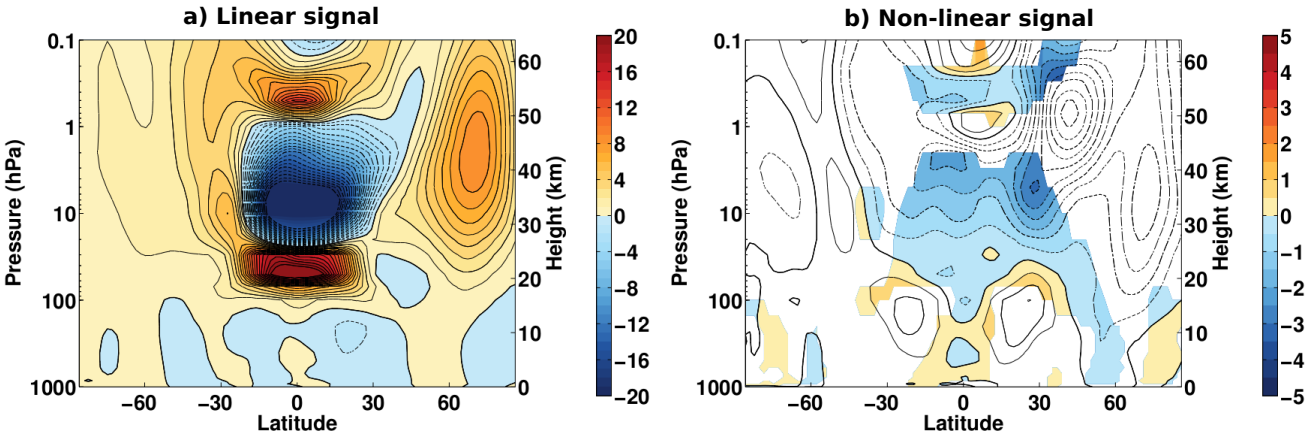

641 FIG. 8. Composite differences for QBOW minus QBOE conditions of zonal mean zonal wind in NDJF for
642 the sum of the NOQBO and the FixedSST experiments (a; contour interval 1 m/s) and difference of the sum of
643 the NOQBO and the FixedSST experiment to the NATURAL experiment (b; contour interval 0.5 m/s; colour
644 shading indicates 90% statistical significance).

5 Summary

In this thesis, the importance of different natural and anthropogenic factors for the dynamical coupling between the stratosphere and the troposphere was investigated. Special emphasis was placed on the Quasi-Biennial Oscillation (QBO) of equatorial stratospheric winds; other factors considered were the variability of (mainly tropical) sea surface temperatures (SSTs), anthropogenic greenhouse gases (GHGs) and ozone depleting substances (ODSs). Analyses were performed on the basis of model simulations with either NCAR's CESM model, a coupled model system which includes an interactively coupled atmosphere, ocean, land and sea ice module, or the stand-alone atmospheric WACCM model, a fully interactive chemistry-climate model which is also used as CESM's atmospheric component. Sensitivity experiments were performed where the respective factor of interest was switched off, so that its influence on stratosphere-troposphere coupling could be investigated in comparison with a control simulation where all factors were included. Here, the questions raised in the introductory chapter of this thesis shall be revisited, and the answers to them obtained in the different chapters will be summarized.

- **How do the different natural and anthropogenic factors influence the extreme events in the NH stratosphere - major Stratospheric Sudden Warmings (SSWs) - which are a prominent example of stratosphere-troposphere coupling?**

  → The answer to this question is manifold as different aspects of SSWs are affected by the different factors. First, the frequency of major SSWs is significantly decreased by the stratospheric variability induced by the QBO, and significantly increased by interannual SST variability. The QBO reduces planetary wave propagation from the troposphere into the stratospheric polar night jet (PNJ) region, leading to reduced wave-mean flow interaction and hence to a weaker deceleration of the PNJ. Hence, the PNJ and the polar vortex are stronger and more stable, and less SSWs occur. By introducing SST variability, the tropospheric wave forcing is enhanced, the PNJ is weakened and the SSW frequency is increased.

  Second, the different phases of the SSWs' life cycles are influenced by the different factors. CESM-WACCM is able to simulate these life cycles realistically. Anthropogenic GHGs and ODSs modulate the prewarming phase of SSWs, while the QBO and SST variability seem to alter the phase after the event when the anomalous stratospheric SSW signals propagate down to the troposphere. These coupling processes happen with

a delay (compared to the average timing) of about 10 days when no QBO variability is included, and over a smaller area and a shorter period of time when no SST variability is included.
Third, the average amplitude and duration of major SSWs is not changed significantly by the different factors.
Compared to reanalysis data, CESM-WACCM like many other models underestimates the frequency of major SSWs; though, the differences are not statistically significant. One problem, however, is the ratio between the two types of major warmings: almost all simulated SSWs are vortex displacement events; the observed frequency of vortex split events is not achieved at all. This is probably attributed to the underestimation of tropospheric blockings in the model, as these blockings have been shown to precede SSWs in many cases.

- **How does the width of the QBO in a climate model influence the connection between the equatorial and the polar stratosphere, which is often referred to as the Holton-Tan mechanism?**

  → The width of the QBO nudging along the equator influences the mean state in the NH polar stratosphere during winter. The Holton-Tan effect, i.e., stronger zonal mean zonal winds in the stratospheric PNJ region during the westerly phase of the QBO (QBOW) compared to the easterly phase (QBOE), is enhanced when a wider QBO nudging is chosen. In this case, wave propagation as well as wave-mean flow interaction are influenced in such a way that the meridional temperature gradient is strengthened compared to a smaller nudging case. This leads to an intensification of the stratospheric PNJ.
  Chemical tracers like ozone, water vapour and methane react accordingly: their high-latitude stratospheric response to the QBO is enhanced when a wider QBO nudging is applied. Below 10hPa, the concentration and composition of these chemical constituents are mainly determined by transport processes; above that height, temperature-dependent chemical reactions are more important. The differences in chemical tracers between a wider and a smaller nudging are entirely consistent with the differences in circulation and reaction velocities (through temperature changes) in the respective height ranges.
  The dynamics of the QBO influence on high latitudes is not yet fully understood. However, the results of this thesis suggest that at least two processes are involved: first, the effect of the zero wind line in the *low-latitude lower stratosphere* which is shifted away from the equator during QBOE conditions, leading to planetary waves being reflected towards the pole and therefore a more disturbed stratospheric polar vortex; and second the effect of the secondary QBO circulation in the *mid-latitude middle to upper stratosphere*, where a "barrier" to planetary waves is created during QBOE conditions in

mid-latitudes so that these waves converge in the polar region.

- **How does the stratospheric QBO influence tropospheric weather and climate?**

  → The tropospheric influence of the QBO interacts with the tropospheric signals of ENSO, and large differences thereby occur between the North Pacific and North Atlantic. The stratospheric equatorial QBO anomalies extend down to the troposphere over the North Pacific during NH winter, but only during La Niña and not during El Niño phases. During La Niña, the conditions for the genesis and intensification of synoptic-scale waves are improved during QBOW compared to QBOE through a strengthening of the meridional SST gradient which leads to enhanced baroclinic instability. The Aleutian low is deepened, and the subtropical jet is stronger and shifted northward. The combined QBO-ENSO signal seems to be a linear superposition of the anomaly signals coming from the QBO or ENSO alone.

  In the North Atlantic, the combination of QBOW with La Niña (QBOE with El Niño) establishes a positive (negative) North Atlantic Oscillation (NAO) pattern. These NAO patterns are generated as a non-linear amplification of the respective QBO and ENSO phase responses. The other two combinations counteract the general North Atlantic ENSO signals.

  Hence, the stratospheric QBO together with ENSO affect both NH storm tracks, which are key regions when extreme extra-tropical cyclones - one of the most important natural hazards, at least in Europe - are considered.

Altogether, several new aspects of the dynamical coupling between the stratosphere and the troposphere and how this coupling is influenced by different factors have been obtained within this thesis, as summarized above. These results are useful, as they help to improve our general understanding of physical processes of stratosphere-troposphere coupling which are still not well explored. This thesis does not only provide quantitative estimates about how the different natural and anthropogenic factors alter stratosphere-troposphere coupling (e.g., for the example of SSWs), but also presents some ideas for possible underlying mechanisms (e.g., changes in planetary wave generation, propagation and its interaction with the mean flow due to the different factors; see summary above).

In this thesis, GHGs and ODSs were considered together as representing the anthropogenic factors which influence atmospheric variability in general and particularly stratosphere-troposphere coupling. Some studies exist which distinguish between the impacts of GHGs and ODSs [e.g., McLandress et al., 2010; Stolarski et al., 2010; Previdi and Polvani, 2014]; however, the sensitivity simulations performed here did not allow to analyze their impacts separately.

It has to be kept in mind that one single model only was used for the analyses, and that this model, as all models, has its biases and limitations. A strong intervention in CESM-WACCM's model physics and momentum balance is done by nudging observed zonal winds in the equatorial

stratosphere to obtain a QBO. By doing this, no feedback processes between middle to high latitudes with the tropics can be investigated. Another issue is the wrong simulated ratio of the two types of SSWs, which is probably attributed to the underestimation of tropospheric blockings in the model. However, the question about the preceding and initializing processes of SSWs is a research topic which is far from being understood, hence the mechanism including tropospheric blockings is just one of probably several possible mechanisms. As long as these mechanisms are not completely understood, we cannot expect any model to simulate such events correctly. A lack of full process-understanding leads to inconsistencies between different models and deviating results for the same or similar questions. Nevertheless, this thesis confirmed that climate models are an irreplaceable tool to study dynamical and chemical mechanisms. The obtained results also highlight the importance of the stratosphere for tropospheric dynamics. Hence, proceeding effort should be put in climate model development and improvement, and in realistically representing middle atmosphere processes therein.

5.1 Outlook

As summarized above, this thesis answered some questions about the importance of the QBO, SSTs, GHGs and ODSs for the stratosphere-troposphere coupling, especially during major SSWs. On the other hand, new questions and ideas for further research developed.

Models which generate the QBO internally (e.g., a recent version of WACCM [Xue et al., 2012] as CESM's atmospheric component) could be used to perform the same experiments as done here to repeat the analysis with an even more "realistic" model. This model would then also allow to study feedback processes between the equatorial stratosphere and the middle and high latitudes in both directions. With such a model, the future behavior of the QBO could be investigated, i.e., projections of its future amplitude, period and global stratospheric and tropospheric influence could be analyzed.

The results obtained in this thesis suggest that the coupling between atmosphere and ocean might be of importance for stratosphere-troposphere coupling processes, e.g., as shown in Chapter 2, for the downward influence of SSWs. Hence, future studies should focus further on investigating the importance of atmosphere-ocean coupling on different time scales.

After the publication of the SSW study of this thesis (Chaper 2), the CESM-WACCM "NOQBO" an "FixedSSTs" simulations have been extended until from 2010 until 2099. The analysis steps performed for this study can be applied to these extended runs to check the robustness of the results. This will be the topic of a Bachelor's thesis at Geomar during the summer semester 2015 which will be supervised by Prof. Dr. Katja Matthes and myself.

Instead of performing sensitivity experiments to investigate the importance of different factors for stratosphere-troposphere coupling as done for this thesis, a different type of experiments can be analyzed which include nudging. In these experiments, one or more parameters in the model are

relaxed towards reanalysis data in a specific region and/or for a specific period of interest. Such kind of experiments have been performed with the European Centre for Medium-Range Weather Forecasts (ECMWF) atmosphere model by Prof. Dr. Thomas Jung at the Alfred-Wegener Institute, Bremerhaven, in collaboration with Prof. Dr. Richard Greatbatch at Geomar. In a set of experiments, the ECMWF model is relaxed towards ERA-Interim reanalysis data in different regions like the NH or SH only, the tropics only, the stratosphere only (globally, on one or both hemispheres, or in the tropics) or the troposphere only. These experiments allow to study the influence of the respective regions and processes, e.g., to analyze from which regions/processes predictive skill for tropospheric weather forecasts or longer-term predictions can be obtained. Their analysis will be part of my future research.

Bibliography

Alexander, M. A., I. Blade, M. Newman, J. R. Lanzante, N. C. Lau, and J. D. Scott, 2002: The atmospheric bridge: The influence of ENSO teleconnections on air-sea interaction over the global oceans. *Journal of Climate*, **15 (16)**, 2205–2231, doi: 10.1175/1520-0442(2002)015⟨2205:TABTIO⟩2.0.CO;2.

Andrews, D. G. and M. E. McIntyre, 1976: Planetary waves in horizontal and vertical shear: The generalized Eliassen-Palm relation and the mean zonal acceleration. *J. Atmos. Sci.*, **33 (11)**, 2031–2048.

Anstey, J. A. and T. G. Shepherd, 2014: High-latitude influence of the quasi-biennial oscillation. *Quarterly Journal of the Royal Meteorological Society*, **140 (678)**, 1–21, doi: 10.1002/qj.2132.

Anstey, J. A., T. G. Shepherd, and J. F. Scinocca, 2010: Influence of the Quasi-Biennial Oscillation on the Extratropical Winter Stratosphere in an Atmospheric General Circulation Model and in Reanalysis Data. *J. Atmos. Sci.*, **67 (5)**, 1402–1419, doi: 10.1175/2009JAS3292.1.

Ayarzagüena, B., U. Langematz, S. Meul, S. Oberlander, J. Abalichin, and A. Kubin, 2013: The role of climate change and ozone recovery for the future timing of Major Stratospheric Warmings. *Geophys. Res. Lett.*, **40**, 2460–2465, doi: 10.1002/grl.50477.

Badin, G. and D. I. V. Domeisen, 2013: A Search for Chaotic Behavior in Northern Hemisphere Stratospheric Variability. *J. Atmos. Sci.*, **71 (4)**, 1494–1507, doi: 10.1175/JAS-D-13-0225.1, URL `http://dx.doi.org/10.1175/JAS-D-13-0225.1`.

Baldwin, M. and T. Dunkerton, 2001: Stratospheric harbingers of anomalous Weather Regimes. *Science*, **294**, 581–584.

Baldwin, M. P. and T. J. Dunkerton, 1999: Propagation of the arctic oscillation from the stratosphere to the troposphere. *J. Geophys. Res.-Atmos.*, **104 (D24)**, 30 937–30 946, doi: 10.1029/1999JD900445.

Baldwin, M. P., D. B. Stephenson, D. W. J. Thompson, T. J. Dunkerton, A. J. Charlton, and A. O'Neill, 2003: Stratospheric memory and skill of extended-range weather forecasts. *Science*, **301 (5633)**, 636–640, doi: 10.1126/science.1087143.

Baldwin, M. P. and D. W. J. Thompson, 2009: A critical comparison of stratosphere-troposphere coupling indices. *Quart. J. Roy. Meteor. Soc.*, **135 (644)**, 1661–1672, doi: 10.1002/qj.479.

Baldwin, M. P., et al., 2001: The quasi-biennial oscillation. *Rev. Geophys.*, **39 (2)**, 179–229.

Belmont, A. D., D. G. Dartt, and G. D. Nastrom, 1974: Periodic Variations In Stratospheric Zonal Wind From 20 To 65 Km, At 80 Degrees N To 70 Degrees S. *Quarterly Journal of the Royal Meteorological Society*, **100 (424)**, 203–211, doi: 10.1002/qj.49710042407.

Black, R. X., 2002: Stratospheric forcing of surface climate in the Arctic oscillation. *Journal of Climate*, **15 (3)**, 268–277, doi: 10.1175/1520-0442(2002)015⟨0268:SFOSCI⟩2.0.CO;2.

Black, R. X. and B. A. McDaniel, 2004: Diagnostic case studies of the northern annular mode. *J. Climate*, **17 (20)**, 3990–4004, doi: 10.1175/1520-0442(2004)017⟨3990:DCSOTN⟩2.0.CO;2.

Blume, C., 2012: Statistical Learning To Model Stratospheric Variability. Ph.D. thesis, Freie Universität Berlin.

Brewer, A. W., 1949: Evidence For A World Circulation Provided By the Measurements of Helium and Water Vapour Distribution In the Stratosphere. *Quarterly Journal of the Royal Meteorological Society*, **75 (326)**, 351–363, doi: 10.1002/qj.49707532603.

Butchart, N., A. A. Scaife, J. Austin, S. H. E. Hare, and J. R. Knight, 2003: Quasi-biennial oscillation in ozone in a coupled chemistry-climate model. *J. Geophys. Res.-Atmos.*, **108 (D15)**, 4486, doi: 10.1029/2002JD003004.

Butler, A. H., L. M. Polvani, and C. Deser, 2014: Separating the stratospheric and tropospheric pathways of El Nino-Southern Oscillation teleconnections. *Environmental Research Letters*, **9 (2)**, 024 014, doi: 10.1088/1748-9326/9/2/024014.

Calvo, N., M. A. Giorgetta, R. Garcia-Herrera, and E. Manzini, 2009: Nonlinearity of the combined warm ENSO and QBO effects on the Northern Hemisphere polar vortex in MAECHAM5 simulations. *J. Geophys. Res.-Atmos.*, **114**, D13 109, doi: 10.1029/2008JD011445.

Charlton, A. J. and L. M. Polvani, 2007: A new look at stratospheric sudden warmings. Part I: Climatology and modeling benchmarks. *J. Climate*, **20 (3)**, 449–469, doi: 10.1175/JCLI3996.1.

Charlton-Perez, A. J., et al., 2013: On the lack of stratospheric dynamical variability in low-top versions of the CMIP5 models. *Journal of Geophysical Research-atmospheres*, **118 (6)**, 2494–2505, doi: 10.1002/jgrd.50125.

Charney, J. G. and P. G. Drazin, 1961: Propagation of planetary-scale disturbances from the lower into the upper atmosphere. *J. Geophys. Res.*, **66**, 83–109.

Christiansen, B., 2000: Chaos, quasiperiodicity, and interannual variability: Studies of a stratospheric vacillation model. *Journal of the Atmospheric Sciences*, **57 (18)**, 3161–3173, doi: 10.1175/1520-0469(2000)057⟨3161:CQAIVS⟩2.0.CO;2.

Davini, P., C. Cagnazzo, and J. A. Anstey, 2014: A blocking view of the stratosphere-troposphere coupling. *J. Geophys. Res. Atmos.*, **119 (19)**, 11,100–11,115, URL http://dx.doi.org/10.1002/2014JD021703.

Dobson, G. M. B., 1952: Ozone In the Earths Atmosphere. *Endeavour*, **11 (44)**, 215–219.

Domeisen, D. I. V., A. H. Butler, K. Fröhlich, M. Bittner, W. A. Müller, and J. Baehr, 2015: Seasonal Predictability over Europe Arising from El Niño and Stratospheric Variability in the MPI-ESM Seasonal Prediction System. *J. Climate*, **28**, 256–271, doi: 10.1175/JCLI-D-14-00207.1.

Domeisen, D. I. V., L. Sun, and G. Chen, 2013: The role of synoptic eddies in the tropospheric response to stratospheric variability. *Geophysical Research Letters*, **40 (18)**, 4933–4937, doi: 10.1002/grl.50943.

Erlebach, P., U. Langematz, and S. Pawson, 1996: Simulations of stratospheric sudden warmings in the Berlin troposphere stratosphere mesosphere GCM. *Ann. Geophys.*, **14 (4)**, 443–463, doi: 10.1007/s00585-996-0443-6.

Frame, T. H. A. and L. J. Gray, 2010: The 11-Yr Solar Cycle in ERA-40 Data: An Update to 2008. *J. Climate*, **23 (8)**, 2213–2222, doi: 10.1175/2009JCLI3150.1.

Garcia, R. R., D. R. Marsh, D. E. Kinnison, B. A. Boville, and F. Sassi, 2007: Simulation of secular trends in the middle atmosphere, 1950-2003. *J. Geophys. Res.-Atmos.*, **112 (D9)**, D09 301, doi: 10.1029/2006JD007485.

Garcia, R. R., W. J. Randel, and D. E. Kinnison, 2011: On the Determination of Age of Air Trends from Atmospheric Trace Species. *J. Atmos. Sci.*, **68 (1)**, 139–154, doi: 10.1175/2010JAS3527.1.

Garfinkel, C. I. and D. L. Hartmann, 2007: Effects of the El Nino-Southern Oscillation and the Quasi-Biennial Oscillation on polar temperatures in the stratosphere. *J. Geophys. Res.-Atmos.*, **112 (D19)**, D19 112, doi: 10.1029/2007JD008481.

Garfinkel, C. I. and D. L. Hartmann, 2011a: The Influence of the Quasi-Biennial Oscillation on the Troposphere in Winter in a Hierarchy of Models. Part I: Simplified Dry GCMs. *J. Atmos. Sci.*, **68 (6)**, 1273–1289, doi: 10.1175/2011JAS3665.1.

Garfinkel, C. I. and D. L. Hartmann, 2011b: The Influence of the Quasi-Biennial Oscillation on the Troposphere in Winter in a Hierarchy of Models. Part II: Perpetual Winter WACCM Runs. *J. Atmos. Sci.*, **68 (9)**, 2026–2041, doi: 10.1175/2011JAS3702.1.

Garfinkel, C. I., T. A. Shaw, D. L. Hartmann, and D. W. Waugh, 2012: Does the Holton-Tan mechanism explain how the quasi-biennial oscillation modulates the polar vortex? *Journal of Atmospheric Sciences*, **69 (5)**, 1713–1733, doi: doi:10.1175/JAS-D-11-0209.1.

Giorgetta, M. A., E. Manzini, and E. Roeckner, 2002: Forcing of the quasi-biennial oscillation from a broad spectrum of atmospheric waves. *Geophys. Res. Lett.*, **29 (8)**, 1245, doi: 10.1029/2002GL014756.

Giorgetta, M. A., E. Manzini, E. Roeckner, M. Esch, and L. Bengtsson, 2006: Climatology and forcing of the quasi-biennial oscillation in the MAECHAM5 model. *J. Climate*, **19 (16)**, 3882–3901, doi: 10.1175/JCLI3830.1.

Gray, L. J. and J. A. Pyle, 1986: The semi-annual oscillation and equatorial tracer distribution. *Quart. J. Roy. Meteor. Soc.*, **112**, 387–407.

Gray, L. J., et al., 2010: Solar Influences On Climate. *Rev. Geophys.*, **48**, RG4001, doi: 10.1029/2009RG000282.

Gray, W. M., J. D. Sheaffer, and J. A. Knaff, 1992: Influence of the Stratospheric QBO on ENSO Variability. *J. Meteor. Soc. Japan*, **70 (5)**, 975–995.

Haigh, J. D., 1994: The Role of Stratospheric Ozone In Modulating the Solar Radiative Forcing of Climate. *Nature*, **370 (6490)**, 544–546, doi: 10.1038/370544a0.

Haigh, J. D., 1996: The impact of solar variability on climate. *Science*, **272 (5264)**, 981–984, doi: 10.1126/science.272.5264.981.

Hansen, F., K. Matthes, and L. J. Gray, 2013: Sensitivity of stratospheric dynamics and chemistry to QBO nudging width in the chemistry-climate model WACCM. *J. Geophys. Res.-Atmos.*, **118**, 10 464–10 474, doi: 10.1002/jgrd.50812.

Hansen, F., K. Matthes, C. Petrick, and W. Wang, 2014: The influence of natural and anthropogenic factors on major Stratospheric Sudden Warmings. *J. Geophys. Res.-Atmos.*, **119**, 8117–8136, doi: 10.1002/2013JD021397.

Hansen, F., K. Matthes, and S. Wahl, 2015: Tropospheric QBO-ENSO interactions and differences between Atlantic and Pacific. *Submitted to J. Climate*.

Harnik, N., 2009: Observed stratospheric downward reflection and its relation to upward pulses of wave activity. *J. Geophys. Res.-Atmos.*, **114**, D08 120, doi: 10.1029/2008JD010493.

Harnik, N. and R. S. Lindzen, 2001: The effect of reflecting surfaces on the vertical structure and variability of stratospheric planetary waves. *J. Atmos. Sci.*, **58 (19)**, 2872–2894, doi: 10.1175/

1520-0469(2001)058⟨2872:TEORSO⟩2.0.CO;2.

Hartley, D. E., J. T. Villarin, R. X. Black, and C. A. Davis, 1998: A new perspective on the dynamical link between the stratosphere and troposphere. *Nature*, **391 (6666)**, 471–474, doi: 10.1038/35112.

Haynes, P. H., C. J. Marks, M. E. McIntyre, T. G. Shepherd, and K. P. Shine, 1991: On the Downward Control of Extratropical Diabatic Circulations By Eddy-induced Mean Zonal Forces. *Journal of the Atmospheric Sciences*, **48 (4)**, 651–679, doi: 10.1175/1520-0469(1991)048⟨0651:OTCOED⟩2.0.CO;2.

Hitchcock, P. and I. R. Simpson, 2014: The Downward Influence of Stratospheric Sudden Warmings. *J. Atmos. Sci.*, **71 (10)**, 3856–3876, doi: 10.1175/JAS-D-14-0012.1, URL `http://dx.doi.org/10.1175/JAS-D-14-0012.1`.

Ho, C. H., H. S. Kim, J. H. Jeong, and S. W. Son, 2009: Influence of stratospheric quasi-biennial oscillation on tropical cyclone tracks in the western north pacific. *Geophys. Res. Lett.*, **36**, L06 702, doi: 10.1029/2009GL037163.

Holton, J. R. and C. Mass, 1976: Stratospheric Vacillation Cycles. *Journal of the Atmospheric Sciences*, **33 (11)**, 2218–2225, doi: 10.1175/1520-0469(1976)033⟨2218:SVC⟩2.0.CO;2.

Holton, J. R. and H.-C. Tan, 1980: The influence of the equatorial quasi-biennial oscillation on the global circulation at 50 mb. *J. Atmos. Sci.*, **37**, 2200–2208.

Holton, J. R. and H.-C. Tan, 1982: The quasi-biennial oscillation in the Northern Hemisphere lower stratosphere. *J. Meteor. Soc. Japan*, **60**, 140–148.

Ineson, S. and A. A. Scaife, 2009: The role of the stratosphere in the European climate response to El Nino. *Nature Geoscience*, **2 (1)**, 32–36, doi: 10.1038/NGEO381.

Ineson, S., A. A. Scaife, J. R. Knight, J. C. Manners, N. J. Dunstone, L. J. Gray, and J. D. Haigh, 2011: Solar forcing of winter climate variability in the Northern Hemisphere. *Nature Geoscience*, **4 (11)**, 753–757, doi: 10.1038/NGEO1282.

IPCC, 2014: Summary for Policymakers. In: *Climate Change 2014: Impacts, Adaptation, and Vulnerability. Part A: Global and Sectoral Aspects. Contribution of Working Group II to the Fifth Assessment Report of the Intergovernmental Panel on Climate Change* [Field, C. B., V. R. Barros, D. J. Dokken, K. J. Mach, M. D. Mastrandrea, T. E. Bilir, M. Chatterjee, K. L. Ebi, Y. O. Estrada, R. C. Genova, B. Girma, E. S. Kissel, A. N. Levy, S. MacCracken, P. R. Mastrandrea and L. L. White (eds.)]. Cambridge University Press, Cambridge, United Kingdom, and New York, NY, USA, 1–32 pp.

Julian, P. R. and K. B. Labitzke, 1965: A Study of Atmospheric Energetics During January-febrauary 1963 Stratospheric Warming. *Journal of the Atmospheric Sciences*, **22 (6)**, 597–&, doi: 10.1175/1520-0469(1965)022⟨0597:ASOAED⟩2.0.CO;2.

Kawatani, Y. and K. Hamilton, 2013: Weakened stratospheric quasibiennial oscillation driven by increased tropical mean upwelling. *Nature*, **497 (7450)**, 478–+, doi: 10.1038/nature12140.

Kawatani, Y., K. Sato, T. J. Dunkerton, S. Watanabe, S. Miyahara, and M. Takahashi, 2010: The roles of equatorial trapped waves and internal inertia-gravity waves in driving the quasi-biennial oscillation. part i: Zonal mean wave forcing. *J. Atmos. Sci.*, **67 (4)**, 963–980, doi: 10.1175/2009JAS3222.1.

Kodera, K. and Y. Kuroda, 2002: Dynamical response to the solar cycle. *Journal of Geophysical*

Research-atmospheres, **107 (D24)**, 4749, doi: 10.1029/2002JD002224.

Krüger, K., B. Naujokat, and K. Labitzke, 2005: The unusual midwinter warming in the Southern Hemisphere stratosphere 2002: A comparison to northern hemisphere phenomena. *Journal of the Atmospheric Sciences*, **62 (3)**, 603–613, doi: 10.1175/JAS-3316.1.

Kulyamin, D. V., E. M. Volodin, and V. P. Dymnikov, 2009: Simulation of the quasi-biennial oscillations of the zonal wind in the equatorial stratosphere: Part II. Atmospheric general circulation models. *Izvestiya Atmospheric and Oceanic Physics*, **45 (1)**, 37–54, doi: 10.1134/S0001433809010046.

Kunz, T. and R. J. Greatbatch, 2013: On the Northern Annular Mode Surface Signal Associated with Stratospheric Variability. *Journal of the Atmospheric Sciences*, **70 (7)**, 2103–2118, doi: 10.1175/JAS-D-12-0158.1.

Kushner, P. J. and L. M. Polvani, 2004: Stratosphere-troposphere coupling in a relatively simple AGCM: The role of eddies. *Journal of Climate*, **17 (3)**, 629–639, doi: 10.1175/1520-0442(2004)017⟨0629:SCIARS⟩2.0.CO;2.

Labitzke, K. and B. Naujokat, 2000: The lower Arctic stratosphere in winter since 1952. *SPARC Newsletter*, **15**, 11–14.

Lean, J. L., G. J. Rottman, H. L. Kyle, T. N. Woods, J. R. Hickey, and L. C. Puga, 1997: Detection and parameterization of variations in solar mid- and near-ultraviolet radiation (200-400 nm). *Journal of Geophysical Research-atmospheres*, **102 (D25)**, 29 939–29 956, doi: 10.1029/97JD02092.

Lee, Y.-Y. and R. X. Black, 2015: The Structure and Dynamics of the Stratospheric Northern Annular Mode in CMIP5 Simulations. *J. Climate*, **28**, 86–107, doi: 10.1175/JCLI-D-13-00570.1.

Limpasuvan, V., J. H. Richter, Y. J. Orsolini, F. Stordal, and O. K. Kvissel, 2012: The roles of planetary and gravity waves during a major stratospheric sudden warming as characterized in WACCM. *J. Atmos. Sol.-Terr. Phy.*, **78-79**, 84–98, doi: 10.1016/j.jastp.2011.03.004.

Lindzen, R. S. and J. R. Holton, 1968: A theory of the quasi-biennial oscillation. *Journal of Atmospheric Sciences*, **25**, 1095–1107.

Linkin, M. E. and S. Nigam, 2008: The north pacific oscillation-west Pacific teleconnection pattern: Mature-phase structure and winter impacts. *Journal of Climate*, **21 (9)**, 1979–1997, doi: 10.1175/2007JCLI2048.1.

Mantua, N. J., S. R. Hare, Y. Zhang, J. M. Wallace, and R. C. Francis, 1997: A Pacific interdecadal climate oscillation with impacts on salmon production. *Bulletin of the American Meteorological Society*, **78 (6)**, 1069–1079, doi: 10.1175/1520-0477(1997)078⟨1069:APICOW⟩2.0.CO;2.

Manzini, E., M. A. Giorgetta, M. Esch, L. Kornblueh, and E. Roeckner, 2006: The influence of sea surface temperatures on the northern winter stratosphere: Ensemble simulations with the MAECHAM5 model. *J. Climate*, **19 (16)**, 3863–3881, doi: 10.1175/JCLI3826.1.

Marsh, D., M. J. Mills, D. E. Kinnison, J.-F. Lamarque, N. Calvo, and L. M. Polvani, 2013: Climate Change from 1850 to 2005 simulated in CESM1(WACCM). *J. Climate*, doi: 10.1175/JCLI-D-12-00558.1.

Marshall, A. G. and A. A. Scaife, 2009: Impact of the QBO on surface winter climate. *J. Geophys. Res.-Atmos.*, **114**, D18 110, doi: 10.1029/2009JD011737.

Matsuno, T., 1971: Dynamical Model of Stratospheric Sudden Warming. *J. Atmos. Sci.*, **28 (8)**, 1479–1494, doi: 10.1175/1520-0469(1971)028⟨1479:ADMOTS⟩2.0.CO;2.

Matthes, K., K. Kodera, R. R. Garcia, Y. Kuroda, D. R. Marsh, and K. Labitzke, 2013: The importance of time-varying forcing for QBO modulation of the atmospheric 11 year solar cycle signal. *Journal of Geophysical Research-atmospheres*, **118 (10)**, 4435–4447, doi: 10.1002/jgrd.50424.

Matthes, K., Y. Kuroda, K. Kodera, and U. Langematz, 2006: Transfer of the solar signal from the stratosphere to the troposphere: Northern winter. *Journal of Geophysical Research-atmospheres*, **111 (D6)**, D06 108, doi: 10.1029/2005JD006283.

Matthes, K., D. R. Marsh, R. R. Garcia, D. E. Kinnison, F. Sassi, and S. Walters, 2010: Role of the QBO in modulating the influence of the 11 year solar cycle on the atmosphere using constant forcings. *J. Geophys. Res.-Atmos.*, **115**, D18 110, doi: 10.1029/2009JD013020.

McLandress, C., A. I. Jonsson, D. A. Plummer, M. C. Reader, J. F. Scinocca, and T. G. Shepherd, 2010: Separating the Dynamical Effects of Climate Change and Ozone Depletion. Part I: Southern Hemisphere Stratosphere. *Journal of Climate*, **23 (18)**, 5002–5020, doi: 10.1175/2010JCLI3586.1.

Mitchell, D. M., L. J. Gray, J. Anstey, M. P. Baldwin, and A. J. Charlton-Perez, 2013: The Influence of Stratospheric Vortex Displacements and Splits on Surface Climate. *J. Climate*, **26 (8)**, 2668–2682, doi: 10.1175/JCLI-D-12-00030.1.

Mitchell, D. M., et al., 2014: Signatures of naturally induced variability in the atmosphere using multiple reanalysis datasets. *Q.J.R. Meteorol. Soc.*, n/a–n/a, URL `http://dx.doi.org/10.1002/qj.2492`.

Naoe, H. and K. Shibata, 2010: Equatorial quasi-biennial oscillation influence on northern winter extratropical circulation. *J. Geophys. Res.-Atmos.*, **115**, D19 102, doi: 10.1029/2009JD012952.

O'Callaghan, A., M. Joshi, D. Stevens, and D. Mitchell, 2014: The effects of different sudden stratospheric warming types on the ocean. *Geophys. Res. Lett.*, **41 (21)**, 7739–7745, URL `http://dx.doi.org/10.1002/2014GL062179`.

Perlwitz, J. and N. Harnik, 2003: Observational evidence of a stratospheric influence on the troposphere by planetary wave reflection. *J. Climate*, **16 (18)**, 3011–3026, doi: 10.1175/1520-0442(2003)016⟨3011:OEOASI⟩2.0.CO;2.

Perlwitz, J. and N. Harnik, 2004: Downward coupling between the stratosphere and troposphere: The relative roles of wave and zonal mean processes. *J. Climate*, **17 (24)**, 4902–4909, doi: 10.1175/JCLI-3247.1.

Plumb, R. A. and R. C. Bell, 1982: A model of the quasi-biennial oscillation on an equatorial beta-plane. *Quart. J. Roy. Meteor. Soc.*, **108**, 335–352.

Previdi, M. and L. M. Polvani, 2014: Climate system response to stratospheric ozone depletion and recovery. *Quarterly Journal of the Royal Meteorological Society*, **140 (685)**, 2401–2419, doi: 10.1002/qj.2330.

Quiroz, R. S., 1977: Tropospheric-stratospheric Polar Vortex Breakdown of January 1977. *Geophys. Res. Lett.*, **4 (4)**, 151–154, doi: 10.1029/GL004i004p00151.

Reed, R. J., 1966: Zonal Wind Behavior In Equatorial Stratosphere and Lower Mesosphere. *Journal of Geophysical Research*, **71 (18)**, 4223–&.

Reichler, T., J. Kim, E. Manzini, and J. Kroger, 2012: A stratospheric connection to Atlantic climate variability. *Nature Geoscience*, **5 (11)**, 783–787, doi: 10.1038/NGEO1586.

Richter, J. H., F. Sassi, R. R. Garcia, K. Matthes, and C. A. Fischer, 2008: Dynamics of the middle atmosphere as simulated by the Whole Atmosphere Community Climate Model, version 3 (WACCM3). *J. Geophys. Res.-Atmos.*, **113 (D8)**, D08 101, doi: 10.1029/2007JD009269.

Richter, J. H., A. Solomon, and J. T. Bacmeister, 2014: On the simulation of the quasi-biennial oscillation in the Community Atmosphere Model, version 5. *Journal of Geophysical Research-atmospheres*, **119 (6)**, 3045–3062, doi: 10.1002/2013JD021122.

Rind, D., J. Jonas, N. K. Balachandran, G. A. Schmidt, and J. Lean, 2014: The qbo in two giss global climate models: 1. generation of the qbo. *J. Geophys. Res. Atmos.*, **119 (14)**, 2014JD021 678–, URL `http://dx.doi.org/10.1002/2014JD021678`.

Robock, A., 2000: Volcanic eruptions and climate. *Rev. Geophys.*, **38 (2)**, 191–219, doi: 10.1029/1998RG000054.

Sassi, F., D. Kinnison, B. A. Boville, R. R. Garcia, and R. Roble, 2004: Effect of El Nino-Southern Oscillation on the dynamical, thermal, and chemical structure of the middle atmosphere. *J. Geophys. Res.-Atmos.*, **109 (D17)**, D17 108, doi: 10.1029/2003JD004434.

Scaife, A. A., N. Butchart, C. D. Warner, D. Stainforth, W. Norton, and J. Austin, 2000: Realistic quasi-biennial oscillations in a simulation of the global climate. *Geophys. Res. Lett.*, **27 (21)**, 3481–3484.

Schlesinger, M. E. and N. Ramankutty, 1994: An Oscillation In the Global Climate System of Period 65-70 Years. *Nature*, **367 (6465)**, 723–726, doi: 10.1038/367723a0.

Shapiro, L. J., 1989: The relationship of the quasi-biennial oscillation to atlantic tropical storm activity. *Mon. Wea. Rev.*, **117 (7)**, 1545–1552, doi: 10.1175/1520-0493(1989)117⟨1545:TROTQB⟩2.0.CO;2.

Shaw, T. A., J. Perlwitz, and N. Harnik, 2010: Downward Wave Coupling between the Stratosphere and Troposphere. The Importance of Meridional Wave Guiding and Comparison with Zonal-Mean Coupling. *J. Climate*, **23 (23)**, 6365–6381, doi: 10.1175/2010JCLI3804.1.

Shaw, T. A., J. Perlwitz, and O. Weiner, 2014: Troposphere-stratosphere coupling: Links to North Atlantic weather and climate, including their representation in CMIP5 models. *J. Geophys. Res. Atmos.*, **119**, n/a–n/a, doi: 10.1002/2013JD021191, URL `http://dx.doi.org/10.1002/2013JD021191`.

Shibata, K. and M. Deushi, 2005: Partitioning between resolved wave forcing and unresolved gravity wave forcing to the quasi-biennial oscillation as revealed with a coupled chemistry-climate model. *Geophys. Res. Lett.*, **32 (12)**, L12 820, doi: 10.1029/2005GL022885.

Sigmond, M., J. F. Scinocca, V. V. Kharin, and T. G. Shepherd, 2013: Enhanced seasonal forecast skill following stratospheric sudden warmings. *Nature Geoscience*, **6 (2)**, 98–102, doi: 10.1038/NGEO1698.

Simpson, I. R., M. Blackburn, and J. D. Haigh, 2009: The Role of Eddies in Driving the Tropospheric Response to Stratospheric Heating Perturbations. *J. Atmos. Sci.*, **66 (5)**, 1347–1365, doi: 10.1175/2008JAS2758.1.

Smith, A. K., R. R. Garcia, D. R. Marsh, and J. H. Richter, 2011: WACCM simulations of the mean circulation and trace species transport in the winter mesosphere. *J. Geophys. Res.-Atmos.*, **116**, D20 115, doi: 10.1029/2011JD016083.

Solomon, S., 1999: Stratospheric ozone depletion: a review of concepts and history. *Rev. Geophys.*,

37, 275–316.

Song, Y. C. and W. A. Robinson, 2004: Dynamical mechanisms for stratospheric influences on the troposphere. *Journal of the Atmospheric Sciences*, **61 (14)**, 1711–1725, doi: 10.1175/1520-0469(2004)061⟨1711:DMFSIO⟩2.0.CO;2.

SPARC CCMVal, 2010: *SPARC Report on the Evaluation of Chemistry-Climate Models, SPARC-Report No. 5, WCRP-132,WMO/TD-No. 1526*. SPARC CCMVal.

Stolarski, R. S., A. R. Douglass, P. A. Newman, S. Pawson, and M. R. Schoeberl, 2010: Relative Contribution of Greenhouse Gases and Ozone-Depleting Substances to Temperature Trends in the Stratosphere: A Chemistry-Climate Model Study. *Journal of Climate*, **23 (1)**, 28–42, doi: 10.1175/2009JCLI2955.1.

Taguchi, M., 2010: Observed connection of the stratospheric quasi-biennial oscillation with El Nino-Southern Oscillation in radiosonde data. *J. Geophys. Res.-Atmos.*, **115**, D18 120, doi: 10.1029/2010JD014325.

Taylor, K., R. J. Stouffer, and G. A. Meehl, 2009: A summary of the CMIP5 Experiment Design. *from http cmip-pcmdi.llnl.gov cmip5 docs Taylor CMIP5 design.pdf*.

Taylor, K., R. J. Stouffer, and G. A. Meehl, 2012: An overview of CMIP5 and the experiment design. *Bull. Amer. Meteor. Soc.*, **93**, 485–498.

Thompson, D. W. J., M. P. Baldwin, and J. M. Wallace, 2002: Stratospheric connection to Northern Hemisphere wintertime weather: Implications for prediction. *J. Climate*, **15 (12)**, 1421–1428, doi: 10.1175/1520-0442(2002)015⟨1421:SCTNHW⟩2.0.CO;2.

Trenberth, K. E., 1997: The definition of El Niño. *Bull. Amer. Meteor. Soc.*, **78**, 2771–2777.

van Loon, H. and K. Labitzke, 1987: The Southern Oscillation .5. The Anomalies In the Lower Stratosphere of the Northern-hemisphere In Winter and A Comparison With the Quasi-biennial Oscillation. *Mon. Wea. Rev.*, **115 (2)**, 357–369, doi: 10.1175/1520-0493(1987)115⟨0357:TSOPVT⟩2.0.CO;2.

Wallace, J. M. and D. S. Gutzler, 1981: Teleconnections In the Geopotential Height Field During the Northern Hemisphere Winter. *Mon. Wea. Rev.*, **109 (4)**, 784–812, doi: 10.1175/1520-0493(1981)109⟨0784:TITGHF⟩2.0.CO;2.

Xue, X. H., H. L. Liu, and X. K. Dou, 2012: Parameterization of the inertial gravity waves and generation of the quasi-biennial oscillation. *J. Geophys. Res.-Atmos.*, **117**, D06 103, doi: 10.1029/2011JD016778.

Yoden, S., 1987a: Bifurcation Properties of A Stratospheric Vacillation Model. *Journal of the Atmospheric Sciences*, **44 (13)**, 1723–1733, doi: 10.1175/1520-0469(1987)044⟨1723:BPOASV⟩2.0.CO;2.

Yoden, S., 1987b: Dynamical Aspects of Stratospheric Vacillations In A Highly Truncated Model. *Journal of the Atmospheric Sciences*, **44 (24)**, 3683–3695, doi: 10.1175/1520-0469(1987)044⟨3683:DAOSVI⟩2.0.CO;2.

Yuan, W., M. A. Geller, and P. T. Love, 2014: ENSO influence on the QBO modulations of the tropical tropopause. *Q. J. R. Meteorol. Soc.*, **140**, 1670–1676, doi: 10.1002/qj.2247.

Own Publications

Martin-Puertas, C., K. Matthes, A. Brauer, R. Muscheler, **F. Hansen**, C. Petrick, A. Aldahan, G. Possnert, and B. van Geel, 2012: Regional atmospheric circulation shifts induced by a grand solar minimum. *Nature Geosci.*, **5 (6)**, 397–401, doi: 10.1038/NGEO1460.

Hansen, F., K. Matthes, and L. J. Gray, 2013: Sensitivity of stratospheric dynamics and chemistry to QBO nudging width in the chemistry-climate model WACCM. *J. Geophys. Res.-Atmos.*, **118**, 10464–10474, doi: 10.1002/jgrd.50812.

Hansen, F., K. Matthes, C. Petrick, and W. Wang, 2014: The influence of natural and anthropogenic factors on major Stratospheric Sudden Warmings. *J. Geophys. Res.-Atmos.*, **119**, 8117–8136, doi: 10.1002/2013JD021397.

Thiéblemont, R., K. Matthes, N.-E. Omrani, K. Kodera and **F. Hansen**, 2015: Solar forcing synchronizes decadal North Atlantic climate variability. Under review with *Nat. Commun.*.

Hansen, F., K. Matthes, and S. Wahl, 2015: Tropospheric QBO-ENSO interactions and their differences between Atlantic and Pacific. Submitted to *J. Climate*.

Appendix

A.1 Multiple Linear Regression (MLR) Analysis

Multiple Linear Regression (MLR) is a relatively simple and robust statistical method which makes it quite popular for analyzing stratospheric variability. In a MLR, a target time series, e.g., a time series representing stratospheric temperature, is modeled using a linear and stationary model, which means that no non-linear interactions between the so-called forcing factors, i.e., the factors that influence the variability of the target time series, are taken into account and that the underlying processes that govern the evolution of the target time series are assumed to not change their characteristics significantly over time. The target time series y is modeled so that

$$y(x) = x^T \beta + \beta_0 \tag{5.1}$$

where x is a matrix containing the time series of the forcing factors , β the coefficients in the linear equation, and β_0 the so-called offset. The impact or statistical importance of the factor k on the model response is then computed as

$$I_k = |\beta_k| \sqrt{var(x_k)} \tag{5.2}$$

To compare the impacts of different factors, they are normalized via:

$$I_k^{rel} = \frac{I_k}{\sum_{i=1}^{n} I_i} \tag{5.3}$$

with n being the number of all factors.

In Figure 1.4, the target time series is the time series of daily zonal mean temperature. An MLR is performed for every grid point in the latitude-height plane separately. The forcings and their representing time series are:

- SSTs: represented by the principal components (PCs) of the first four Empirical Orthogonal Functions (EOFs) of daily detrended SST anomalies between 60°S and N; these EOFs include the El Niño Southern Oscillation, the Pacific Decadal Oscillation and the North Pacific Oscillation/West Pacific pattern. For Figure 1.4, the sum of the impacts of the four single time series is computed.
- QBO: represented by the PCs of the first two EOFs of daily detrended zonal mean zonal wind

anomalies between 5°S and N, 100 and 1hPa. For Figure 1.4, the sum of the impacts of the two single time series is computed.

- Solar forcing: represented by daily detrended anomalies of the 10.7 cm solar radio flux (also referred to as F10.7 index).
- Volcanic eruptions: represented by daily absolute values of globally averaged aerosol optical depth.
- Semi-annual oscillation (SAO): represented by daily detrended anomalies of zonal mean zonal wind, averaged between 5°S and N, and between 0.03 and 0.05hPa.
- Annual cycle: represented by sine and cosine functions with the period of one year.
- Linear trend term

For all forcings, a 5-day running mean is applied, then all time series are normalized such that the maximum is $+1$ and the minimum is -1.

Danksagung

DANKE an meine Doktormutter Prof. Dr Katja Matthes für die intensive, anregende, diskussionsreiche, motivierende, persönliche Betreuung in den letzten vier Jahren. Ich habe so viel gelernt und weiß das wirklich zu schätzen! Danke, dass du es mir von Anfang an ermöglicht hast, an internationalen Konferenzen und Sommer(bzw. Winter-)schulen teilzunehmen, und dass du es möglich gemacht hast, meinen am Ende vielleicht etwas ambitionierten Zeitplan einzuhalten. Danke für so vieles, was über eine einfache PhD-Betreuung hinausgeht!
DANKE, THANKS und MERCI an die gesamte Arbeitsgruppe (erst NATHAN in Potsdam, jetzt Physik der Atmosphäre in Kiel), die in den letzten vier Jahren fast so etwas wie meine zweite internationale Familie war. In diesem Zusammenhang auch noch ein besonderer Dank an Prof. Dr. Maik Thomas vom GFZ Postdam und an die dortige Sektion 1.3. Danke für die wissenschaftlichen Diskussionen, die unwissenschaftlichen Kaffee- und Mittagspausen und die "after work" Zusammenkünfte (besonders mit Christof). Danke an alle aus der Gruppe, die speziell auf den letzten Metern noch unterstützt haben, besonders Lisa für die Korrektur des Abstracts!
DANKE und THANKS an Prof. Dr. Mojib Latif, Prof. Dr. Douglas Maraun und Prof. Dr. Richard Greatbatch vom GEOMAR für herausfordernde Fragen und Hilfe bei deren Beantwortung.
DANKE an meine Eltern und meine Schwestern für so vieles! Am meisten für die ständige moralische Unterstützung, fürs Anfeuern und Motivieren am Ende und für die praktische Hilfe bei allen Umzügen und mit Silas. Mama, danke auch fürs Ausleihen des beheizbaren Fußsacks für den Endspurt!
DANKE an den Rest der Familie Hansen und an die gesamte Familie Kruschke für die Unterstützung aus der Nähe und der Ferne.
DANKE endlich mal an alle Freunde, besonders an die Flensburger Mädels Rebecca, Davina, Sophie und Inga, die "Berliner" Nico, Stefan, Mareike, Christopher und Dennis, die Kieler Geomar-Truppe, die FBOB-Frauen und an Viky und Tilia.
DANKE an die Deutsche Bahn dafür, dass sie mich zwei Jahre lang etwa jedes zweite Wochenende ziemlich zuverlässig zwischen Kiel und Berlin hin und her transportiert hat.
DANKE an Silas, das objektiv betrachtet süßeste Baby der Welt, der die letzten Monaten so viel schlafärmer, aber doch so viel reicher gemacht hat. Du bringst jeden Tag so viel Freude in mein Leben!
DANKE an Tim, den allerwichtigsten, ohne den gar nichts geht, den besten Freund und Freund, den ich mir wünschen kann. Danke für deine Geduld, deinen Enthusiasmus, deine Unterstützung in allem und deine Liebe! Bekomme ich nun den Staubsauger-Roboter?

Selbstständigkeitserklärung

Hiermit erkläre ich an Eides Statt, dass ich die vorliegende Dissertation - abgesehen von der Beratung durch meine Betreuerin Prof. Dr. Katja Matthes - selbstständig und ohne fremde Hilfe angefertigt, keine anderen als die angegebenen Quellen und Hilfsmittel benutzt und die den benutzten Quellen wörtlich oder inhaltlich entnommenen Stellen als solche kenntlich gemacht habe. Diese Arbeit hat in gleicher oder ähnlicher Form noch keiner Prüfungsbehörde vorgelegen. Sie ist unter Einhaltung der Regeln guter wissenschaftlicher Praxis der Deutschen Forschungsgemeinschaft entstanden.

Kiel, März 2015